

# Supporting Information

## Au→M bonds promote catalytic alkyne hydrofunctionalisation

M. Alexander Eltester<sup>a</sup>, Hans Gildenast<sup>a</sup>, Kristína Rabatinová<sup>a</sup>, Christopher Pütz<sup>a</sup>, Christopher Cremer<sup>a</sup>, Patrick Lanzerath<sup>a</sup>, Julian P. Schroers<sup>a</sup> and Michael E. Tauchert<sup>a\*</sup>

<sup>a</sup>Institute of Inorganic Chemistry, RWTH Aachen University, Landoltweg 1A, D-52074 Aachen, Germany

1	Experimental procedures.....	S2
1.1	General.....	S2
1.1.1	Analytics .....	S2
1.1.2	Chemicals .....	S2
1.1.3	Solvents .....	S2
1.2	Syntheses .....	S3
1.2.1	[Zn( <b>dpptpa</b> )(MeOH)](NTf <sub>2</sub> ) <sub>2</sub> ( <b>6</b> ) .....	S3
1.2.2	[Au( <b>dpptpa</b> )Ag(SMe <sub>2</sub> )](NTf <sub>2</sub> ) <sub>2</sub> ( <b>9</b> ) .....	S5
1.2.3	[Au( <b>dpptpa</b> )Cl] ( <b>10</b> ).....	S7
1.2.4	[AuZn( <b>dpptpa</b> )Cl](NTf <sub>2</sub> ) <sub>2</sub> ( <b>7</b> ) .....	S8
1.2.5	[AuZn( <b>dpptpa</b> )](NTf <sub>2</sub> ) <sub>3</sub> ( <b>8</b> ) .....	S9
1.2.6	[AuCu( <b>dpptpa</b> )Cl]OTf ( <b>11</b> ) .....	S10
1.2.7	[AuAg( <b>dpptpa</b> )](NTf <sub>2</sub> ) <sub>2</sub> ( <b>12</b> ) .....	S11
1.2.8	[AuZn( <b>dpptpa</b> )Br](SbF <sub>6</sub> ) <sub>2</sub> ( <b>17</b> ) .....	S12
2	Determination of Lewis acidity .....	S15
3	Single crystal X-ray diffraction analyses .....	S16
4	Overview of known Au complexes featuring a short Au–M distances .....	S19
5	Computational studies .....	S21
6	Catalytic experiments .....	S24
6.1	Hydroamination of alkynes .....	S24
6.2	Cycloisomerisation of <i>N</i> -(prop-2-yn-1-yl)benzamide ( <b>14</b> ) .....	S30
7	NMR spectra .....	S34
8	References .....	S61

## 1 Experimental procedures

### 1.1 General

#### 1.1.1 Analytics

All manipulations were carried out in an MBraun glove box under an inert argon atmosphere. NMR-experiments were performed in Wilmad® quick pressure valve NMR tubes.  $^1\text{H}$ ,  $^{13}\text{C}\{^1\text{H}\}$ ,  $^{19}\text{F}\{^1\text{H}\}$  and  $^{31}\text{P}\{^1\text{H}\}$  NMR spectra were recorded on a Bruker Avance II (400.1 MHz, probe: BBO) or a Bruker Avance (400.3 MHz, probe: ATM BBFO) spectrometer.  $^1\text{H}$  and  $^{13}\text{C}\{^1\text{H}\}$  NMR spectra were referenced to residual solvent resonances.<sup>1</sup>

**Table S1** Shifts of residual solvent resonances used to reference NMR spectra.

Solvent	$^1\text{H-NMR Shift in ppm}$	$^{13}\text{C-NMR Shift in ppm}$
DCM-d <sub>2</sub>	5.32	53.8
	1.72	67.2
THF-d <sub>8</sub>	3.58	25.3

CHN combustion analysis were carried out on an Elementar EL device by Elementar Analysesysteme GmbH. Infrared spectra were recorded on a FTIR IRSpirit spectrometer (Shimadzu). High resolution mass spectra (HRMS) were obtained by a maXis II spectrometer (Bruker).

#### 1.1.2 Chemicals

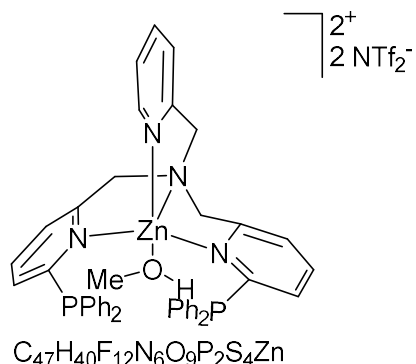
Unless stated otherwise all chemicals were purchased from Aldrich, ABCR, TCI, Merck or Alfa Aesar and used with no further purification. Zn(NTf<sub>2</sub>)<sub>2</sub> was purchased from TCI and sublimed using a Kugelrohr short-path distillation apparatus. **DPPTA** was synthesized as described earlier.<sup>2</sup> NaBArF was purchased from Alfa Aesar and purified/dried using literature techniques.<sup>3</sup> N-(Prop-2-yn-1-yl)benzamide was synthesized according to literature procedure<sup>4</sup>. DPB<sup>5</sup> and **1**<sup>6</sup> were synthesized using literature procedures. CO<sub>2</sub> 4.5 was purchased from Air Products and was passed through a sicapent column prior to use.

#### 1.1.3 Solvents

DCM-d<sub>2</sub> and was degassed employing the freeze-pump-thaw technique and stored over activated molecular sieves (3 Å). THF-d<sub>8</sub> was dried over sodium, distilled under an argon atmosphere and degassed employing the freeze-pump-thaw technique. Toluene, diethylether, dichloromethane, tetrahydrofurane, and pentane were dried by an MBraun solvent purification system (SPS800). *n*-Hexane and hexamethyldisiloxane were dried over sodium and distilled under argon prior to use and stored over activated molecular sieves (4 Å). Methanol was dried over molecular sieves (3 Å) overnight prior to use.

## 1.2 Syntheses

### 1.2.1 $[\text{Zn}(\text{dpptpa})(\text{MeOH})](\text{NTf}_2)_2$ (**6**)



**DPPTA** (152 mg, 230 µmol, 1.0 equiv.) and  $\text{Zn}(\text{NTf}_2)_2$  (144 mg, 230 µmol, 1.0 equiv.) were dissolved in THF (10 mL) and stirred for 72 h. The volatiles were removed *in vacuo* and Complex **6** yielded 284 mg (96 %). Complex **6** (77 mg) was dissolved in MeOH (1.5 mL) and cooled to – 30 °C for crystallization. Crystals suitable for SCXRD were grown from cooling a saturated solution of **6** in MeOH in the freezer.

$^1\text{H}$  NMR (400 MHz, DCM-d<sub>2</sub>)  $\delta$ /ppm = 8.04 – 7.96 (m, 2H,  $\text{CH}_{\text{arom}}$ ), 7.96 – 7.89 (m, 1H,  $\text{CH}_{\text{arom}}$ ), 7.59 (d,  $^3J_{\text{HH}} = 7.4$  Hz, 3H,  $\text{CH}_{\text{arom}}$ ), 7.50 (d,  $^3J_{\text{HH}} = 8.1$  Hz, 1H,  $\text{CH}_{\text{arom}}$ ), 7.44 – 7.38 (m, 3H,  $\text{CH}_{\text{arom}}$ ), 7.38 – 7.29 (m, 11H,  $\text{CH}_{\text{arom}}$ ), 7.25 – 7.19 (m, 1H,  $\text{CH}_{\text{arom}}$ ), 7.15 (s, 8H,  $\text{CH}_{\text{arom}}$ ), 4.51 (d,  $^2J_{\text{HH}} = 17.3$  Hz, 2H,  $\text{CH}_2$ ), 4.45 (d,  $^2J_{\text{HH}} = 17.6$  Hz, 2H,  $\text{CH}_2$ ), 4.33 (s, 2H,  $\text{CH}_2$ ), 3.53 (s, 2.6H,  $\text{CH}_3\text{OH}$ ), 2.26 (s, 0.8H,  $\text{CH}_3\text{OH}$ ).

$^{13}\text{C}\{\text{H}\}$  NMR (151 MHz, DCM-d<sub>2</sub>)  $\delta$ /ppm = 162.4, 157.2 (pt,  $J_{\text{CP}} = 7$  Hz), 154.5, 148.5, 142.8, 142.3, 134.0 (pt,  $J_{\text{CP}} = 10$  Hz), 133.9 (pt,  $J_{\text{CP}} = 10$  Hz), 132.2, 131.6, 131.4, 131.3, 131.3, 130.2 (pt,  $J_{\text{CP}} = 4$  Hz), 130.0 (pt,  $J_{\text{CP}} = 4$  Hz), 126.2, 126.2, 125.4, 120.3 (q,  $^1J_{\text{CF}} = 322$  Hz), 58.0, 57.7, 52.3.

$^{19}\text{F}\{\text{H}\}$  NMR (377 MHz, DCM-d<sub>2</sub>)  $\delta$ /ppm = -79.3 (s).

$^{31}\text{P}\{\text{H}\}$  NMR (162 MHz, DCM-d<sub>2</sub>)  $\delta$ /ppm = 6.9 (s).

IR (neat)  $\nu/\text{cm}^{-1}$  = 3431 (m), 1613 (w), 1593 (vw), 1438 (m), 1351 (s), 1197 (vs), 1135 (m), 1057 (m), 746 (w), 698 (w), 612 (m), 570 (m), 512 (m).

CHN calculated for  $\text{C}_{46}\text{H}_{36}\text{F}_{12}\text{N}_6\text{O}_9\text{P}_2\text{S}_4\text{Zn} + 0.8 \text{ CH}_3\text{OH}$ : C, 42.4 %; H, 3.0 %; N, 6.3 %;  
Found: C, 42.0 %; H, 2.7 %; N, 6.3 %.

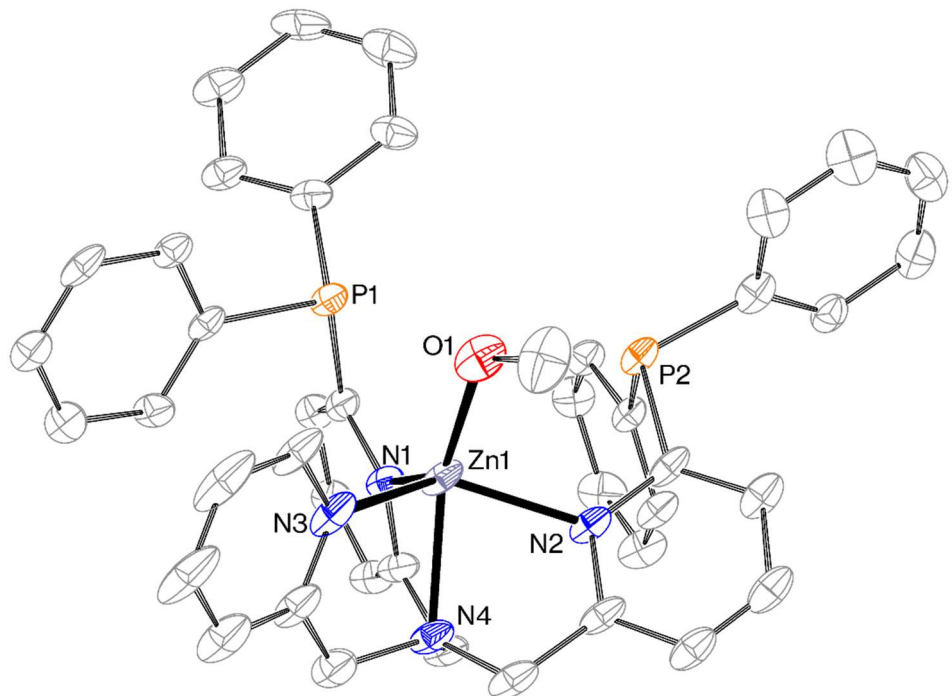
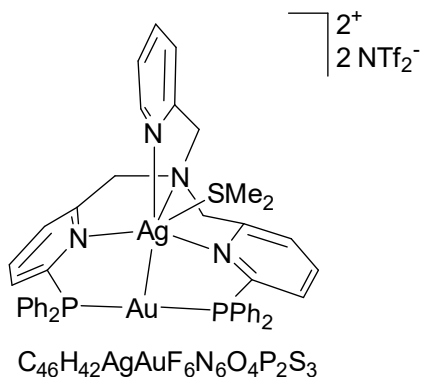


**Figure S1.** Displacement ellipsoid plot of **6** (30% probability, *P*-1, *Z* = 2). Two NTf<sub>2</sub>-anions and H atoms have been omitted for clarity. Crystal data for **6**: C<sub>47</sub>H<sub>40</sub>F<sub>12</sub>N<sub>6</sub>O<sub>9</sub>P<sub>2</sub>S<sub>4</sub>Zn, *M* = 1316.40 g mol<sup>-1</sup>, triclinic, space group P-1, *a* = 12.6499(18) Å, *b* = 14.203(3), *c* = 16.800(3) Å,  $\alpha$  = 77.885(3),  $\beta$  = 75.560(3),  $\gamma$  = 77.008(3), *V* = 2810.1(9) Å<sup>3</sup>, *Z* = 2, *T* = 100(2) K,  $\mu(\text{Mo-}K\alpha)$  = 0.740 mm<sup>-1</sup>, collected/unique reflections 31734/10297, *R*<sub>1</sub> = 0.0835, *wR*<sub>2</sub> = 0.2250, GOF = 1.041

### 1.2.2 [Au(**dpptpa**)Ag(SMe<sub>2</sub>)<sub>2</sub>](NTf<sub>2</sub>)<sub>2</sub> (**9**)



**DPPTPA** (20 mg, 30  $\mu\text{mol}$ ) and [Au(SMe<sub>2</sub>)Cl] (9 mg, 30  $\mu\text{mol}$ , 1.0 equiv.) were solved in DCM (1.2 mL) and thoroughly mixed. AgNTf<sub>2</sub> (24 mg, 61  $\mu\text{mol}$ , 2.0 equiv.) was added and the suspension was filtered through glass wool. The product **9** was crystallized by slow diffusion of Et<sub>2</sub>O into the solution. The solution was decanted, and the solid residue was dried *in vacuo*. The product **9** was obtained as a white crystalline solid (33 mg, 21  $\mu\text{mol}$ , 68 %). Crystals suitable for SCXRD were grown from slow diffusion of Et<sub>2</sub>O into a saturated solution of **9** in DCM.

<sup>1</sup>H NMR (400 MHz, DCM-d<sub>2</sub>)  $\delta$ /ppm = 7.91 (tt, <sup>3</sup>J<sub>HH</sub> = 7.8 Hz, J = 2.0 Hz, 2H, CH<sub>arom</sub>), 7.77 (m, 2H, CH<sub>arom</sub>), 7.71 (td, <sup>3</sup>J<sub>HH</sub> = 4.5 Hz, <sup>4</sup>J<sub>HH</sub> = 2.1 Hz, 11H, CH<sub>arom</sub>), 7.64 (m, 4H, CH<sub>arom</sub>), 7.58 (m, 4H, CH<sub>arom</sub>), 7.50 (m, 2H, CH<sub>arom</sub>), 7.35 (d, <sup>3</sup>J<sub>HH</sub> = 7.8 Hz, 1H, CH<sub>arom</sub>), 7.29 (dq, <sup>3</sup>J<sub>HH</sub> = 7.7 Hz, J = 1.4 Hz, 2H, CH<sub>arom</sub>), 7.16 (m, 1H, CH<sub>arom</sub>), 7.03 (ddd, <sup>3</sup>J<sub>HH</sub> = 7.7 Hz, <sup>3</sup>J<sub>HH</sub> = 4.9 Hz, J = 1.2 Hz, 1H, CH<sub>arom</sub>), 4.05 (s, 4H, CH<sub>2</sub>), 4.01 (s, 2H, CH<sub>2</sub>), 1.76 (s, 6H, S(CH<sub>3</sub>)<sub>2</sub>).

<sup>13</sup>C{<sup>1</sup>H} NMR (101 MHz, DCM-d<sub>2</sub>)  $\delta$ /ppm = 159.7 (pt, J<sub>CP</sub> = 9 Hz), 155.6, 153.2 (pt, <sup>1</sup>J<sub>CP</sub> = 43 Hz), 150.3, 140.4 (pt, J<sub>CP</sub> = 3 Hz), 138.9, 135.4 (pt, J<sub>CP</sub> = 8 Hz), 134.5 (pt, J<sub>CP</sub> = 8 Hz), 134.3, 134.1, 131.0 (pt, J<sub>CP</sub> = 6 Hz), 130.7 (pt, J<sub>CP</sub> = 6 Hz), 130.5 (pt, J<sub>CP</sub> = 10 Hz), 127.6, 126.1, 125.5 (pt, <sup>1</sup>J<sub>CP</sub> = 29 Hz), 125.2 (pt, <sup>1</sup>J<sub>CP</sub> = 28 Hz), 124.1, 120.3 (q, <sup>1</sup>J<sub>CF</sub> = 322 Hz), 62.4, 60.0, 20.2

<sup>19</sup>F{<sup>1</sup>H} -NMR (377 MHz, DCM-d<sub>2</sub>)  $\delta$ /ppm = -79.3 (s).

<sup>31</sup>P{<sup>1</sup>H} -NMR (162 MHz, DCM-d<sub>2</sub>)  $\delta$ /ppm = 48.9 (s).

IR (neat)  $\nu/\text{cm}^{-1}$  = 3071 (w), 2976(w), 2928(w), 2860(w), 1585 (m), 1560 (sh), 1482 (sh), 1437 (m), 1346 (vs), 1332 (s), 1226 (sh), 1174 (vs), 1134 (vs), 1100 (s), 1053 (vs), 997 (m), 972 (sh), 947 (sh), 924 (sh), 881 (sh), 844 (w), 786 (m), 769 (m), 754 (m), 738 (m), 715 (m), 692 (s), 652 (w), 612 (m), 598 (m), 568 (s), 537, 506 (s), 482 (sh), 463 (sh), 404 (w)

HRMS (ESI, m/z) calculated for [AuAg(**dpptpa**)]<sup>2+</sup> (**9** – SMe<sub>2</sub> – 2 NTf<sub>2</sub><sup>-</sup>): 481.05658, found 481.05747 (1.8 ppm)

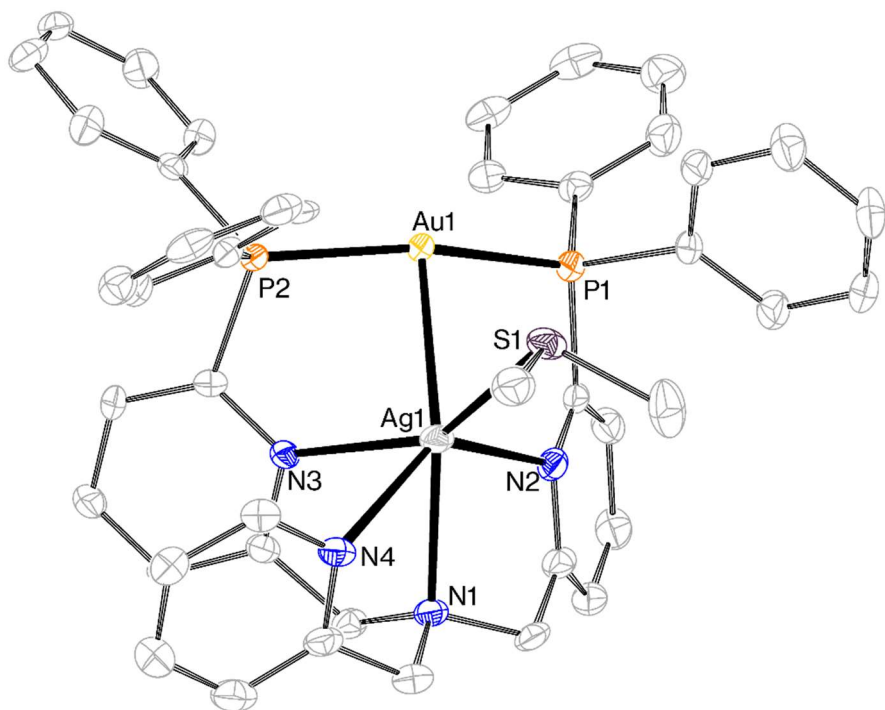
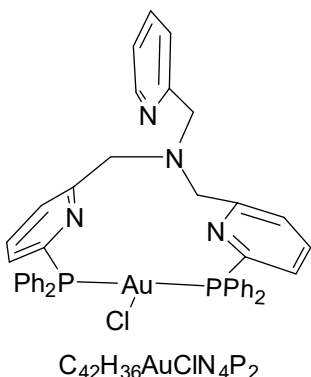


**Figure S2.** Displacement ellipsoid plot of **9** (50% probability, *P*-1, *Z* = 2). Two NTf<sub>2</sub>-anions, one THF molecule and H atoms have been omitted for clarity. Crystal data for **9**: C<sub>52</sub>H<sub>52</sub>AgAuF<sub>12</sub>N<sub>6</sub>O<sub>8</sub>P<sub>2</sub>S<sub>5</sub>, *M* = 1644.07 g mol<sup>-1</sup>, triclinic, space group *P*-1, *a* = 14.1986(13) Å, *b* = 15.7612(15), *c* = 15.7808(15) Å,  $\alpha$  = 96.576(2),  $\beta$  = 108.838(2),  $\gamma$  = 107.971(2), *V* = 3088.0(5) Å<sup>3</sup>, *Z* = 2, *T* = 100(2) K,  $\mu(\text{Mo-}K\alpha)$  = 3.003 mm<sup>-1</sup>, collected/unique reflections 61181/18445, *R*<sub>1</sub> = 0.0478, *wR*<sub>2</sub> = 0.1031, *GOF* = 1.046.

### 1.2.3 [Au(dpptpa)Cl] (**10**)



**DPPTPA** (100 mg, 152  $\mu\text{mol}$ ) and  $[\text{Au}(\text{SMe}_2)\text{Cl}]$  (45 mg, 152  $\mu\text{mol}$ , 1.0 equiv.) was solved in DCM (2 mL) and thoroughly mixed for 30 min. The solvent was removed *in vacuo* and the residue was washed with hexane (3 x 2 mL). The washing solution was discarded, and the solid was dried *in vacuo*. The product **10** was obtained as a white powder (104 mg, 117  $\mu\text{mol}$ , 77 %).

$^1\text{H}$  NMR (400 MHz, THF-d<sub>8</sub>)  $\delta/\text{ppm}$  = 8.24 (m, 2H,  $\text{CH}_{\text{arom}}$ ), 7.92 (d,  $^3J_{\text{HH}} = 8$  Hz, 2H,  $\text{CH}_{\text{arom}}$ ), 7.61 (m, 24H,  $\text{CH}_{\text{arom}}$ ), 6.74 (m, 2H,  $\text{CH}_{\text{arom}}$ ), 4.84 (d,  $^2J_{\text{HH}} = 17$  Hz, 2H,  $\text{CH}_{\text{arom}}$ ), 4.69 (d,  $^2J_{\text{HH}} = 1$  Hz, 4H,  $\text{CH}_2$ ), 4.52 (s, 2H,  $\text{CH}_2$ )

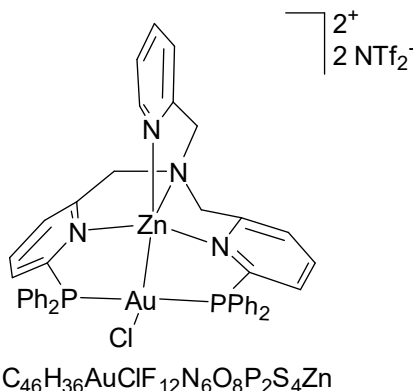
$^{13}\text{C}\{\text{H}\}$  NMR (101 MHz, THF-d<sub>8</sub>)  $\delta/\text{ppm}$  = 160.6, 159.0, 158.5, 150.0, 137.5 (d,  $J_{\text{CP}} = 7.5$  Hz), 137.0, 135.5 (d,  $J_{\text{CP}} = 17$  Hz), 134.2 (d,  $J = 30$  Hz), 131.4, 129.7 (d,  $J_{\text{CP}} = 10$  Hz), 129.1 (d,  $J = 27$  Hz), 124.7, 123.9, 122.7, 61.1, 60.6.

$^{31}\text{P}\{\text{H}\}$  NMR (162 MHz, THF-d<sub>8</sub>)  $\delta/\text{ppm}$  = 17.5 (s)

IR (neat)  $\nu/\text{cm}^{-1}$  = 3047 (w), 3004 (w), 2961 (w), 2921 (w), 2830 (w), 2359 (m), 2343 (m), 1478 (sh), 1433 (s), 1352 (w), 1261 (w), 1259 (w), 1229 (sh), 1184 (m), 1097 (s), 1025 (w), 796 (m), 742 (s), 689 (vs), 610 (sh), 545 (m), 502 (vs), 405 (m).

HRMS (ESI, m/z) calculated for  $[\text{Au}(\text{dpptpa})]^+$  (**10** – Cl): 855.20807, found 855.22269 (1.7 ppm).

#### 1.2.4 [AuZn(**dpptpa**)Cl](NTf<sub>2</sub>)<sub>2</sub> (**7**)



**DPPTPA** (210 mg, 320  $\mu\text{mol}$ ) and Zn(NTf<sub>2</sub>)<sub>2</sub> (200 mg, 320  $\mu\text{mol}$ , 1.0 equiv.) was solved in DCM (4 mL) and thoroughly mixed. [Au(SMe<sub>2</sub>)Cl] (94 mg, 320  $\mu\text{mol}$ , 1.0 equiv.) was added as a solid and the mixture was stirred for 30 min. The solution was concentrated *in vacuo* to approximately 1 mL and further stirred until a white precipitate formed. The solvent was decanted, and the residue was washed with DCM (1 x 1 mL) and hexane (2 x 2 mL). All volatiles were removed *in vacuo* and the product **7** was obtained as a rose-white powder (425 mg, 280  $\mu\text{mol}$ , 88 %). Crystals suitable for SCXRD were grown from a cooled solution of **7** in THF.

<sup>1</sup>H NMR (400 MHz, THF-d<sub>8</sub>)  $\delta/\text{ppm}$  = 8.24 (m, 2H, CH<sub>arom</sub>), 7.92 (d, <sup>3</sup>J<sub>HH</sub> = 8.0 Hz, 2H, CH<sub>arom</sub>), 7.61 (m, 24H, CH<sub>arom</sub>), 6.74 (m, 2H, CH<sub>arom</sub>), 4.84 (d, <sup>2</sup>J<sub>HH</sub> = 16.9 Hz, 2H, CH<sub>2</sub>), 4.69 (d, <sup>2</sup>J<sub>HH</sub> = 16.9 Hz, 2H, CH<sub>2</sub>), 4.52 (s, 2H, CH<sub>2</sub>).

<sup>13</sup>C{<sup>1</sup>H} NMR (101 MHz, THF-d<sub>8</sub>)  $\delta/\text{ppm}$  = 159.6 (pt, J<sub>CP</sub> = 8 Hz), 155.6, 149.7 (pt, <sup>1</sup>J<sub>CP</sub> = 37 Hz), 147.5, 143.9, 142.2, 135.9 (pt, J<sub>CP</sub> = 8 Hz), 135.0 (pt, J<sub>CP</sub> = 7 Hz), 134.1, 134.0, 132.9 (pt, J<sub>CP</sub> = 7 Hz), 131.0 (pt, J<sub>CP</sub> = 6 Hz), 130.7 (pt, J<sub>CP</sub> = 6 Hz), 129.2, 126.7 (pt, <sup>1</sup>J<sub>CP</sub> = 32 Hz), 127.0 (pt, <sup>1</sup>J<sub>CP</sub> = 31 Hz), 125.9, 125.6, 121.1 (q, <sup>1</sup>J<sub>CF</sub> = 322 Hz), 60.9, 60.9.

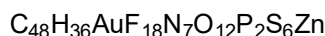
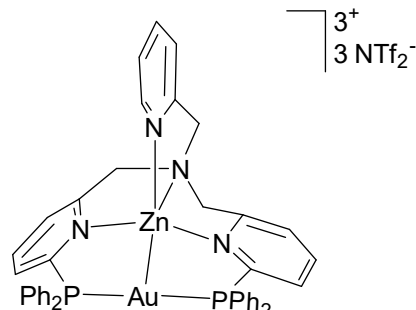
<sup>31</sup>P{<sup>1</sup>H} NMR (162 MHz, THF-d<sub>8</sub>)  $\delta/\text{ppm}$  = 58.2 (s).

IR (neat)  $\nu/\text{cm}^{-1}$  = 3077 (w), 3053 (w), 2363 (w), 1611 (w), 1592 (w), 1573 (w), 1559 (w), 1480 (w), 1435 (m), 1356 (m), 1334 (s), 1323 (s), 1177 (vs), 1127 (vs), 1055 (s), 1021 (sh), 997 (sh), 972 (sh), 964 (sh), 924 (sh), 898 (sh), 884 (sh), 786 (m), 772 (m), 762 (m), 746 (m), 738 (m), 729 (m), 713 (m), 689 (m), 645 (m), 616 (w), 593 (w), 580 (w), 569 (vs), 533 (s), 516 (s), 506 (vs), 490 (m), 475 (m), 463 (m), 442 (m), 427 (m), 403 (m).

HRMS (ESI, m/z) calculated for [AuZn(**dpptpa**)Cl](NTf<sub>2</sub>)<sup>+</sup> (**7** – NTf<sub>2</sub><sup>-</sup>) 1234.02283, found 1234.02594 (2.5 ppm).

CHN calculated for C<sub>46</sub>H<sub>36</sub>AuClF<sub>12</sub>N<sub>6</sub>O<sub>8</sub>P<sub>2</sub>S<sub>4</sub>Zn C: 36.4, H: 2.4, N: 5.5, found: C: 36.4 %, H: 2.5 %, N: 5.2 %.

### 1.2.5 [AuZn(**dpppta**)](NTf<sub>2</sub>)<sub>3</sub> (**8**)



Complex **7** (40 mg, 26 μmol, 1.0 equiv.) and AgNTf<sub>2</sub> (10 mg, 26 μmol, 1.0 equiv.) were suspended in DCM and thoroughly mixed. The precipitate (AgCl) was filtered off using glass wool. The product **8** was isolated as colourless needles by crystallisation via slow diffusion of Et<sub>2</sub>O into the solution (31 mg, 20 μmol, 77 %).

<sup>1</sup>H NMR (400 MHz, THF-d<sub>8</sub>) δ/ppm = 8.39 (tt, <sup>3</sup>J<sub>HH</sub> = 7.9 Hz, J = 1.7 Hz, 2H, CH<sub>arom</sub>), 8.05 (dt, <sup>3</sup>J<sub>HH</sub> = 8.1 Hz, J = 1.4 Hz, 2H, CH<sub>arom</sub>), 7.92 – 7.56 (m, 23H, CH<sub>arom</sub>), 7.52 (dd, <sup>3</sup>J<sub>HH</sub> = 8.0 Hz, J = 1.1 Hz, 1H, CH<sub>arom</sub>), 7.06 – 6.95 (m, 2H, CH<sub>arom</sub>), 4.93 (d, <sup>2</sup>J<sub>HH</sub> = 17.5 Hz, 2H, CH<sub>2</sub>), 4.79 (d, <sup>2</sup>J<sub>HH</sub> = 17.4 Hz, 2H, CH<sub>2</sub>), 4.55 (s, 2H, CH<sub>2</sub>).

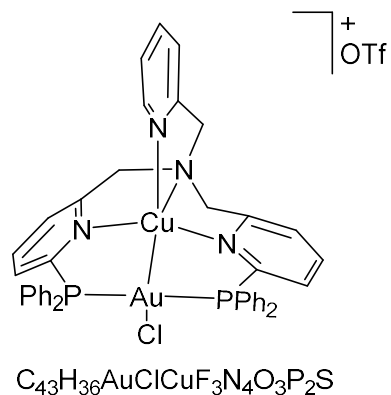
<sup>13</sup>C{<sup>1</sup>H} NMR (101 MHz, THF-d<sub>8</sub>) δ/ppm = 160.9 (pt, J<sub>CP</sub> = 7 Hz), 156.4, 149.4 (pt, <sup>1</sup>J<sub>CP</sub> = 40 Hz), 147.4, 145.2, 143.3, 135.4 (pt, J = 8 Hz), 135.3, 135.1, 133.7 (pt, J<sub>CP</sub> = 8 Hz), 132.3 (pt, J<sub>CP</sub> = 6 Hz), 131.3 (pt, J<sub>CP</sub> = 6 Hz), 130.1, 126.6, 126.4, 125.9, 124.6 (pt, <sup>1</sup>J<sub>CP</sub> = 29 Hz), 123.5 (t, <sup>1</sup>J<sub>CP</sub> = 29 Hz), 121.1 (q, <sup>1</sup>J<sub>CF</sub> = 322 Hz), 60.6, 60.5.

<sup>31</sup>P{<sup>1</sup>H} NMR (162 MHz, THF-d<sub>8</sub>) δ/ppm = 58.6 (s).

IR (neat) ν/cm<sup>-1</sup> = 3077 (w), 2961 (w), 1613 (w), 1595 (w), 1560 (w), 1483 (w), 1439 (m), 1347 (s), 1323 (m), 1176 (vs), 1101 (s), 1050 (vs), 1023 (m), 997, 972 (sh), 958 (sh), 895 (sh), 788 (m), 748 (m), 738 (m), 719 (m), 689 (m), 651 (m), 610 (s), 596 (m), 569 (s), 539 (m), 523 (m), 509 (s), 466 (m), 427 (m), 409 (m).

CHN calculated for C<sub>48</sub>H<sub>36</sub>AuF<sub>18</sub>N<sub>7</sub>O<sub>12</sub>P<sub>2</sub>S<sub>6</sub>Zn C: 32.7, H: 2.1, N: 5.6, found: C: 32.6 %, H: 2.4 %, N: 5.5 %.

### 1.2.6 [AuCu(dpptpa)Cl]OTf (11)



[Au(dpptpa)Cl] (**10**) (50 mg, 56  $\mu$ mol, 1.0 equiv) and [CuOTf]<sub>2</sub>·C<sub>6</sub>H<sub>6</sub> (14 mg, 28  $\mu$ mol, 0.5 equiv) were solved in DCM (0.95 mL), yielding a red-orange solution. The solution was crystallized with n-hexane (1.00 mL). The solution was decanted and the residue was dried in vacuo yielding **11** (38 mg, 34  $\mu$ mol, 61%). Crystals suitable for SCXRD were grown from a saturated solution of **11** in THF/DCM layered with n-hexane.

<sup>1</sup>H NMR (400 MHz, DCM-d<sub>2</sub>)  $\delta$ /ppm = 7.88 (t, <sup>3</sup>J<sub>HH</sub> = 7.7 Hz, 2H, CH<sub>Arom</sub>), 7.75 – 7.17 (m, 28H, CH<sub>Arom</sub>), 7.11 (d, <sup>3</sup>J<sub>HH</sub> = 7.8 Hz, 1H, CH<sub>Arom</sub>), 6.57 (d, <sup>3</sup>J<sub>HH</sub> = 5.1 Hz, 1H, CH<sub>Arom</sub>), 6.44 (t, <sup>3</sup>J<sub>HH</sub> = 6.3 Hz, 1H, CH<sub>Arom</sub>), 4.34 (d, <sup>2</sup>J<sub>HH</sub> = 16.4 Hz, 2H), 4.20 (d, <sup>2</sup>J<sub>HH</sub> = 16.4 Hz, 2H), 3.98 (s, 2H).

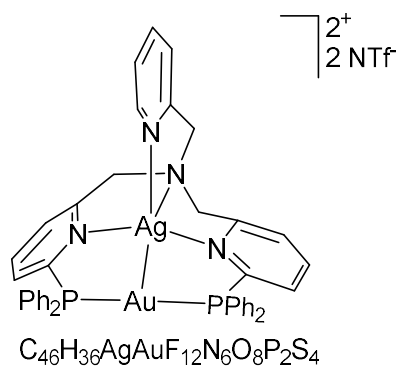
<sup>13</sup>C{<sup>1</sup>H} NMR (101 MHz, DCM-d<sub>2</sub>)  $\delta$ /ppm = 158.4 (pt, J<sub>CP</sub> = 7 Hz), 155.0, 152.7 (pt, <sup>1</sup>J<sub>CP</sub> = 37 Hz), 148.2, 138.4, 136.7, 134.6 (pt, J<sub>CP</sub> = 8 Hz), 133.3 (pt, J<sub>CP</sub> = 7 Hz), 132.3, 131.6, 129.4 (pt, J<sub>CP</sub> = 6 Hz), 129.3 (pt, J<sub>CP</sub> = 6 Hz), 128.7 (pt, <sup>1</sup>J<sub>CP</sub> = 26 Hz), 128.0 (pt, <sup>1</sup>J<sub>CP</sub> = 25 Hz), 126.0, 123.5, 123.4, 121.1 (q, <sup>1</sup>J<sub>CF</sub> = 322 Hz), 58.5, 58.1.

<sup>31</sup>P{<sup>1</sup>H} NMR (162 MHz, DCM-d<sub>2</sub>)  $\delta$ /ppm = 46.9 (s).

IR (neat)  $\nu$ /cm<sup>-1</sup> = 3056 (w), 2913 (w), 2844 (w), 1602 (w), 1583 (w), 1556 (w), 1480 (w), 1435 (s), 1403 (sh), 1261 (vs), 1221 (m), 1146 (m), 1100 (m), 1030 (vs), 997 (w), 970 (w), 895 (w), 877 (w), 749 (s), 691 (s), 661 (sh), 635 (vs), 570 (m), 563 (w), 546 (w), 509 (s), 490 (m), 462 (w).

CHN: calc for C<sub>43</sub>H<sub>36</sub>AuClCuF<sub>3</sub>N<sub>4</sub>O<sub>3</sub>P<sub>2</sub>S x 0.5 CH<sub>2</sub>Cl<sub>2</sub>: C 45.6, H 3.3, N 4.9, found: C 45.8, H 3.4, N 4.9.

### 1.2.7 [AuAg(dpptpa)](NTf<sub>2</sub>)<sub>2</sub> (**12**)



**10** (32 mg, 36 µmol) and AgNTf<sub>2</sub> (28 mg, 72 µmol, 2.0 equiv.) was suspended in DCM (2 mL) and thoroughly mixed. The formed AgCl was removed by filtration using glass wool. The solvent was removed *in vacuo*. The remaining solids were washed with Et<sub>2</sub>O and pentane (2 mL each) and dried *in vacuo*. **12** was obtained as a white powder (34 mg, 22 µmol, 62 %) Crystals suitable for SCXRD were grown from a saturated solution of **12** in CHCl<sub>3</sub> layered with benzene.

<sup>1</sup>H-NMR (400 MHz, THF d<sub>8</sub>)  $\delta$ /ppm = 8.03 (tt, <sup>3</sup>J<sub>HH</sub> = 7.8 Hz, J = 2.1 Hz, 2H, CH<sub>Arom</sub>), 7.95 – 7.62 (m, 23H, CH<sub>Arom</sub>), 7.46 – 7.37 (m, 3H, CH<sub>Arom</sub>), 7.24 – 7.14 (m, 2H, CH<sub>Arom</sub>), 4.07 (d, <sup>2</sup>J<sub>HH</sub> = 15.7 Hz, 2H, CH<sub>2</sub>), 4.02 (d, <sup>2</sup>J<sub>HH</sub> = 15.7 Hz, 2H, CH<sub>2</sub>), 3.94 (s, 2H, CH<sub>2</sub>).

<sup>13</sup>C{<sup>1</sup>H} NMR (101 MHz, THF d<sub>8</sub>)  $\delta$ /ppm = 160.8 (pt, J<sub>CP</sub> = 9 Hz), 157.7, 153.9 (pt, <sup>1</sup>J<sub>CP</sub> = 43 Hz), 151.6, 141.1 (pt, J<sub>CP</sub> = 3 Hz), 139.9, 136.3 (pt, J<sub>CP</sub> = 8 Hz), 135.5 (pt, J<sub>CP</sub> = 8 Hz), 134.5, 134.3, 131.4 (pt, J<sub>CP</sub> = 6 Hz), 131.2 (pt, J<sub>CP</sub> = 6 Hz), 130.9 (pt, J<sub>CP</sub> = 10 Hz), 128.1, 127.6 (pt, <sup>1</sup>J<sub>CP</sub> = 29 Hz), 126.5, 126.3 (pt, <sup>1</sup>J<sub>CP</sub> = 25 Hz), 124.9, 121.2 (q, <sup>1</sup>J<sub>CF</sub> = 322 Hz), 60.1, 59.0.

<sup>31</sup>P{<sup>1</sup>H} NMR (162 MHz, THF d<sub>8</sub>, 300 K)  $\delta$ /ppm = 47.3 (s).

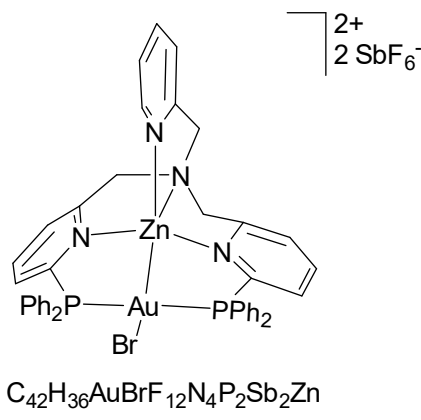
<sup>31</sup>P{<sup>1</sup>H} NMR (162 MHz, THF d<sub>8</sub>, 225 K)  $\delta$ /ppm = 47.2 (d, <sup>2</sup>J<sub>P,Ag</sub> = 3 Hz).

<sup>19</sup>F{<sup>1</sup>H} NMR (377 MHz, THF d<sub>8</sub>)  $\delta$ /ppm = -79.2 (s).

HRMS (ESI, m/z) calc for C<sub>44</sub>H<sub>36</sub>N<sub>5</sub>O<sub>4</sub>F<sub>6</sub>P<sub>2</sub>S<sub>2</sub>AgAu 1242.02991, found 1242.02699 (-2.35 ppm)

IR (neat, cm<sup>-1</sup>)  $\nu$ /cm<sup>-1</sup> = 3064 (w), 2847 (w), 1601 (w), 1585 (w), 1559 (w), 1482 (w), 1437 (m), 1346 (s), 1224 (sh), 1174 (vs), 1128 (s), 1101 (m), 1051 (s), 998 (sh), 920 (sh), 877 (w), 786 (w), 738 (w), 716 (m), 691 (m), 651 (w), 610 (s), 596 (s), 568(s), 505 (vs), 480 (m), 419 (w), 404 (s).

### 1.2.8 [AuZn(**dpptpa**)Br](SbF<sub>6</sub>)<sub>2</sub> (**17**)



**7** (9 mg, 6  $\mu$ mol, 1 mol%), AgSbF<sub>6</sub> (2 mg, 6  $\mu$ mol, 1 mol%) was suspended in DCM and the resulting solution was filtered through glass wool. This filtrate was added to a mixture of 1-octyne (619  $\mu$ mol, 1 equiv.), 2,6 dimethylaniline (619  $\mu$ mol, 1 equiv.) in a J Young NMR in DCM and heated to 40 °C for 2 h in a water bath. After one week, crystals grew in the Young NMR. After picking crystals suitable for SCXRD and HRMS the remaining solids were washed with hexane and THF and then dissolved in MeCN-d<sub>3</sub> for NMR analysis.

<sup>1</sup>H-NMR (400 MHz, MeCN-d<sub>3</sub>)  $\delta$ /ppm = 8.23 (tt, <sup>3</sup>J<sub>HH</sub> = 7.9 Hz, J = 1.6 Hz, 2H, CH<sub>Arom</sub>), 7.86 (d, <sup>3</sup>J<sub>HH</sub> = 7.9 Hz, 2H, CH<sub>Arom</sub>), 7.73 (m, 3H, CH<sub>Arom</sub>), 7.61 (m, 14H, CH<sub>Arom</sub>), 7.42 (m, 6H, CH<sub>Arom</sub>), 7.35 (d, <sup>3</sup>J<sub>HH</sub> = 8.0 Hz, 1H, CH<sub>Arom</sub>), 6.95 (d, <sup>3</sup>J<sub>HH</sub> = 5.4 Hz, 1H, CH<sub>Arom</sub>), 6.75 (m, 1H, CH<sub>Arom</sub>), 4.67 (d, <sup>2</sup>J<sub>HH</sub> = 17.2 Hz, 2H, CH<sub>2</sub>), 4.50 (d, <sup>2</sup>J<sub>HH</sub> = 17.2 Hz, 2H, CH<sub>2</sub>), 4.25 (s, 2H, CH<sub>2</sub>).

<sup>13</sup>C{<sup>1</sup>H} NMR (101 MHz, MeCN-d<sub>3</sub>) four C<sub>quart</sub> not observed,  $\delta$ /ppm = 159.1, 148.1, 144.3, 142.3, 135.4 (pt, J = 7 Hz), 134.6 (pt, J = 7 Hz), 134.4, 134.2, 132.7 (pt, J<sub>CP</sub> = 7 Hz), 131.0 (pt, J = 6 Hz), 130.6 (pt, J = 6 Hz), 128.8, 126.1, 125.7, 59.8, 59.7.

<sup>31</sup>P{<sup>1</sup>H} NMR (162 MHz, MeCN-d<sub>3</sub>)  $\delta$ /ppm = 63.5 (s).

HRMS, (ESI, m/z) calculated for [AuZn(**dpptpa**)Br](SbF<sub>6</sub>)<sup>+</sup> (M – SbF<sub>6</sub><sup>-</sup>) 1232.94925, found 1232.95207 (2.2 ppm); [AuZn(**dpptpa**)Br]<sup>2+</sup> (M - 2 SbF<sub>6</sub><sup>-</sup>) 499.02723, found 499.02804 (1.6 ppm)

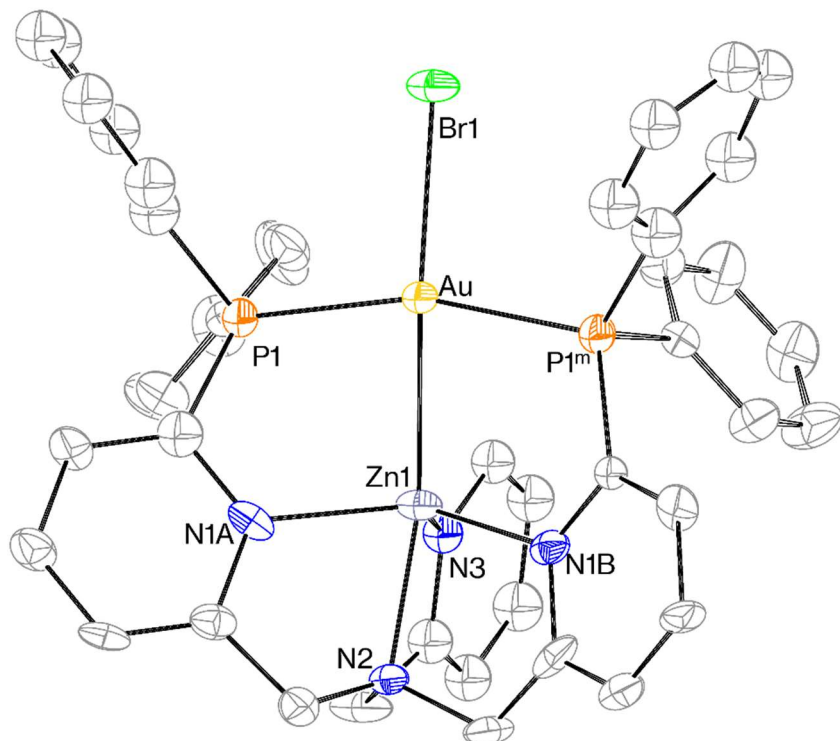


**Figure S3.** Displacement ellipsoid plot of **17** (50% probability, *Pnma*,  $Z = 4$ ). Two  $\text{SbF}_6$ -anions, one THF-molecule and H atoms have been omitted for clarity. The molecule resides on the mirror plane causing a static disorder of the pyridyl rings which is not shown for clarity. Symmetry operator  $m$ :  $x$ ,  $0.5-y$ ,  $z$ . Crystal data for **17** x THF :  $\text{C}_{46}\text{H}_{44}\text{AuBrF}_{12}\text{N}_4\text{OP}_2\text{Sb}_2\text{Zn}$ ,  $M = 1544.54 \text{ g mol}^{-1}$ , orthorhombic, space group *Pnma*,  $a = 34.469(7) \text{ \AA}$ ,  $b = 13.371(3) \text{ \AA}$ ,  $c = 11.347(2) \text{ \AA}$ ,  $V = 5229.7(18) \text{ \AA}^3$ ,  $Z = 4$ ,  $T = 250(2) \text{ K}$ ,  $\mu(\text{Mo}-\text{K}\alpha) = 5.179 \text{ mm}^{-1}$ , collected/unique reflections 53385 / 6782,  $R_1 = 0.0600$ ,  $wR_{2\sigma} = 0.1210$ ,  $GOF = 1.157$  Selected bond lengths ( $\text{\AA}$ ) and angles ( $^\circ$ ): Au-Zn = 2.5998(14), Au-P1 = 2.309(2), P-Au-P = 162.49(11)

The crystal structure of compound **17** we report here was measured at a temperature of 250 K. This discrepancy to the other structures was deliberately chosen as single crystals of **17** undergo a gradual low temperature phase transition. At room temperature the space group is quite unambiguously *Pnma* with distinct systematic absences for the three  $21$  axes as well as the two glide planes (Table S2). A measurement at 100 K was performed as well, and the data shows signs of pseudo-symmetry. Two of the three screw axes as well as the  $n$  glide plane display significant intensities for reflections which should be absent for a structure in *Pnma*, but they are still too weak for the symmetry element to be clearly absent. Consequently, the structure refinement yields highly unsatisfactory results in both *Pnma* as well as its subgroups with large residual electron density maxima, unreasonable anisotropic displacement parameters as well as bad agreement factors. Thus, we decided to report the dataset measured at 250 K. Pseudo-symmetry occurs quite frequently for structures with heavy atoms as they cause pseudo extinctions when they are close to potential special positions.<sup>7</sup> In the structure of **17** all of the atoms that are heavier than phosphorus are located on the mirror plane of *Pnma*.

**Table S2.** Ratio between intensities in agreement ( $I_{\text{true}}$ ) and those not matching ( $I_{\text{false}}$ ) with the reflection condition for the SCXRD measurements of **17** at 100 K and 250 K.

	$I_{\text{true}} / I_{\text{false}}$ (100 K)	$I_{\text{true}} / I_{\text{false}}$ (250 K)
$2_1 \parallel a$ ( $h00 \ h \neq 2n$ )	5.4	10.5
$2_1 \parallel b$ ( $0k0 \ h \neq 2n$ )	3.7	16.9
$2_1 \parallel c$ ( $00l \ h \neq 2n$ )	17.9	22.7
$n \perp a$ ( $0kl \ k+l \neq 2n$ )	3.3	7.4
$a \perp c$ ( $hk0 \ h \neq 2n$ )	19.1	30.4

## 2 Determination of Lewis acidity

- a) **8** (11  $\mu\text{mol}$ ) was dissolved in DCM-d<sub>2</sub> (0.6 mL) and added to triphenylphosphine oxide (3.1 mg, 11  $\mu\text{mol}$ ) in a J Young NMR tube.
- b) **10** (10 mg, 11  $\mu\text{mol}$ ) and AgNTf<sub>2</sub> (8.7 mg, 22  $\mu\text{mol}$ , 2 equiv.) were mixed in DCM-d<sub>2</sub> and filtered through glass wool. The solution was added together with triphenylphosphine oxide (3.1 mg, 11  $\mu\text{mol}$ ) to a J Young NMR tube.
- c) **12** (12 mg, 11  $\mu\text{mol}$ ) was mixed with AgOTf (2.8 mg, 11  $\mu\text{mol}$ , 1 equiv.) in DCM-d<sub>2</sub> and filtered through glass wool. The solution was added together with triphenylphosphine oxide (3.1 mg, 11  $\mu\text{mol}$ ) to a J Young NMR tube.
- d) **1** (9.2 mg, 11  $\mu\text{mol}$ ) was mixed with AgNTf<sub>2</sub> (4.4 mg, 11  $\mu\text{mol}$ , 1 equiv.) in DCM-d<sub>2</sub> and filtered through glass wool. The solution was added together with triphenylphosphine oxide (3.1 mg, 11  $\mu\text{mol}$ ) to a J Young NMR tube.

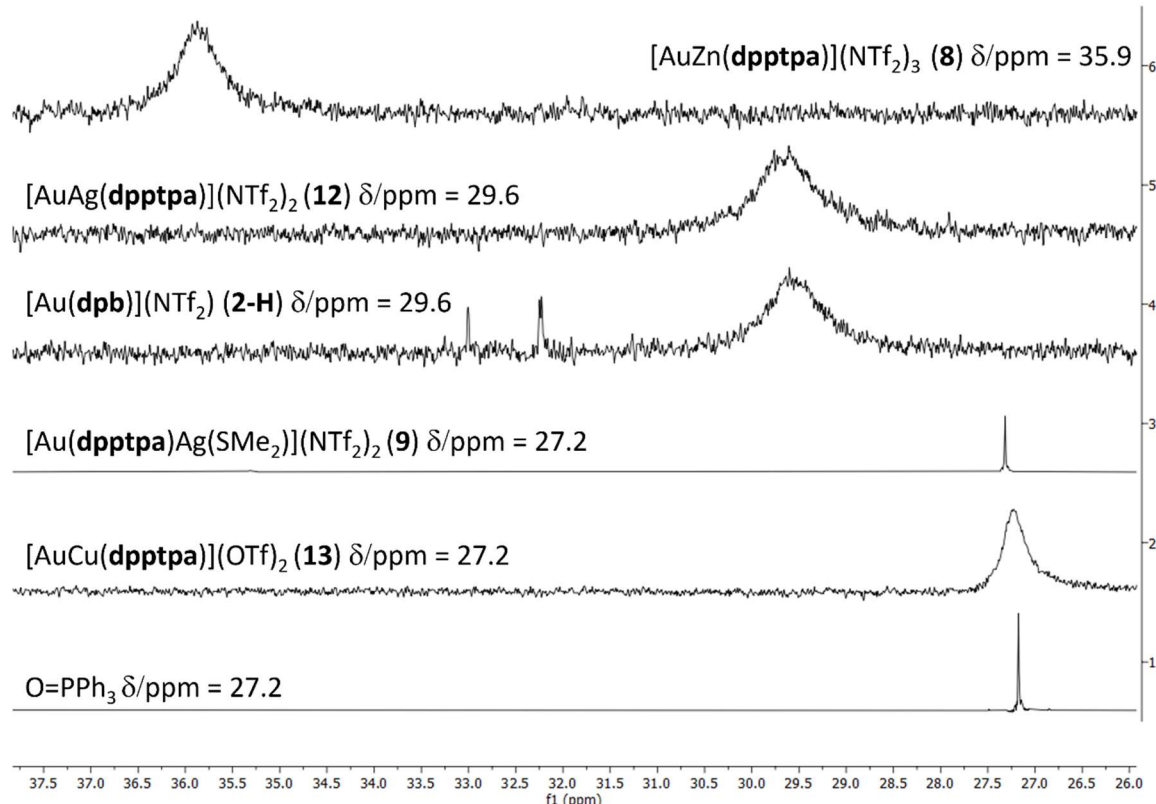


**Figure S4** <sup>31</sup>P-NMR spectra of the Gutmann-Beckett analysis for Lewis acidity.  $\delta/\text{ppm}$  specifies the chemical shift of triphenylphosphine oxide.

### 3 Single crystal X-ray diffraction analyses

For the intensity data collections summarized in Table S3 the following three instruments were used:

(a): A Bruker D8 goniometer equipped with an APEX CCD area detector and an Incoatec microsource (Mo-K $\alpha$  radiation,  $\lambda = 0.71073 \text{ \AA}$ , multilayer optics) at 100(2) K (Oxford Cryostream 700 instrument, Oxfordshire, UK). Data were integrated with SAINT<sup>8</sup> and corrected for absorption by multi-scan methods with SADABS.<sup>9</sup>

(b): A STOE STADIVARI goniometer equipped with a Dectris Pilatus 200K area detector and a GeniX 3D HF Cu-K $\alpha$  microsource (Mo-K $\alpha$  radiation,  $\lambda = 0.71073 \text{ \AA}$ , multilayer optics) at 100(2) K (Oxford Cryostream 800 instrument, Oxfordshire, UK). Data were integrated with X-Area26 and corrected for absorption by multi-scan methods with LANA.<sup>10</sup>

All structures were solved by intrinsic phasing<sup>11</sup> and refined by full matrix least squares procedures based on  $F^2$ , as implemented in SHELXL-18.<sup>12</sup> Hydrogen atoms were treated as riding with C–H = 0.98  $\text{\AA}$  for CH<sub>3</sub> groups, C–H = 0.95  $\text{\AA}$  for aryl-hydrogen and C–H = 1.00  $\text{\AA}$  for alkyl-hydrogen bonds. Their isotropic displacement parameters were constrained to  $U_{\text{iso}}(\text{H}) = 1.5 U_{\text{eq}}(\text{C})$  for methyl groups and acidic protons or  $U_{\text{iso}}(\text{H}) = 1.2 U_{\text{eq}}(\text{C})$  otherwise.

These data can be obtained free of charge from The Cambridge Crystallographic Data Centre via [www.ccdc.cam.ac.uk/data\\_request/cif](http://www.ccdc.cam.ac.uk/data_request/cif). The presentation of crystal structures was done with Mercury 3.9<sup>13</sup> or Platon.<sup>14-16</sup>

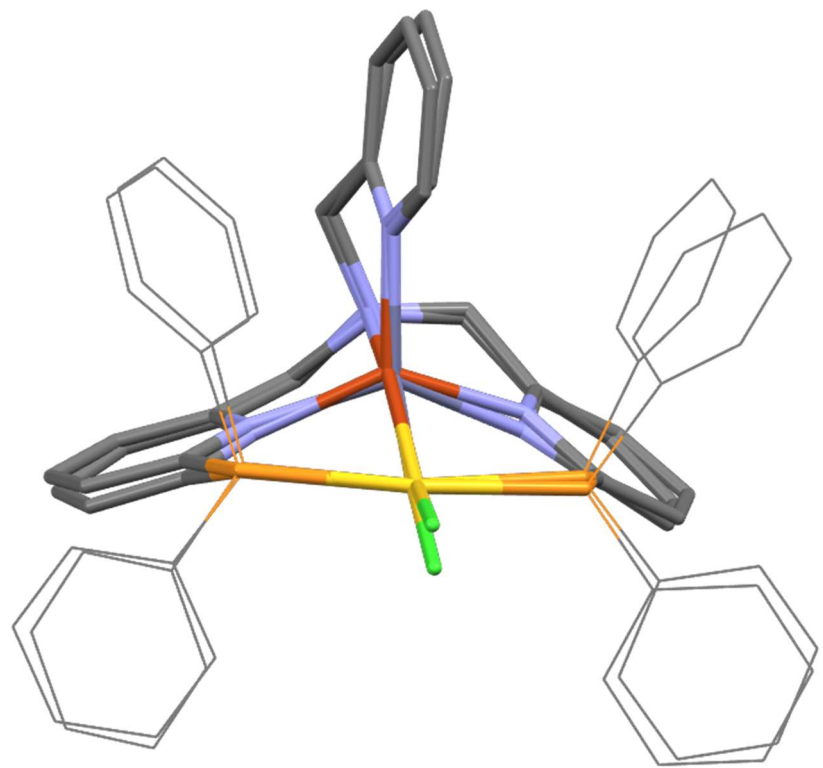


**Figure S5** Overlay of the solid state structures of complexes **7** and **11**.

**Table S3.** Crystal data and structure refinement for **6–9**, **11**, **12** and **17**.

	<b>9</b>	<b>7</b>	<b>8</b>	<b>11</b>	<b>12</b>	<b>17</b>	<b>6</b>
CCDC	2245006	2245003	2245000	2245002	2245008	2244998	2244990
Device	Bruker APEX CCD	Bruker APEX CCD	Stoe Stadivari	Bruker APEX CCD	Bruker APEX CCD	Bruker APEX CCD	Bruker APEX CCD
$\lambda$ [Å]	0.71073	0.71073	0.71073	0.71073	0.71073	0.71073	0.71073
Empirical formula	C <sub>52</sub> H <sub>52</sub> AgAuF <sub>12</sub> N <sub>6</sub> O <sub>8</sub> P <sub>2</sub> S <sub>5</sub>	C <sub>54</sub> H <sub>52</sub> AuClF <sub>12</sub> N <sub>6</sub> O <sub>10</sub> P <sub>2</sub> S <sub>4</sub> Zn	C <sub>49</sub> H <sub>38</sub> AuCl <sub>2</sub> F <sub>18</sub> N <sub>7</sub> O <sub>12</sub> P <sub>2</sub> S <sub>6</sub> Zn	C <sub>47</sub> H <sub>44</sub> AuClCuF <sub>3</sub> N <sub>4</sub> O <sub>4</sub> P <sub>2</sub> S	C <sub>55</sub> H <sub>46</sub> AgAuF <sub>12</sub> N <sub>6</sub> O <sub>8</sub> P <sub>2</sub> S <sub>4</sub>	C <sub>46</sub> H <sub>44</sub> AuBrF <sub>12</sub> N <sub>4</sub> O P <sub>2</sub> Sb <sub>2</sub> Zn	C <sub>47</sub> H <sub>40</sub> F <sub>12</sub> N <sub>6</sub> O <sub>9</sub> P <sub>2</sub> S <sub>4</sub> Zn
M <sub>w</sub> [g mol <sup>-1</sup> ]	1644.07	1660.98	1846.40	1175.82	1640.98	1544.54	1316.40
T [K]	100(2)	100(2)	100(2)	100(2)	100(2)	250(2)	100(2)
Crystal system	Triclinic	Orthorhombic	Monoclinic	Orthorhombic	Orthorhombic	Orthorhombic	Triclinic
Space group	P-1	Pnma	P2 <sub>1</sub>	Pnma	Pbca	Pnma	P-1
<i>a</i> [Å]	14.1986(13)	11.1687(15)	14.81742(16)	27.215(3)	16.5099(14)	34.469(7)	12.6499(18)
<i>b</i> [Å]	15.7612(15)	16.198(2)	17.2560(2)	15.3259(19)	26.641(3)	13.371(3)	14.203(3)
<i>c</i> [Å]	15.7808(15)	34.695(5)	25.0836(3)	11.2478(14)	27.507(3)	11.347(2)	16.800(3)
$\alpha$ [°]	96.576(2)	90	90	90	90	90	77.885(3)
$\beta$ [°]	108.838(2)	90	95.1264(9)	90	90	90	75.560(3)
$\gamma$ [°]	107.971(2)	90	90	90	90	90	77.008(3)
V [Å <sup>3</sup> ]	3088.0(5)	6276.7(14)	6387.96(13)	4691.3(10)	12099(2)	5229.7(18)	2810.1(9)
Z	2	4	4	4	8	4	2
$\rho_{\text{calc}}$ [g cm <sup>-3</sup> ]	1.768	1.758	1.920	1.665	1.802	1.962	1.556
$\mu$ [mm <sup>-1</sup> ]	3.0030	3.040	3.116	3.806	3.033	5.179	0.740
F(000)	1628	3304	3632	2336	6472	2960	1336
Crystal size [mm <sup>3</sup> ]	0.28x0.25x0.23	0.34x0.22x0.10	0.10x0.10x0.10	0.50x0.25x0.20	0.28x0.24x0.14	0.07x0.07x0.07	0.29x0.27x0.21
$\theta$ range [°]	1.398 to 30.873	1.174 to 30.330	1.939 to 39.394	1.496 to 30.725	1.481 to 31.126	1.889 to 28.330	1.794 to 25.348
Index ranges	-20 > <i>h</i> > 20 -22 > <i>k</i> > 22 -22 > <i>l</i> > 22	-15 > <i>h</i> > 13 -22 > <i>k</i> > 20 -49 > <i>l</i> > 49	-25 > <i>h</i> > 26 -30 > <i>k</i> > 29 -44 > <i>l</i> > 21	-37 > <i>h</i> > 38 -21 > <i>k</i> > 21 -15 > <i>l</i> > 16	-23 > <i>h</i> > 23 -38 > <i>k</i> > 38 -39 > <i>l</i> > 39	-45 > <i>h</i> > 45 -17 > <i>k</i> > 17 -15 > <i>l</i> > 15	-15 > <i>h</i> > 15 -17 > <i>k</i> > 17 -20 > <i>l</i> > 20
refl. collected	61181	74553	575018	69650	398068	53385	31734
independent reflections	18445 [R <sub>int</sub> = 0.0910]	9268 [R <sub>int</sub> = 0.1302]	70166 [R <sub>int</sub> = 0.0661]	7419 [R <sub>int</sub> = 0.1026]	19214 [R <sub>int</sub> = 0.1243]	6782 [R <sub>int</sub> = 0.0816]	10297 [R <sub>int</sub> = 0.0639]
data/restraints/parameters	18445/0/750	9268/216/637	70166/1818/1965	7419/203/471	19214/57/893	6782/60/332	10297/911/414
GOF	1.046	1.067	0.941	1.051	1.082	1.157	1.041
final R indices [I > 2σ]	R <sub>1</sub> = 0.0478 wR <sub>2</sub> = 0.1031	R <sub>1</sub> = 0.0552 wR <sub>2</sub> = 0.1221	R <sub>1</sub> = 0.0354 wR <sub>2</sub> = 0.0630	R <sub>1</sub> = 0.0441 wR <sub>2</sub> = 0.1028	R <sub>1</sub> = 0.0389 wR <sub>2</sub> = 0.0863	R <sub>1</sub> = 0.0600 wR <sub>2</sub> = 0.1210	R <sub>1</sub> = 0.0835 wR <sub>2</sub> = 0.2250
final R indices [all data]	R <sub>1</sub> = 0.0674 wR <sub>2</sub> = 0.0674	R <sub>1</sub> = 0.0782 wR <sub>2</sub> = 0.1302	R <sub>1</sub> = 0.0587 wR <sub>2</sub> = 0.0681	R <sub>1</sub> = 0.0559 wR <sub>2</sub> = 0.1070	R <sub>1</sub> = 0.0544 wR <sub>2</sub> = 0.0947	R <sub>1</sub> = 0.0863 wR <sub>2</sub> = 0.1301	R <sub>1</sub> = 0.1323 wR <sub>2</sub> = 0.2667
largest diff. peak/hole [e/Å]	2.008/-1.717	2.409/-3.194	1.472/-1.275	1.173/-1.808	2.171/-1.190	1.587/-1.080	1.166/-1.117
SQUEEZE	Solvent accessible void: 375 Å, e <sup>-</sup> -count 94, good agreement with Et <sub>2</sub> O	-	-	-	-	-	-

#### 4 Overview of known Au complexes featuring a short Au–M distances

The CCDC<sup>17</sup> was searched on February 27<sup>th</sup> 2023 for structures featuring an Au-M (M= Cu, Ag, Zn) or Au-Cl bond. The found heterometallic complexes are displayed in Figure S6 (Au-Ag bond) and Figure S7 (Au-Cu bond). Representative L<sub>2</sub>AuCl-complexes are shown in Figure S8.

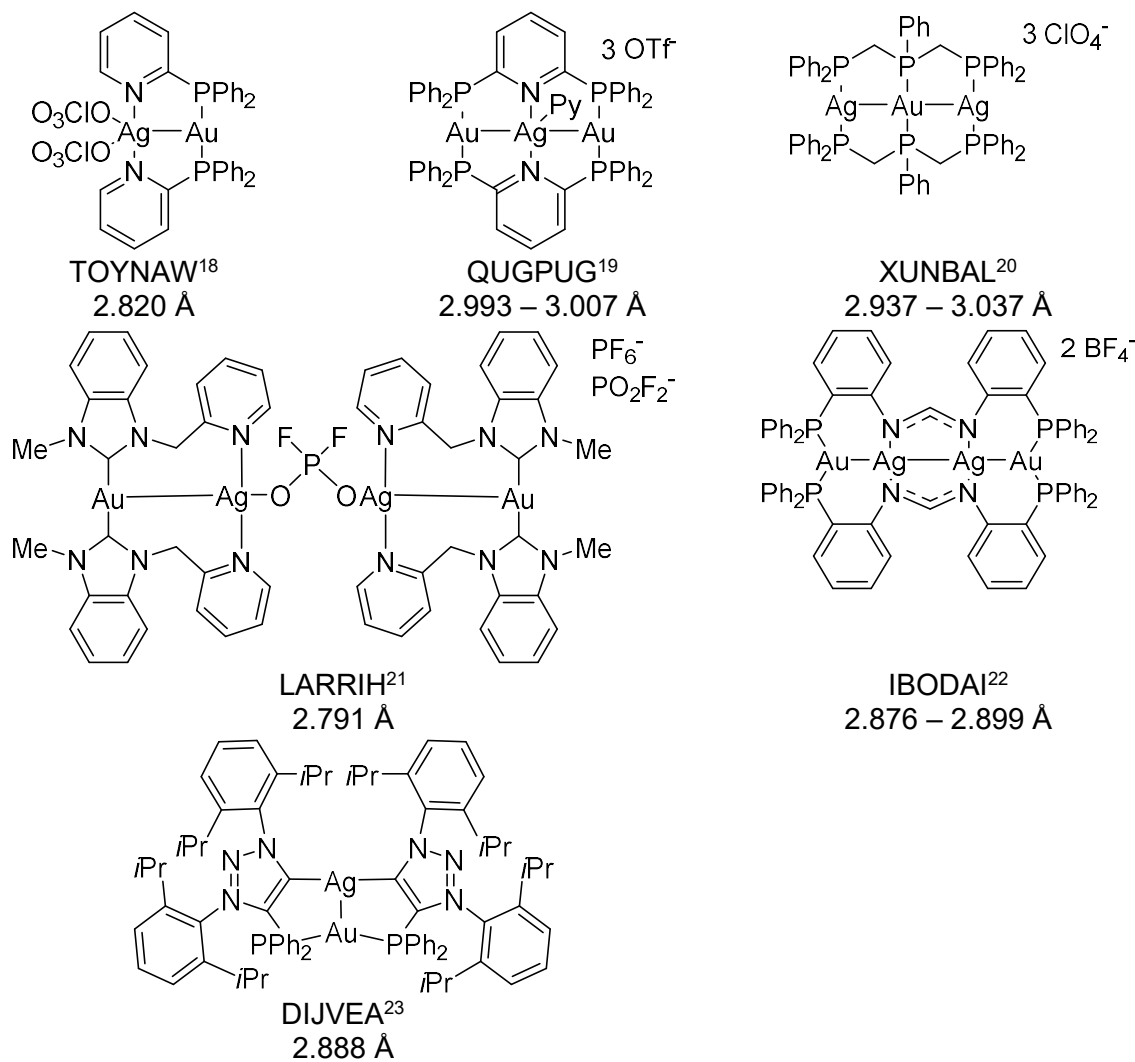


**Figure S6** Selected examples of heterobimetallic Au/Ag-complexes featuring a short Au-Ag-bond. The given distance specifies the Au/Ag distance.

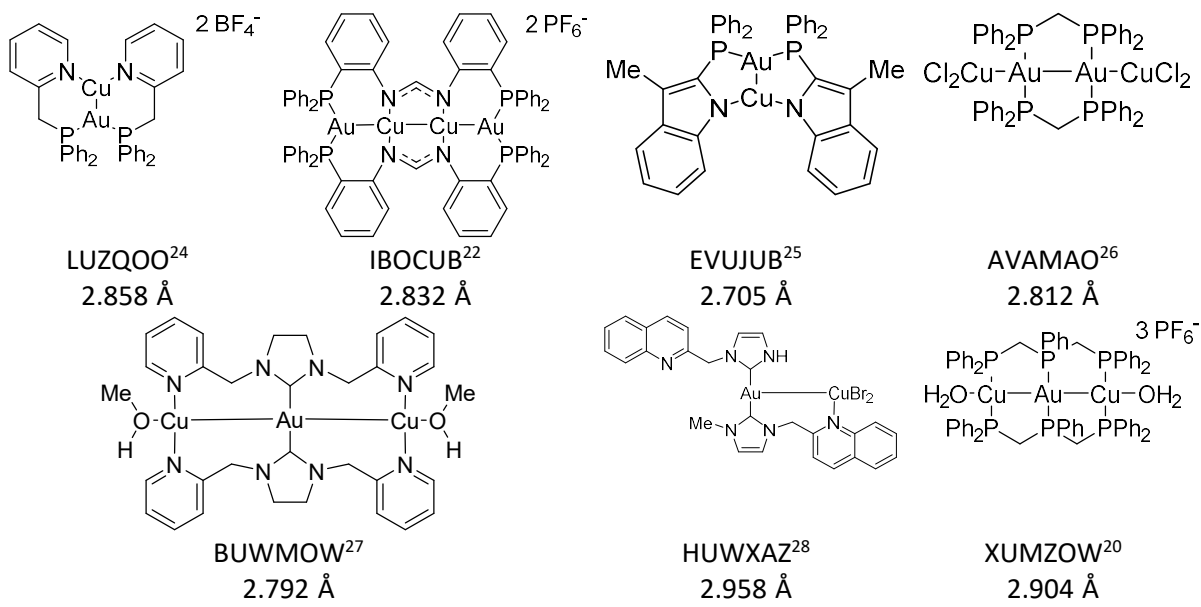


**Figure S7** Selected examples of heterobimetallic Au/Cu-complexes featuring a short Au-Cu-bond. The given distance specifies the Au/Cu distance.

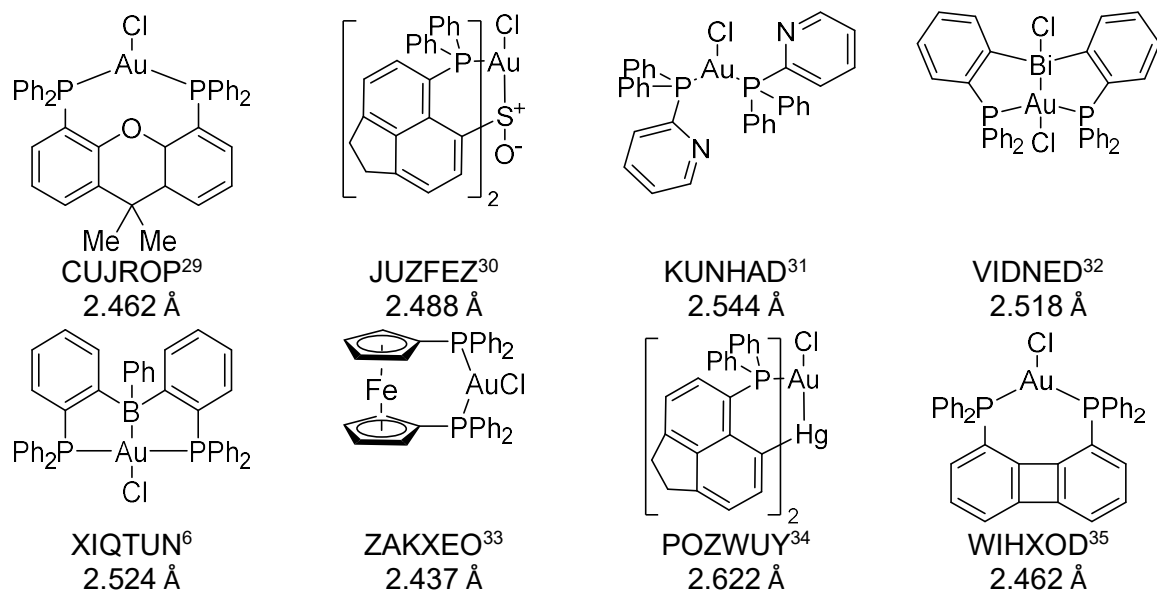


**Figure S8** Selected examples of Au-complexes featuring an Au-Cl-bond. The given distance specifies the Au/Cl distance.

## 5 Computational studies

Geometry optimizations were carried out without any symmetry restrictions. The minimum on the potential energy surface was confirmed by the absence of an imaginary frequency in the vibrational spectrum. Geometry optimizations and frequency analysis were performed using the Gaussian 16 suite of programs (Rev. C.01).<sup>36</sup> The xyz-coordinates from the solid-state structures of complexes **7**, **9**, **11**, **12** and **17** without coordinating solvent and NTf<sub>2</sub>-anion were used as the starting point for structure optimization utilizing the BP86<sup>37, 38</sup> functional, the def2-SV(P)<sup>39, 40</sup> basis set and effective core potentials (SDD)<sup>41-43</sup> for Au, Cu, Zn and Ag. This optimization reproduced the solid state structures well, however, the intermetallic distances were generally too long (ca. 0.1 Å). The optimized structures were used as the starting point for a subsequent structural optimization using the PBE functional,<sup>44-46</sup> the def2-TZVP<sup>47, 48</sup> basis set and effective core potentials (SDD) for Au, Cu, Zn and Ag. Additionally, the BP86 optimized structures of **11** was used to model complex [(dpptpa)CuAu]<sup>2+</sup> (**13**), which was structurally optimised employing PBE/def2-TZVP/SDD. Except for Ag-complexes **9** and **12** intermetallic distances showed a deviation of < 0.04 Å in the calculations from the solid-state.

NBO/NLMO calculations were performed on the PBE/def2-TZVP/SDD level using NBO 7.0<sup>49</sup> / Gaussian 16 Rev. C.01. For all complexes five occupied d-type lone pairs (LP) were found in the valence shell of Au and the respective metalloligand, which is in line with the expected d<sup>10</sup>-configuration of Cu<sup>+</sup>, Zn<sup>2+</sup>, Ag<sup>+</sup> and Au<sup>+</sup>. For all complexes the Au–P bonds were described by a polarized Au–P bond constructed from the Au s-type orbital and the P sp<sup>3</sup>-type orbital and an interaction of the second phosphine LP with the σ\*(Au,P) bond. The Au–M bond is formed by donation of an occupied d-type Au LP to an unoccupied (LV) s-type orbital at the respective metalloligand. Additionally, the LP of the free phosphine as well as the Au–P bond donate electrons into the LV at the metalloligand. The chloride ligand is described as a chloride which donates electrons into the σ\*(Au,P)-bond and the s-type LV of the metalloligand. Detailed results are summarized in Table S4. The NBOs and NLMOs relevant to the Au–M bond are depicted in Figure S9 using complex **7** as a representative example.

**Table S4.** Summary of the structural optimization and NBO/NLMO analysis of heterobimetallic Au complexes.

Complex	M	d(Au,M) XRD [Å]	d(Au,M) DFT [Å]	$\Delta$ d(Au,M) [Å]	WBI Au–M	$\Delta E$ (Au→M) [kcal/mol]	$\Delta E$ (P→M) [kcal/mol]	$\Delta E$ (Au–P→M) [kcal/mol]	$\Delta E$ (X→M) [kcal/mol]	NLMO % Au	NLMO % M
<b>7</b>	Zn	2.608	2.571	-0.037	0.2119	62.61	18.22	50.10	26.46 (Cl)	89.4	7.0
<b>17</b>	Zn	2.600	2.579	-0.021	0.1980	57.89	16.46	44.36	34.36 (Br)	90.9	5.6
<b>8</b>	Zn	2.649	2.690	0.041	0.1448	31.39	14.6	11.22	-	95.9	2.6
<b>11</b>	Cu	2.830	2.735	0.022	0.1133	23.57	4.86	21.95	7.54 (Cl)	94.0	2.1
<b>13</b>	Cu	-	2.738	-	0.0815	11.48	3.70	5.83	-	98.1	1.0
<b>9</b>	Ag	2.899	3.047	0.148	0.0489	5.39	2.01	1.88	-	98.6	0.5
<b>12</b>	Ag	2.768	2.846	0.078	0.0947	13.28	3.32	7.05	-	97.8	1.1

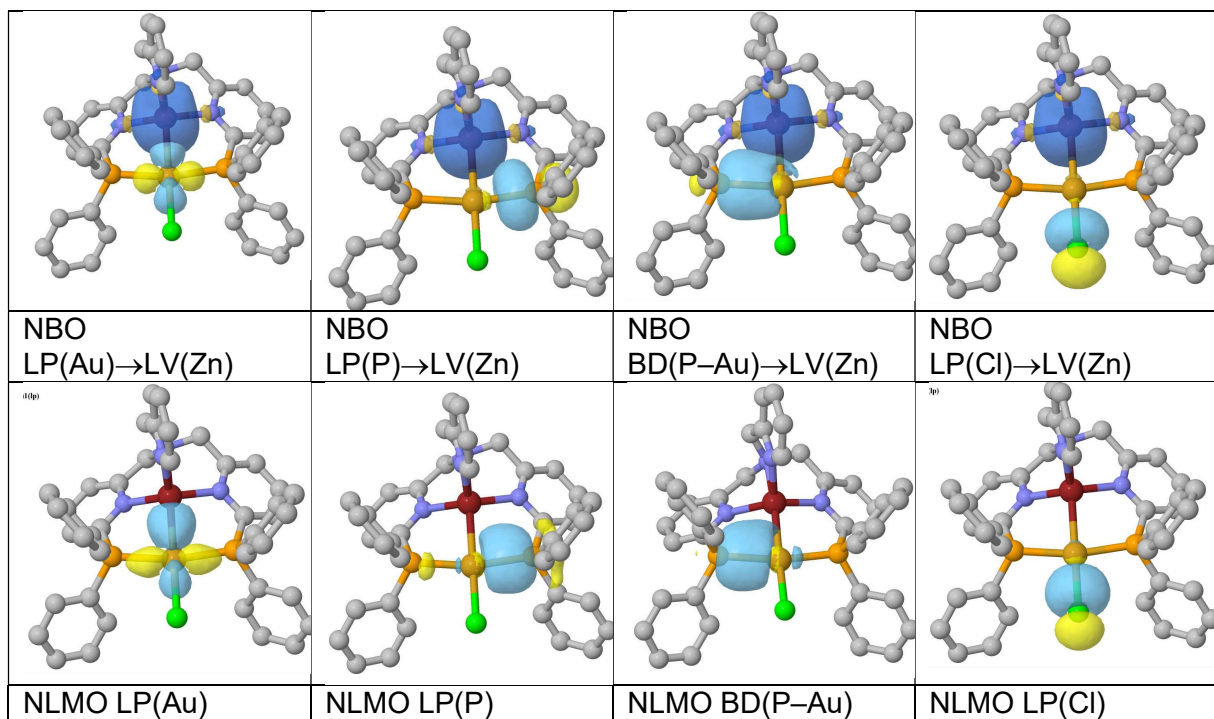
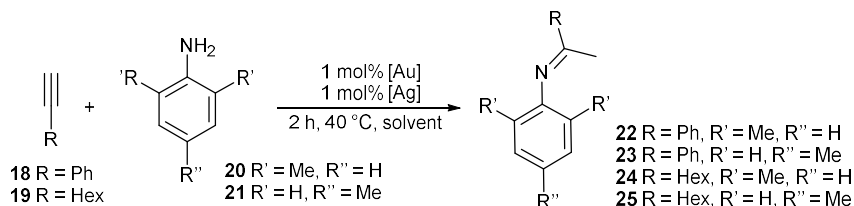


**Figure S9.** Graphical representation of NBOs and NLMOs relevant to the Au–Zn bond in complex **7**.

## 6 Catalytic experiments

### 6.1 Hydroamination of alkynes



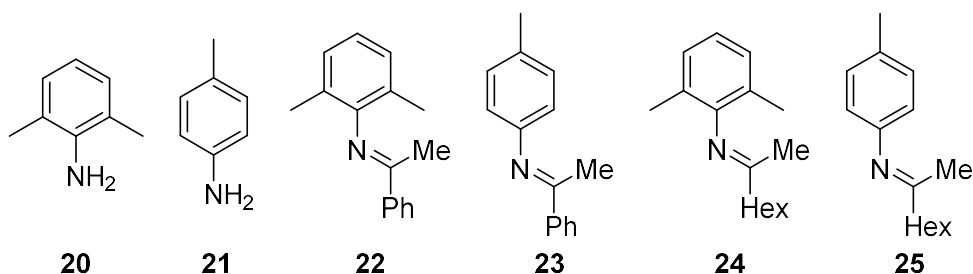
In a glovebox a stock solution of alkyne (1.54 mM), aniline (1.54 mM) and internal standard hexamethyldisiloxane HDMSO (12.5 mg) was prepared with the given solvent in a 1 mL volumetric flask.

The catalyst solutions were prepared in another volumetric flask. For this purpose

- a) **7** or **11** (6  $\mu\text{mol}$ , 1 mol%) and an Ag-salt ( $\text{OTf}^-$ ,  $\text{SbF}_6^-$ ,  $\text{NTf}_2^-$ ) (6  $\mu\text{mol}$ , 1 mol%) were dissolved in 0.2 mL solvent and filtered through glass wool.
- b) **10** (6  $\mu\text{mol}$ , 1 mol%) and  $\text{AgNTf}_2$  (12  $\mu\text{mol}$ , 2 mol%) dissolved in 0.2 mL solvent and filtered through glass wool.
- c) **9** or **8** (6  $\mu\text{mol}$ , 1 mol%) dissolved in 0.2 mL solvent.

0.4 mL of the substrate solution (corresponding to 619  $\mu\text{mol}$ , 1 equiv. of alkyne and aniline and 5 mg HDMSO) was mixed with the catalyst solution in a J Young NMR tube. The tube was sealed and put into a preheated water bath for 1-2 h.

Afterwards the solution was analysed with NMR spectroscopy and the substrates and products were quantified using the following signals: HMDSO:  $\delta = 0.21$  ppm (s, 18 H); **20**:  $\delta = 2.21$  ppm (s, 6 H), **21**:  $\delta = 3.60$  ppm (s, 2 H), **22**:  $\delta = 2.16$  ppm (m, 9 H), **23**:  $\delta = 2.43$  ppm (s, 3 H), **24**:  $\delta = 2.05$  ppm (s, 6 H); **25**:  $\delta = 2.32$  ppm (s, 3 H).



All compounds are known and  $^1\text{H}$  NMR peaks were assigned according to literature:

**20**<sup>50</sup>, **21**<sup>51</sup>, **22**<sup>52</sup>, **23**<sup>53</sup>, **24**<sup>54</sup>, **25**<sup>55</sup>

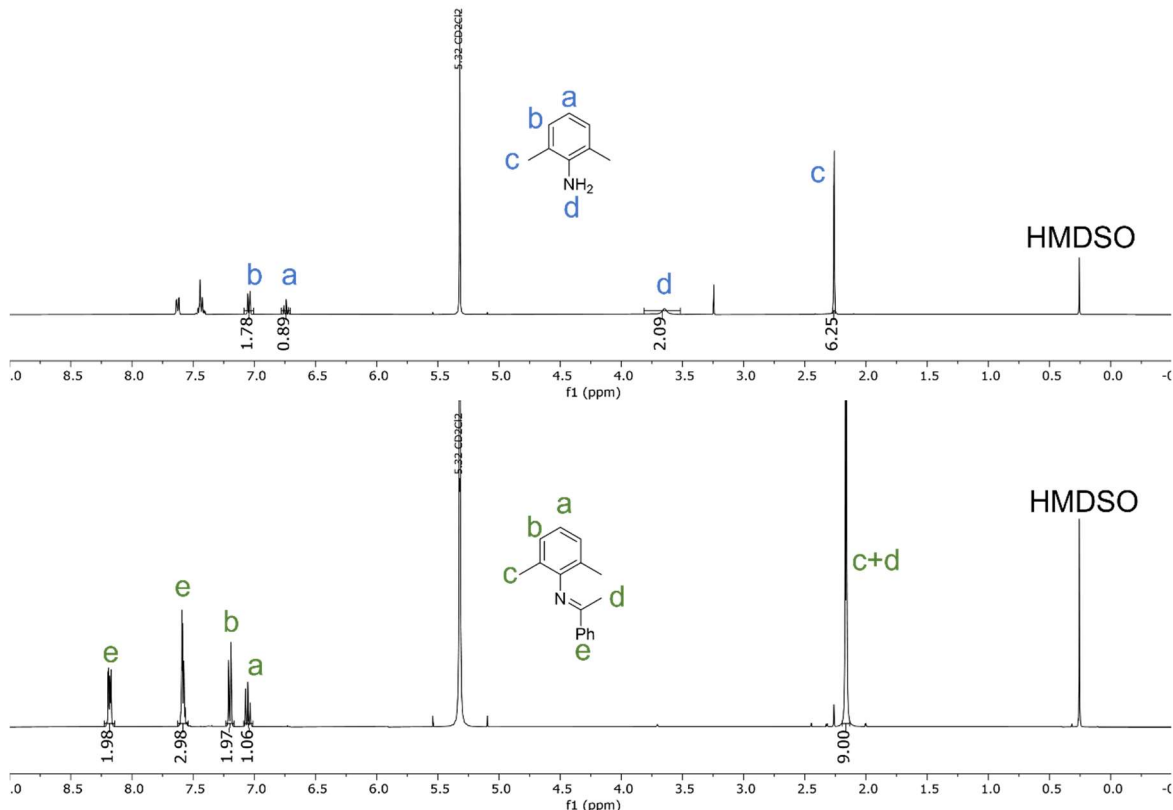


**Figure S10.** Top: Assigned <sup>1</sup>H-NMR spectrum of 2,6-dimethylaniline and phenylacetylene prior to reaction. Bottom: Assigned <sup>1</sup>H-NMR spectrum after completed reaction.

**Table S5.** Integrals and calculated conversion/NMR yield for the reaction of phenylacetylene (**18**) with 2,6-dimethylaniline (**20**) yielding **22** (Table 2, entries 1 – 6).

Entry	n <sub>0</sub> (HMDSO) [μmol] <sup>a</sup>	Integral HMDSO	n <sub>0</sub> ( <b>20</b> ) [μmol] <sup>a</sup>	Reaction completed				Conv. [%]	Yield [%]
				Integral <b>20</b>	Integral <b>22</b>	n <sub>t</sub> ( <b>20</b> ) [μmol]	n <sub>t</sub> ( <b>22</b> ) [μmol]		
1	46	18	622	0.7	123.0	17	627	97	101
2	46	18	622	0.7	119.7	17	610	97	98
3	34	18	617	108.4	0.0	612	0	1	0
4	34	18	617	107.1	0.0	605	0	2	0
5	35	18	622	104.2	0.0	615	0	1	0
6	33	18	628	115.2	0.0	627	0	0	0

<sup>a</sup> Based on weighed sample.

Integrals were determined relative to HMDSO (Integral set to 18). c (**20**) (6 Hs) and c+d (**22**) (9 Hs) were used for the calculations.

Equations used for quantification of substrate and product:

$$n_t(\text{Aniline}) = \frac{\text{Integral}(\text{20})}{6} \times n(\text{HMDSO}) \quad n_t(\text{Product}) = \frac{\text{Integral}(\text{22})}{9} \times n(\text{HMDSO})$$

$$\text{Conv.} = 1 - \frac{n_t(\text{20})}{n_0(\text{20})} \quad \text{Yield} = \frac{n_t(\text{22})}{n_0(\text{20})}$$

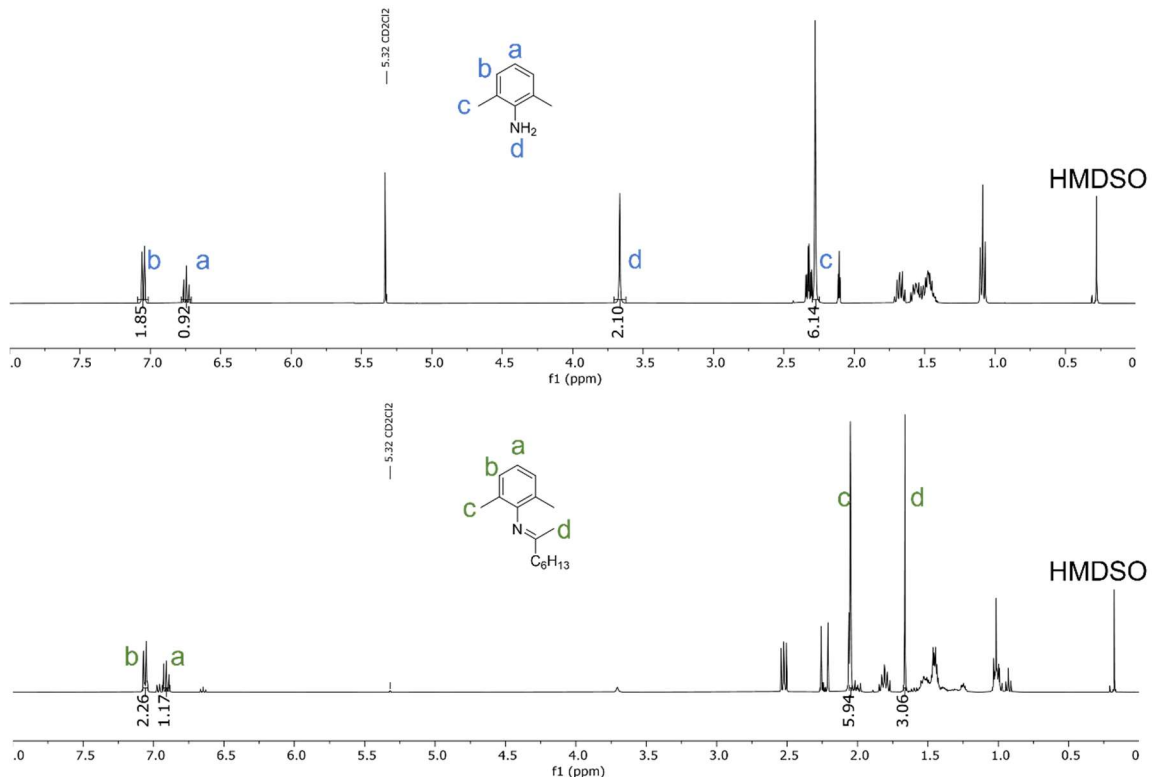


**Figure S11.** Top: Assigned <sup>1</sup>H-NMR spectrum of 2,6-dimethylaniline and octyne prior to reaction. Bottom: Assigned <sup>1</sup>H-NMR spectrum after completed reaction.

**Table S6.** Integrals and calculated conversion/NMR yield for the reaction of octyne (**19**) with 2,6-dimethylaniline (**20**) yielding **24** (Table 2, entries 8 - 14).

Entry	n <sub>0</sub> (HMDSO) [μmol] <sup>a</sup>	Integral HMDSO	n <sub>0</sub> ( <b>20</b> ) [μmol] <sup>a</sup>	Reaction completed				Conv. [%]	Yield [%]
				Integral ( <b>20</b> )	Integral ( <b>24</b> )	n <sub>t</sub> ( <b>20</b> ) [μmol]	n <sub>t</sub> ( <b>24</b> ) [μmol]		
8	20	18	619	29.5	163.1	96	532	84	86
9	30	18	622	15.7	107.7	79	537	87	86
10	30	18	622	28.2	95.2	141	475	77	76
11	30	18	622	61.4	62.6	306	312	51	50
12	58	18	616	61.4	2.4	592	23	4	4
13	58	18	616	61.5	2.1	593	20	4	3
14	31	18	619	121.8	0.0	622	0	0	0

<sup>a</sup> Based on weighed sample.

Integrals were determined relative to HMDSO (Integral set to 18). c (**20**) and c (**24**) (6 Hs each) were used for the calculations.

Equations used for quantification of substrate and product:

$$n_t(\text{Aniline}) = \frac{\text{Integral}(\text{20})}{6} \times n(\text{HMDSO}) \quad n_t(\text{Product}) = \frac{\text{Integral}(\text{24})}{6} \times n(\text{HMDSO})$$

$$\text{Conv.} = 1 - \frac{n_t(\text{20})}{n_0(\text{20})}$$

$$\text{Yield} = \frac{n_t(\text{24})}{n_0(\text{20})}$$

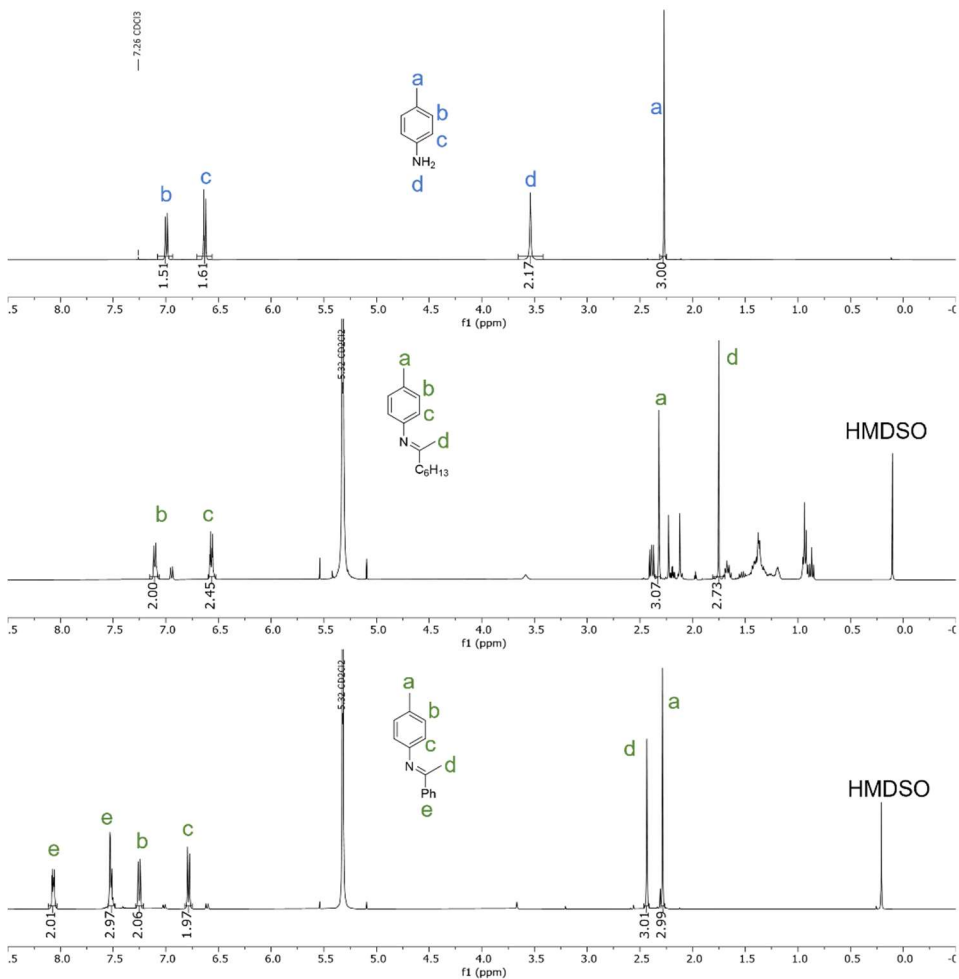


**Figure S12.** top: Assigned <sup>1</sup>H-NMR spectrum of p-toluidine. middle: Assigned <sup>1</sup>H-NMR spectrum after reaction completion with 1-octyne. bottom: Assigned <sup>1</sup>H-NMR spectrum after reaction completion with phenylacetylene.

**Table S7.** Integrals and calculated conversion/NMR yield for the reaction of phenylacetylene (**18**) with *p*-toluidine (**21**) yielding **23**, and ocytne (**19**) with *p*-toluidine (**21**) yielding **25** (Table 2, entries 7, 15 and 16).

Entry	$n_0(\text{HMDSO}) [\mu\text{mol}]^a$	Integral HMDSO	$n_0(\text{21}) [\mu\text{mol}]^a$	Reaction completed				Conv [%]	Yield [%]	Product
				Integral ( <b>21</b> )	Integral Product	$n_t(\text{21}) [\mu\text{mol}]$	$n_t(\text{Product}) [\mu\text{mol}]$			
7	36	18	619	2.8	48.7	49	581	92	94	<b>23</b>
15	36	18	619	23.2	18.1	414	216	33	35	<b>25</b>
16	26	18	633	13.0	53.0	173	468	73	74	<b>25</b>

<sup>a</sup> Based on weighed sample.

Integrals were determined relative to HMDSO (Integral set to 18). d (**21**) (2 Hs) and d (**23** and **25**) (3 Hs each) were used for the calculations.

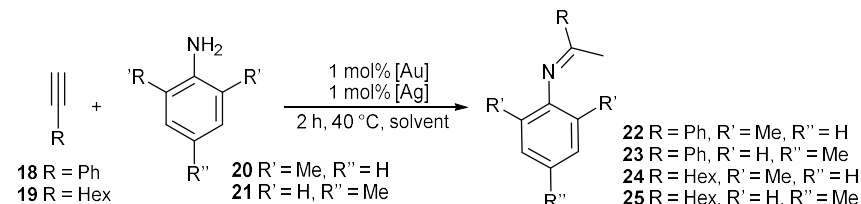
Equations used for quantification of substrate and product:

$$n_t(\text{Aniline}) = \frac{\text{Integral} (\text{21})}{2} \times n(\text{HMDSO}) \quad n_t(\text{Product}) = \frac{\text{Integral} (\text{Product})}{3} \times n(\text{HMDSO})$$

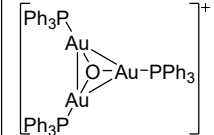
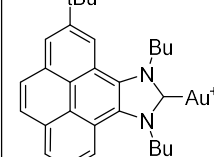
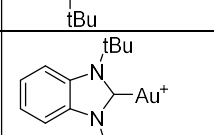
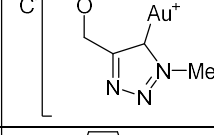
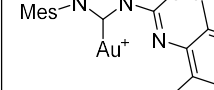
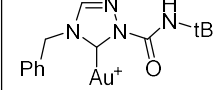
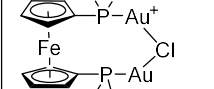
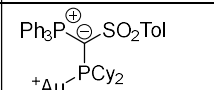
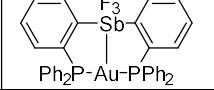
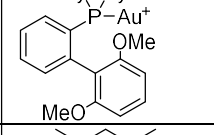
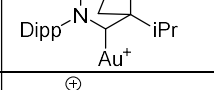
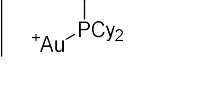
$$\text{Conv.} = 1 - \frac{n_t(\text{21})}{n_0(\text{21})}$$

$$\text{Yield} = \frac{n_t(\text{Product})}{n_0(\text{21})}$$

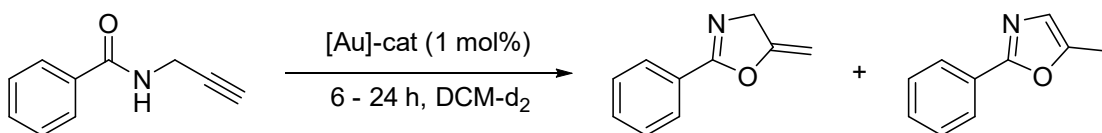
**Table S8.** Overview of known Au<sup>I</sup>-based hydroamination catalysts.



Entry	Aniline	Alkyne	T [°C]	t [h]	Yield [%]	Cat. loading [mol%]	catalyst	Ref
1	<b>21</b>	<b>18</b>	RT	0.66	98	3.5		53
2	<b>21</b>	<b>18</b>	RT	2	100	2		56
3	<b>21</b>	<b>18</b>	RT	4.5	95	2.5		57
4	<b>21</b>	<b>18</b>	RT	24	97	2.5		58
5	<b>21</b>	<b>18</b>	RT	24	98	5		59
6	<b>21</b>	<b>18</b>	40	4	95	2		60
7	<b>21</b>	<b>18</b>	60	16	89	2		61
8	<b>21</b>	<b>18</b>	60	16	73	1		62
9	<b>21</b>	<b>18</b>	70	6	95	0.5		63
10	<b>21</b>	<b>18</b>	70	6	89	0.5		64
11	<b>21</b>	<b>18</b>	70	20	99	5		65

12	<b>21</b>	<b>18</b>	82	4	87	2		66
13	<b>21</b>	<b>18</b>	90	6	80	1		64
14	<b>21</b>	<b>18</b>	90	6	70	1		67
15	<b>20</b>	<b>18</b>	70	6	93	0.5		63
16	<b>20</b>	<b>18</b>	70	6	93	0.5		68
17	<b>20</b>	<b>18</b>	70	20	98	5		65
18	<b>20</b>	<b>18</b>	90	12	88	2		69
19	<b>20</b>	<b>18</b>	120	6	100	1		70
20	Aniline	<b>18</b>	50	3	96	0.2		58
21	<b>21</b>	Hexyne	RT	1	61	3.5		53
22	<b>21</b>	<b>19</b>	RT	24 h	81	2.5		71
23	<b>21</b>	Hexyne	80	3.5 h	92	2.5		57
24	Aniline	Hexyne	80	6 h	98	0.2		58

## 6.2 Cycloisomerisation of *N*-(prop-2-yn-1-yl)benzamide (**14**)



In a glovebox a stock solution of propargylamide (0.78 mM) and internal standard hexamethylbenzene (13 mg) was prepared in DCM in a 1 mL volumetric flask.

The catalyst solutions were prepared as follows:

a) **7**, **11** or **1** (3  $\mu$ mol, 1 mol%) and NaBArF, AgOTf or AgNTf<sub>2</sub> (3  $\mu$ mol, 1 mol%) were dissolved in 0.2 mL DCM-d<sub>2</sub> and filtered through glass wool.

b) **10** (3  $\mu$ mol, 1 mol%) and AgNTf<sub>2</sub> (6  $\mu$ mol, 2 mol%) dissolved in 0.2 mL solvent and filtered through glass wool.

c) **8**, **9**, **10** or **7** (3  $\mu$ mol, 1 mol%) or DPPTPA (3  $\mu$ mol, 1 mol%) and AgNTf<sub>2</sub> and Zn(NTf<sub>2</sub>)<sub>2</sub> (3  $\mu$ mol, 1 mol%) dissolved in 0.2 mL solvent.

0.4 mL of the substrate solution (corresponding to 314  $\mu$ mol; 1.0 equiv. and 5.0 mg hexamethylbenzene) was mixed with the catalyst solution in a J Young NMR tube. The tube was sealed and put into a preheated oil bath for 6-24 h. Afterwards the solution was analysed with NMR spectroscopy. All compounds are known and peaks were assigned according to literature<sup>72</sup>

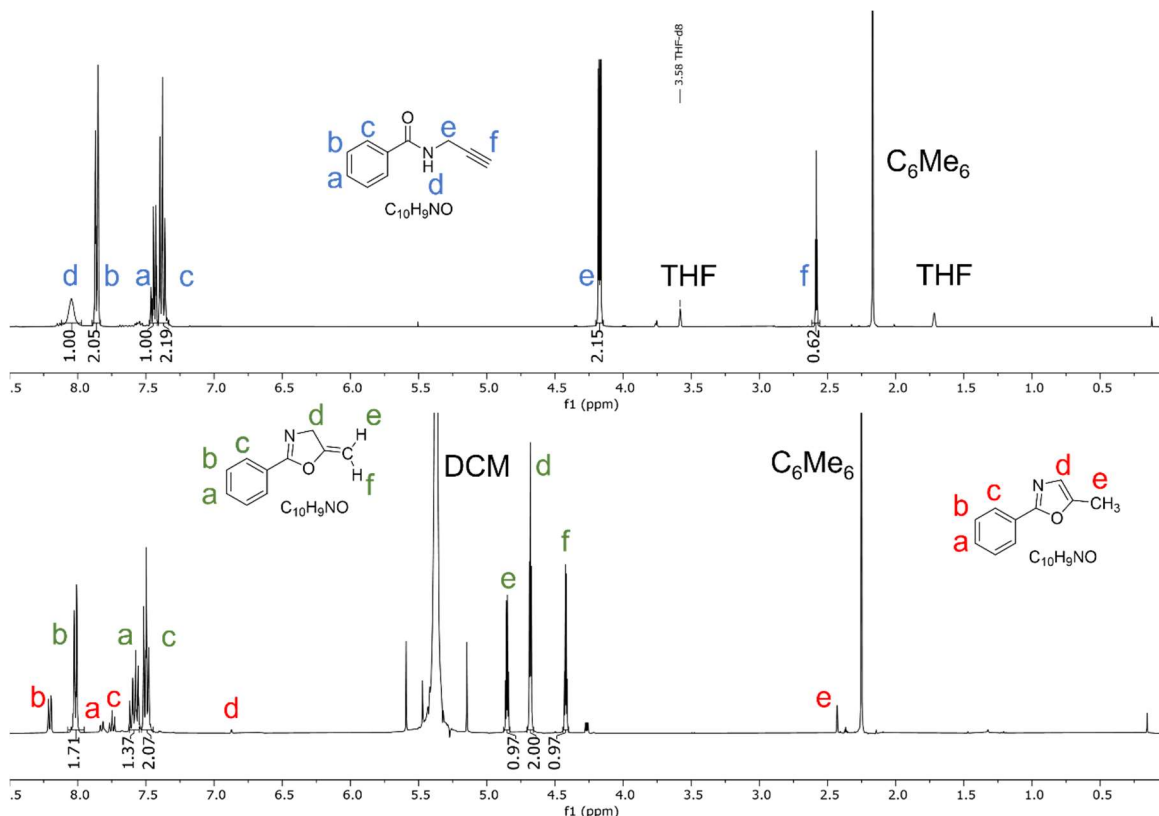


**Figure S13** top: <sup>1</sup>H-NMR spectrum of *N*-(Prop-2-yn-1-yl)benzamide (**14**) prior to reaction with assigned peaks.  
bottom: Assigned <sup>1</sup>H-NMR spectrum after reaction completion.

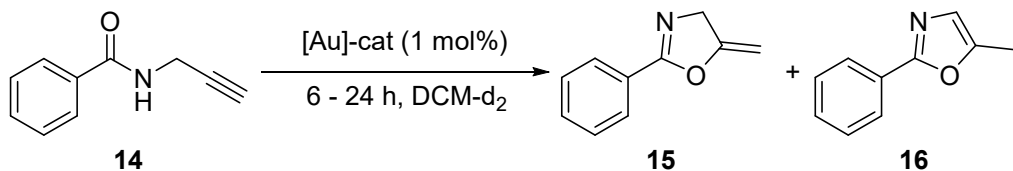


**Table S9.** Calculation of conversion and yields for the cycloisomerisation of 14 corresponding to Table 1 Entry 1 to 11.

Entry	n(C <sub>6</sub> Me <sub>6</sub> ) [μmol] <sup>a</sup>	Integral C <sub>6</sub> Me <sub>6</sub>	n <sub>0</sub> (14) [μmol] <sup>a</sup>	Reaction completed								Conv. [%]	Yield (15) [%]	Yield (16) [%]
				Integral (14)	Integral (15)	Integral (16)	n <sub>t</sub> (14) [μmol]	n <sub>t</sub> (15) [μmol]	n <sub>t</sub> (16) [μmol]					
1	25	18	314	16.23	9.04	0	200	111	0	36	35			0
2	34	18	312	10.84	5.61	2.41	184	95	27	41	30			9
3	39	18	312	3.01	7.45	7.81	58	143	100	81	46			32
4	39	18	312	1.93	12.87	1.74	37	248	22	88	79			7
5	22	18	312	0.64	23.21	4.96	7	258	37	98	83			12
6	32	18	314	20.18	0	0	321	0	0	0	0			0
7	32	18	314	13.75	6.18	0	219	98	0	30	31			0
8	33	18	314	0	16.33	4.1	0	270	45	100	86			14
9	24	18	317	1.29	23.07	1.4	16	278	11	95	88			4
10	23	18	313	27.26	0.25	0	312	3	0	0	0			0
11	23	18	313	27.43	0.25	0	314	3	0	0	0			0

<sup>a</sup> Based on weighed sample.

Integrals were determined relative to C<sub>6</sub>Me<sub>6</sub> (Integral set to 18). Integrals used for the calculations: e (2 Hs) (14), d (2 Hs) (15), e (16)

Equations used for quantification of 14, 15 and 16:

$$n_t(14) = \frac{\text{Integral (14)}}{2} \times n(C_6\text{Me}_6) \quad n_t(15) = \frac{\text{Integral (15)}}{2} \times n(C_6\text{Me}_6) \quad n_t(16) = \frac{\text{Integral (16)}}{3} \times n(C_6\text{Me}_6)$$

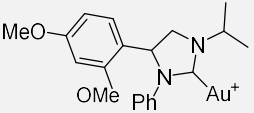
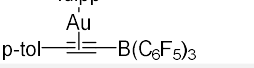
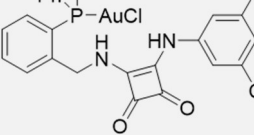
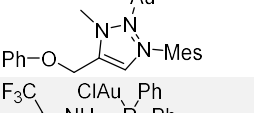
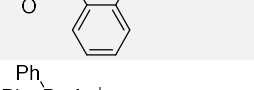
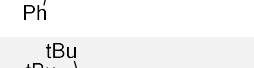
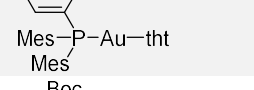
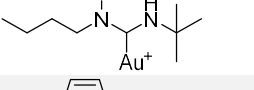
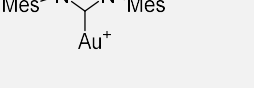
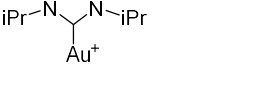
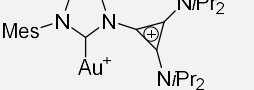
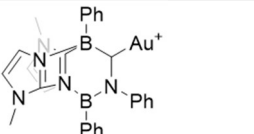
$$\text{Conv.} = 1 - \frac{n_t(14)}{n_0(14)}$$

$$\text{Yield (15)} = \frac{n_t(15)}{n_0(14)}$$

$$\text{Yield (16)} = \frac{n_t(16)}{n_0(14)}$$

**Table S10** Overview of known Au<sup>I</sup>-based catalysts for the cycloisomerisation of *N*-(prop-2-yn-1-yl)benzamide.

Entry	T [°C]	t [h]	Conv [%]	Cat. loading [mol%]	catalyst	Ref
1	RT	0.5	74	2		73
2	RT	1.5	88	2		74
3	RT	2	100	1		75
4	25	3	99	1		76
5	RT	3	99	1		70
6	RT	3	99	1		77
7	RT	6	99	1		78
8	RT	7	99	5		79
9	RT	7.5	100	3		56
10	RT	7.5	35	3		56

11	RT	9	97	1		80
12	RT	11	98	2		81
13	23	24	98	5		82
14	RT	24	76	3		83
15	RT	24	36	5		84
16	RT	36	79	1		72
17	RT	36	79	2		73
18	RT	48	93	1		85
19	RT	48	>98	0.5		86
20	RT	48	>98	0.5		86
21	RT	48	>98	1		86
22	RT	120	57	5		87

## 7 NMR spectra

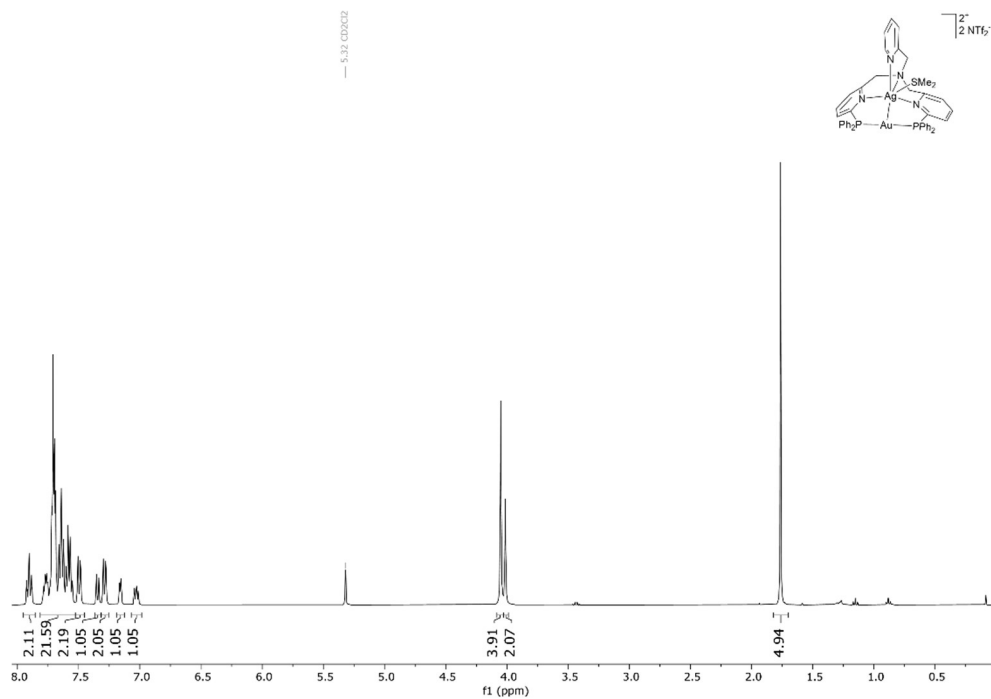


**Figure S14.**  $^1\text{H}$ -NMR (DCM-d<sub>2</sub>) of **9**.

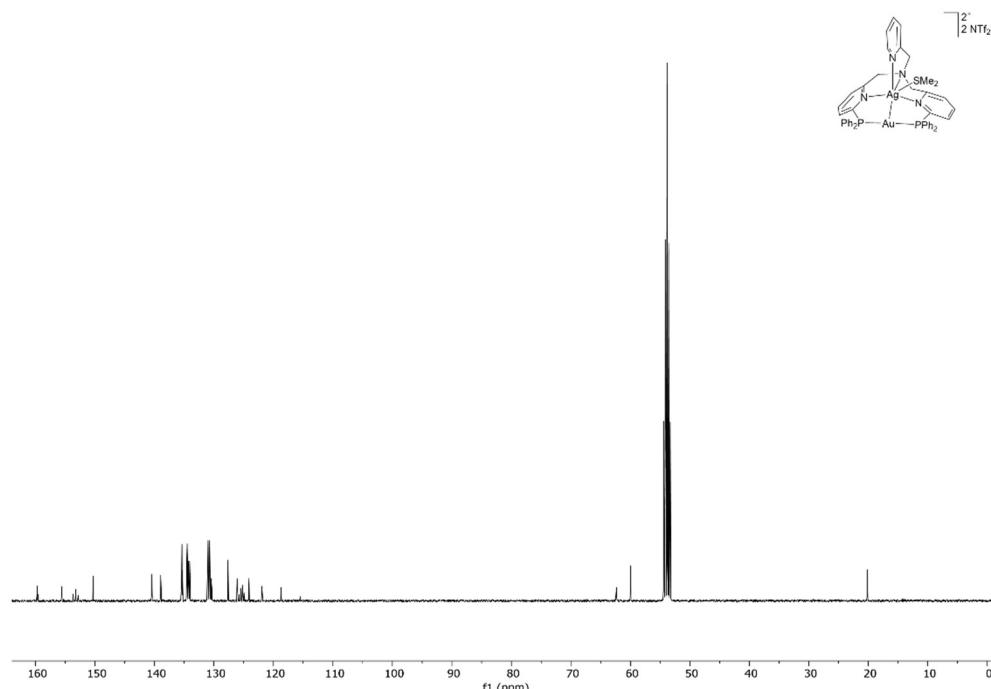


**Figure S15.**  $^{13}\text{C}$ -NMR (DCM-d<sub>2</sub>) of **9**.

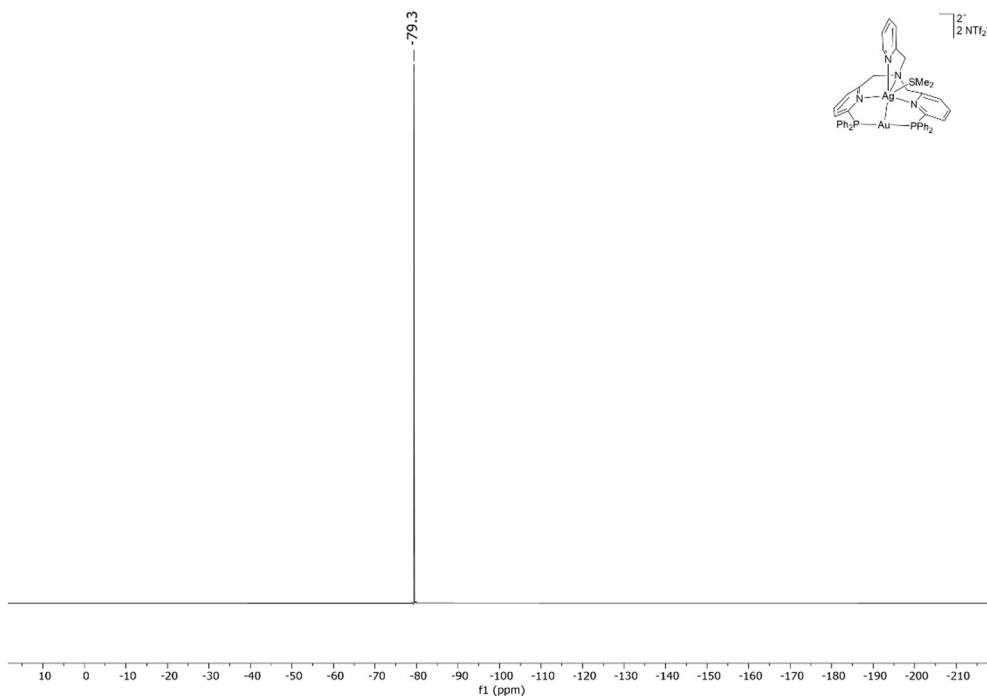


**Figure S16.**  $^{19}\text{F}$ -NMR ( $\text{DCM-d}_2$ ) of **9**.

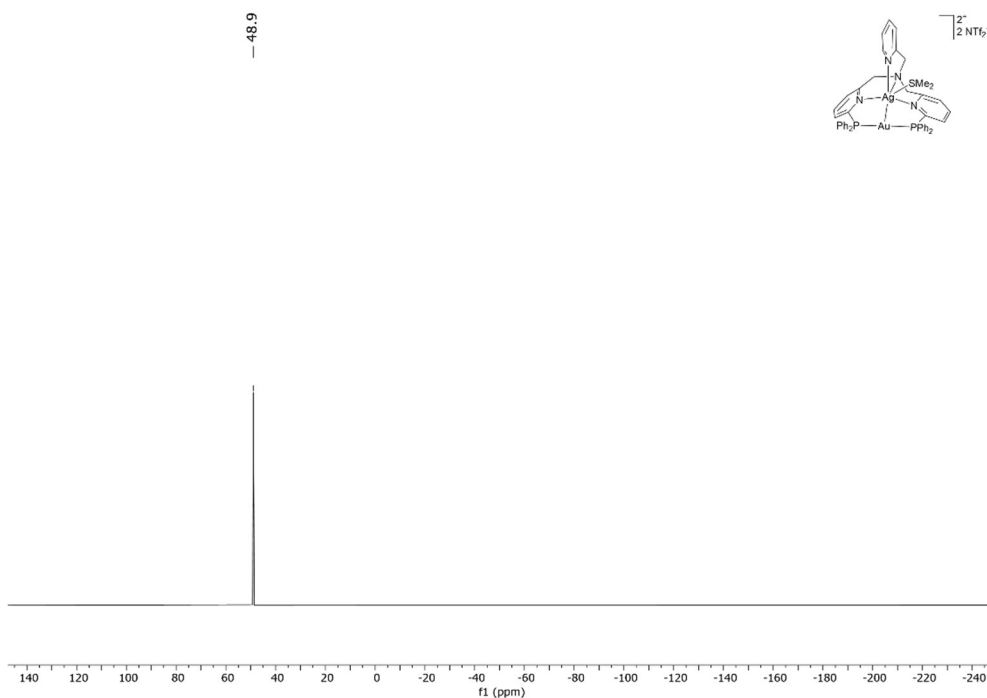


**Figure S17.**  $^{31}\text{P}$ -NMR ( $\text{DCM-d}_2$ ) of **9**.

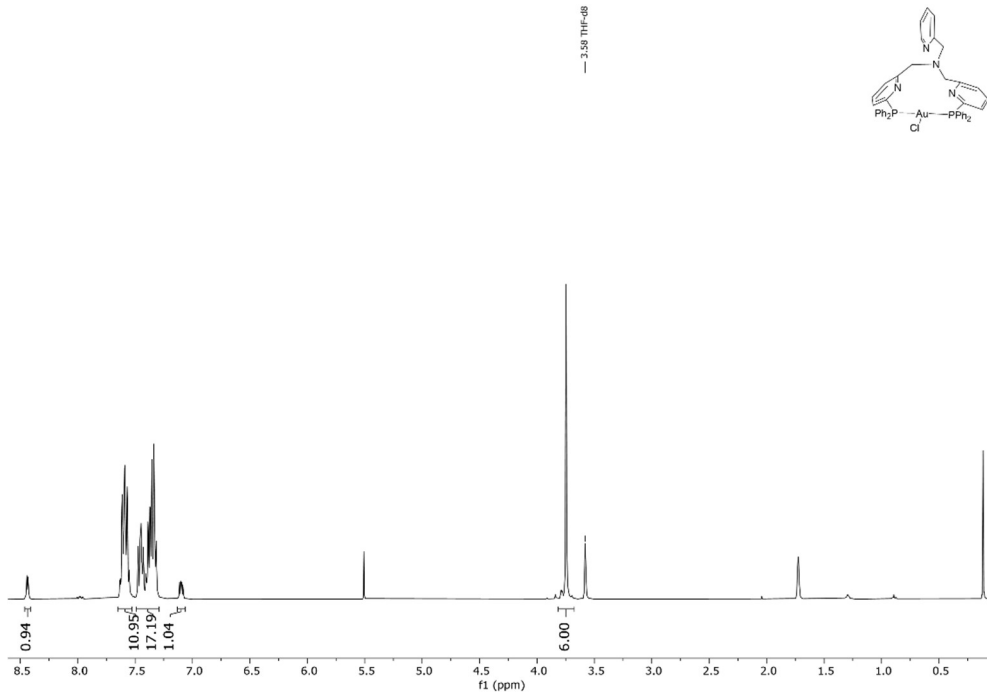


**Figure S18.**  $^1\text{H}$ -NMR (THF- $d_8$ ) of **10**.

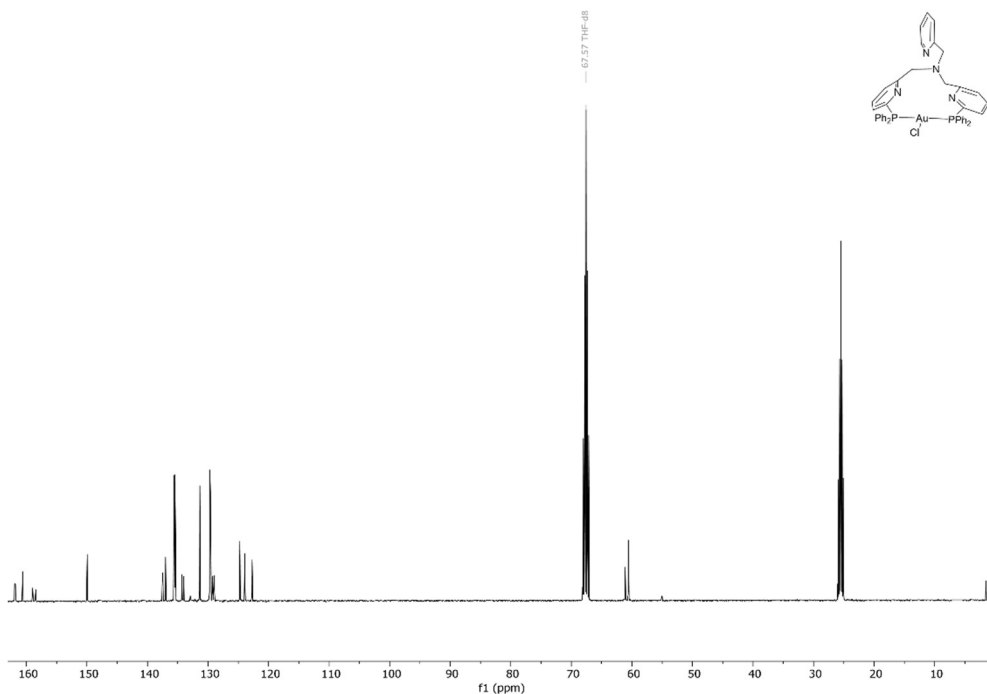


**Figure S19.**  $^{13}\text{C}$ -NMR (THF- $\text{d}_8$ ) of **10**.

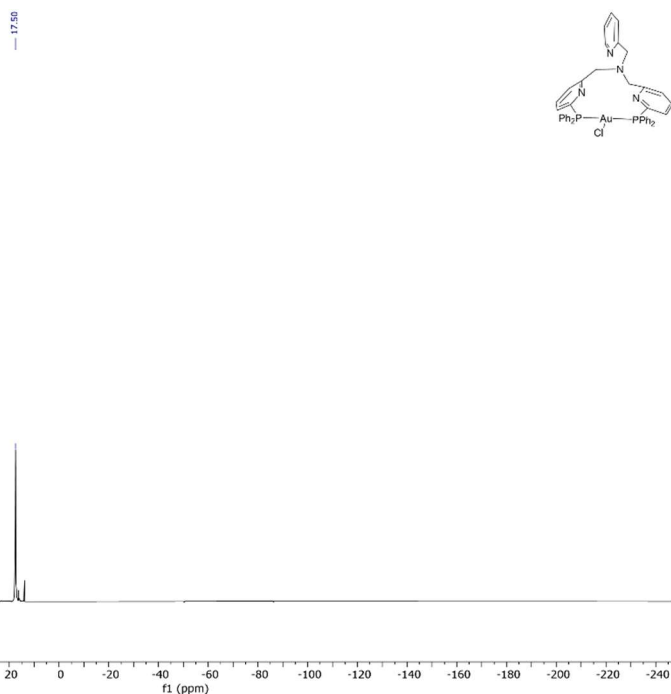


**Figure S20.** <sup>31</sup>P-NMR (THF-d<sub>8</sub>) of 10.

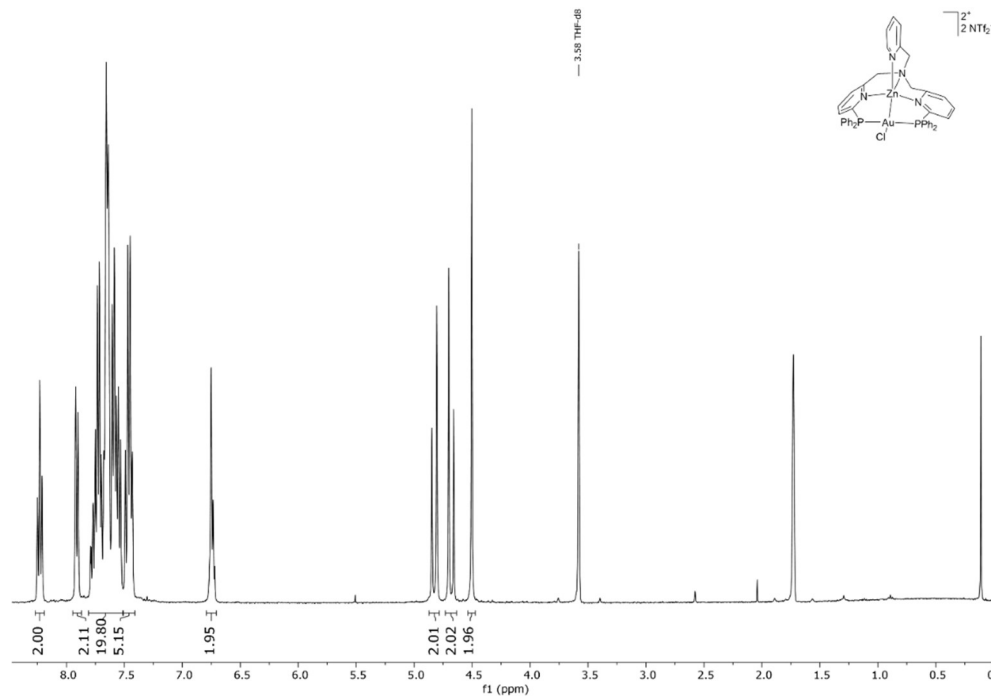


**Figure S21.** <sup>1</sup>H-NMR (THF-d<sub>8</sub>) of 7.

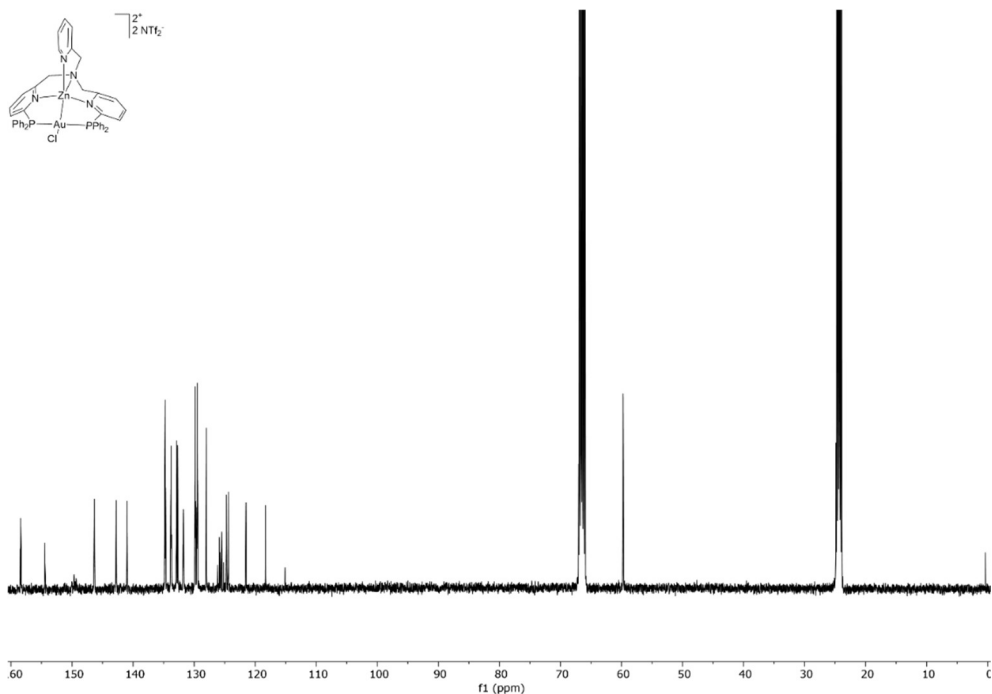


**Figure S22.**  $^{13}\text{C}$ -NMR (THF- $d_8$ ) of 7.

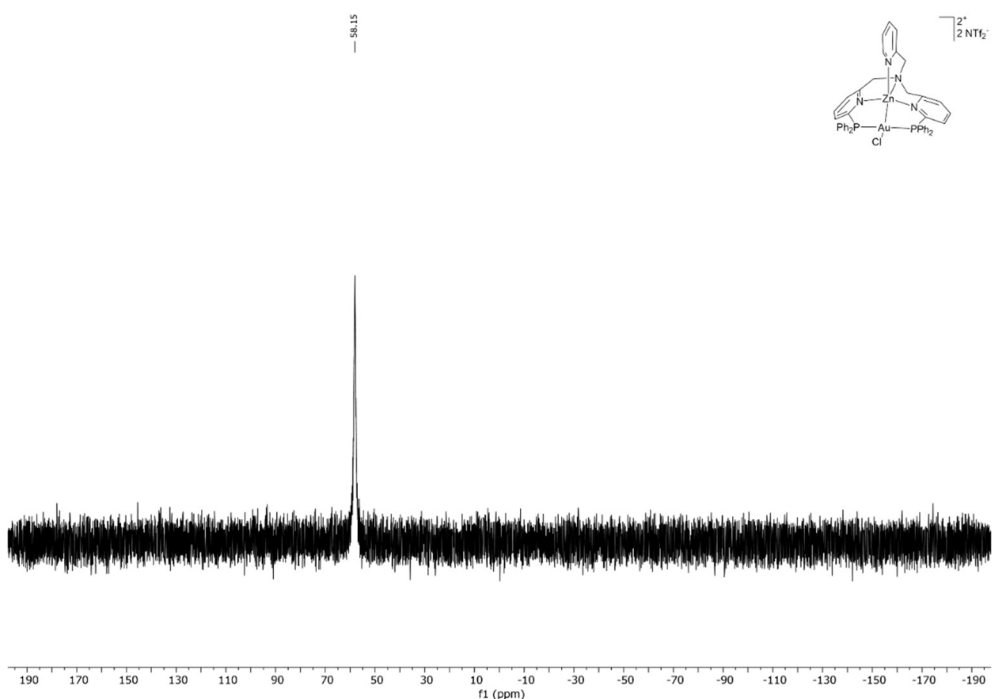


**Figure S23.**  $^{31}\text{P}$ -NMR (THF- $d_8$ ) of 7.

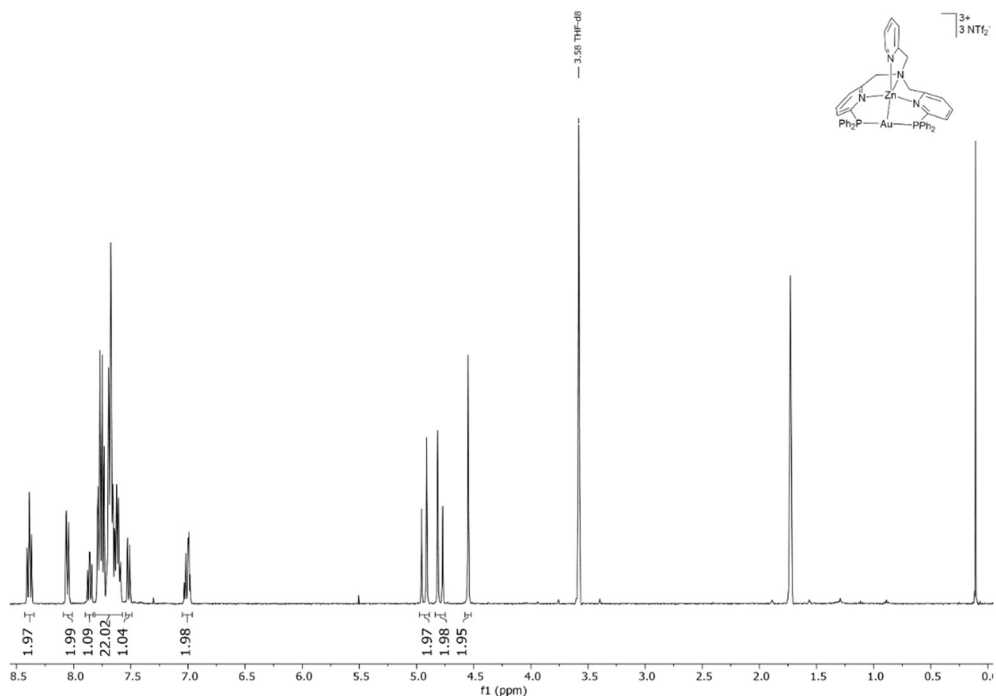


**Figure S24.**  $^1\text{H}$ -NMR (THF- $d_8$ ) of **8**.

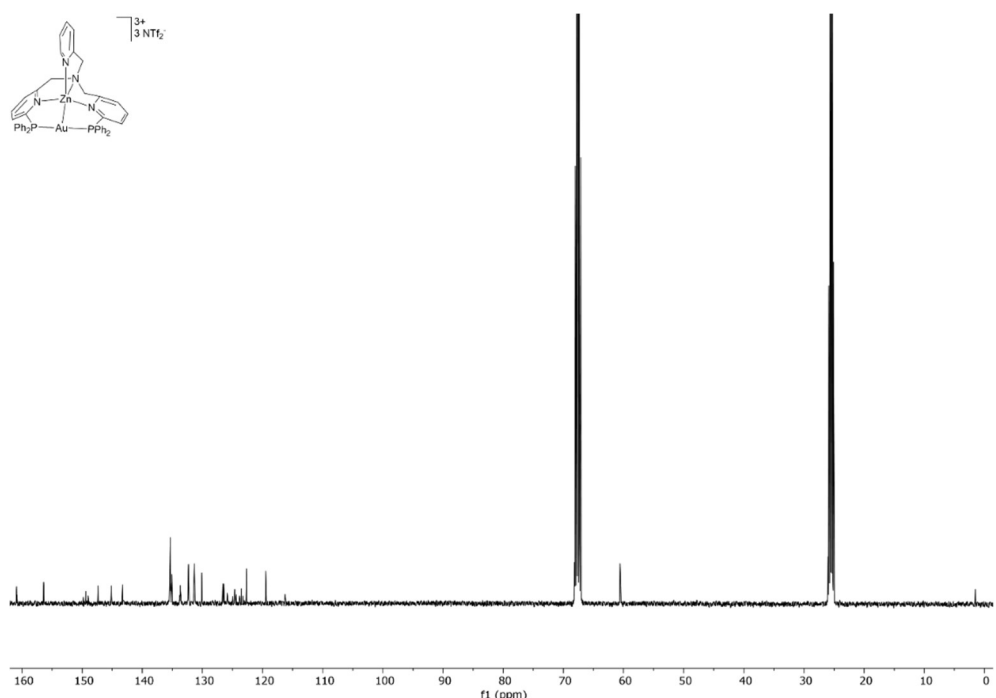


**Figure S25.**  $^{13}\text{C}$ -NMR (THF- $d_8$ ) of **8**.

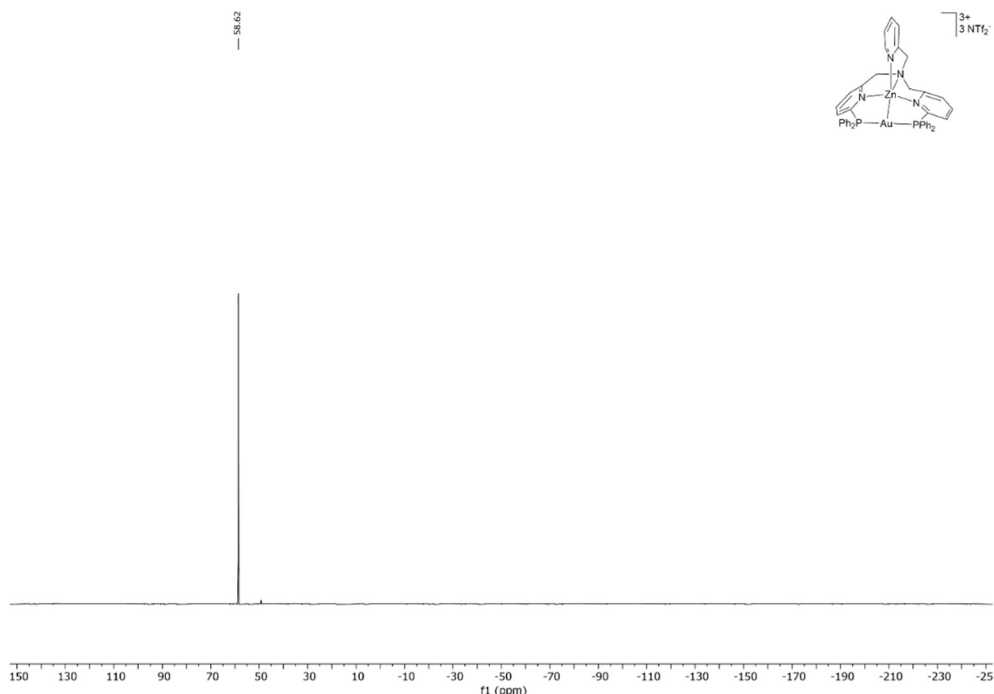


**Figure S26.**  ${}^{31}\text{P}$ -NMR (THF-d<sub>8</sub>) of **8**.

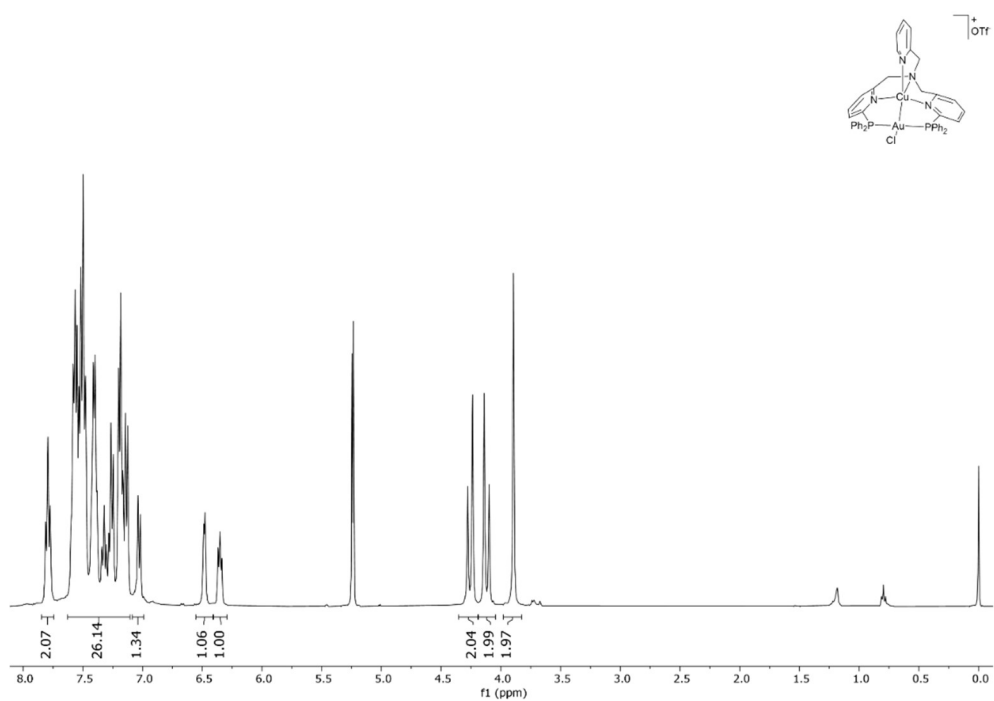


**Figure S27.**  ${}^1\text{H}$ -NMR (DCM-d<sub>2</sub>) of **11**.

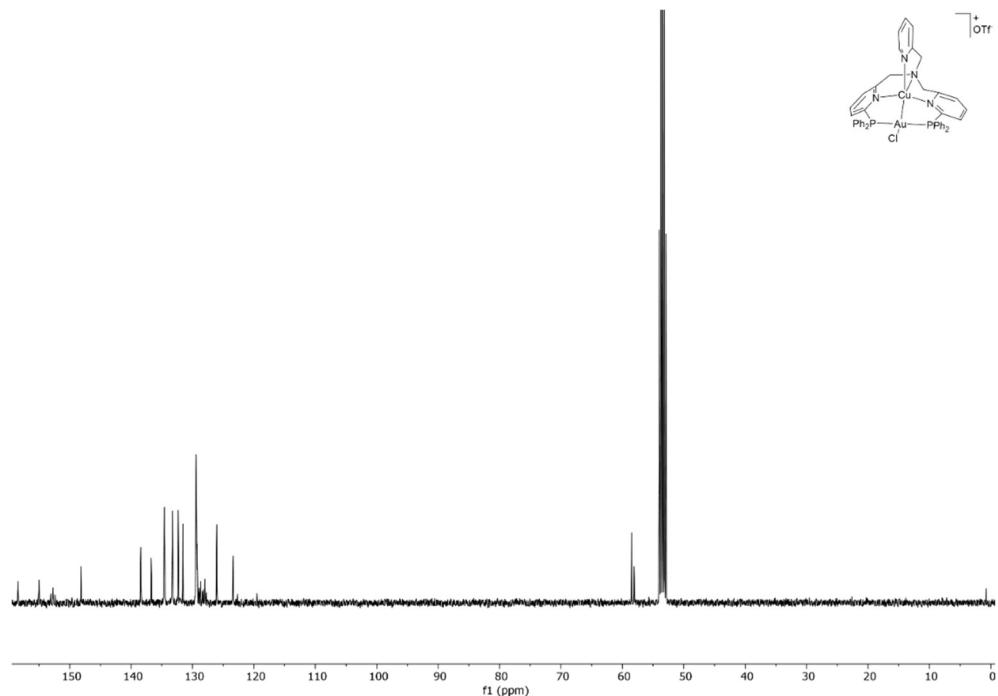


**Figure S28.**  $^{13}\text{C}$ -NMR (DCM-d<sub>2</sub>) of 11.

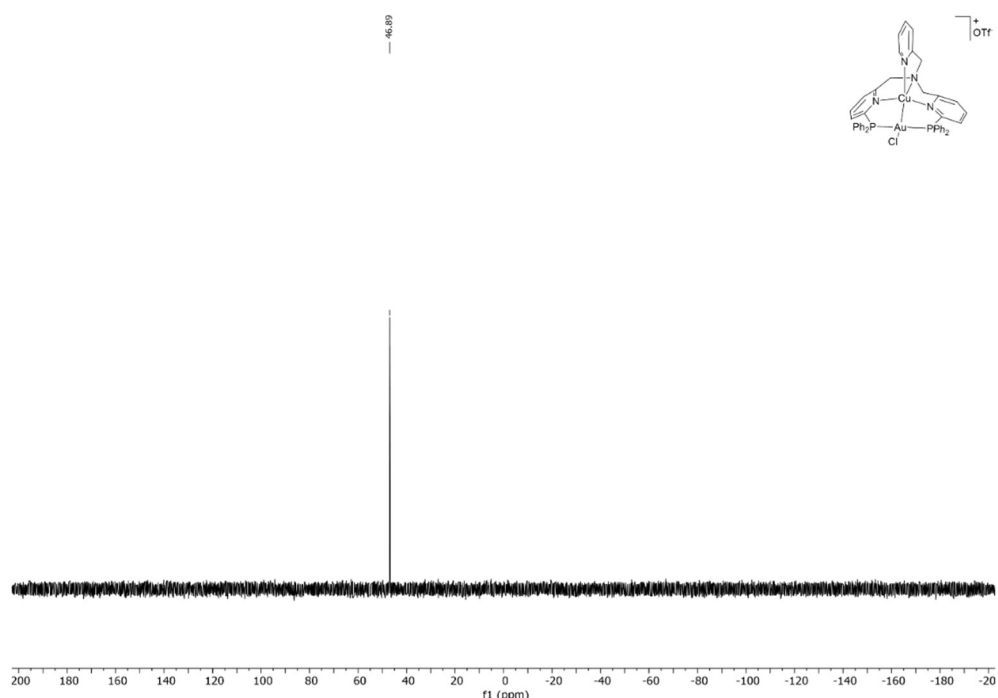


**Figure S29.**  $^{31}\text{P}$ -NMR (DCM-d<sub>2</sub>) of 11.

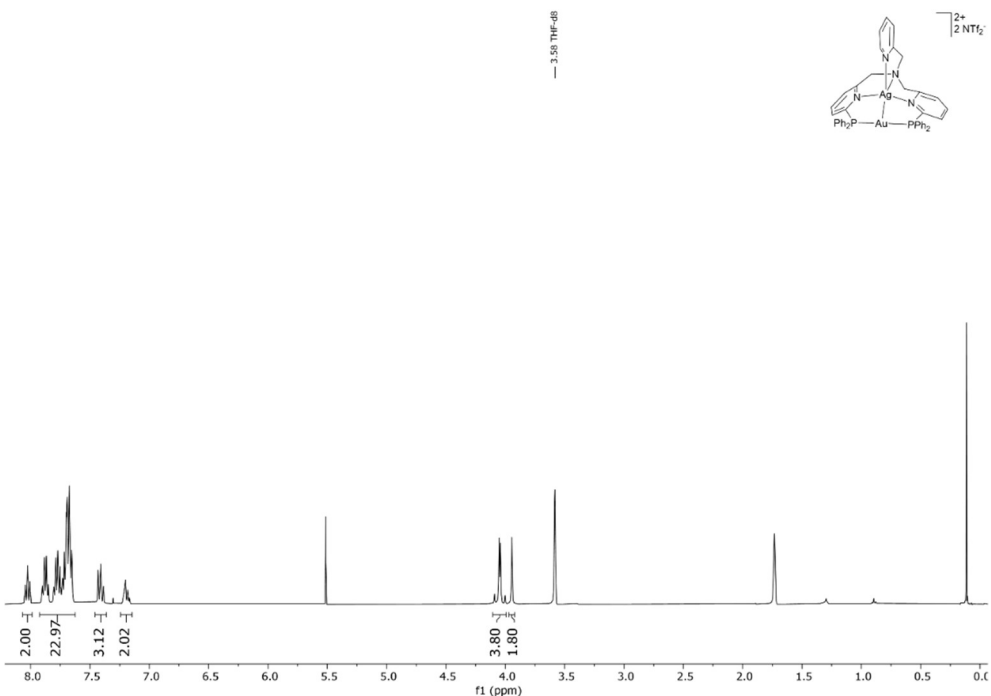


**Figure S30.**  $^1\text{H}$ -NMR (THF- $d_8$ ) of **12**.

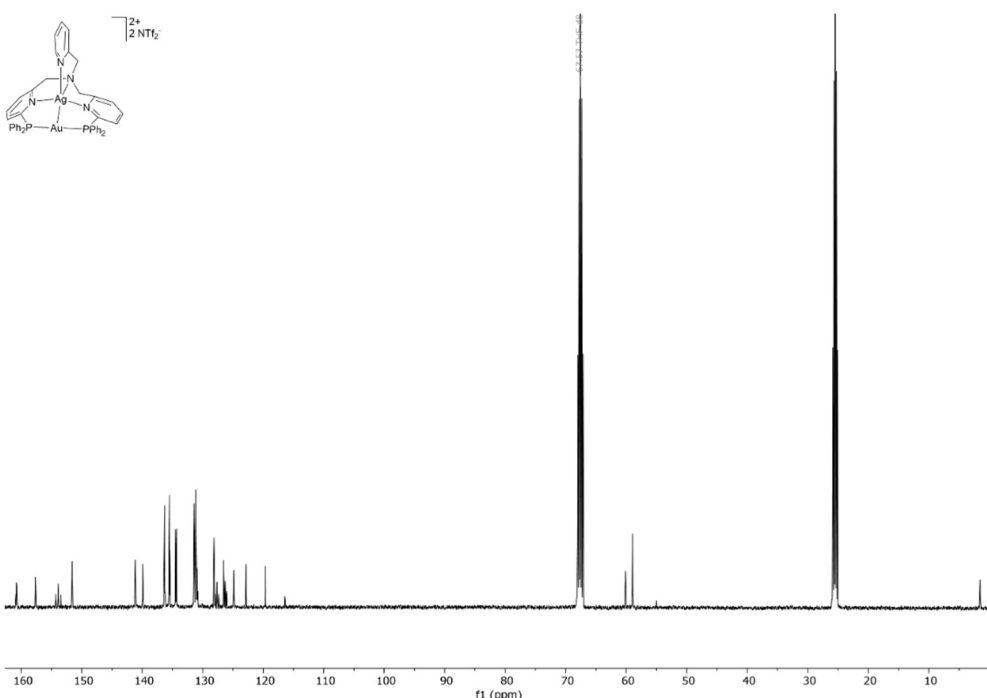


**Figure S31.**  $^{13}\text{C}$ -NMR (THF- $d_8$ ) of **12**.

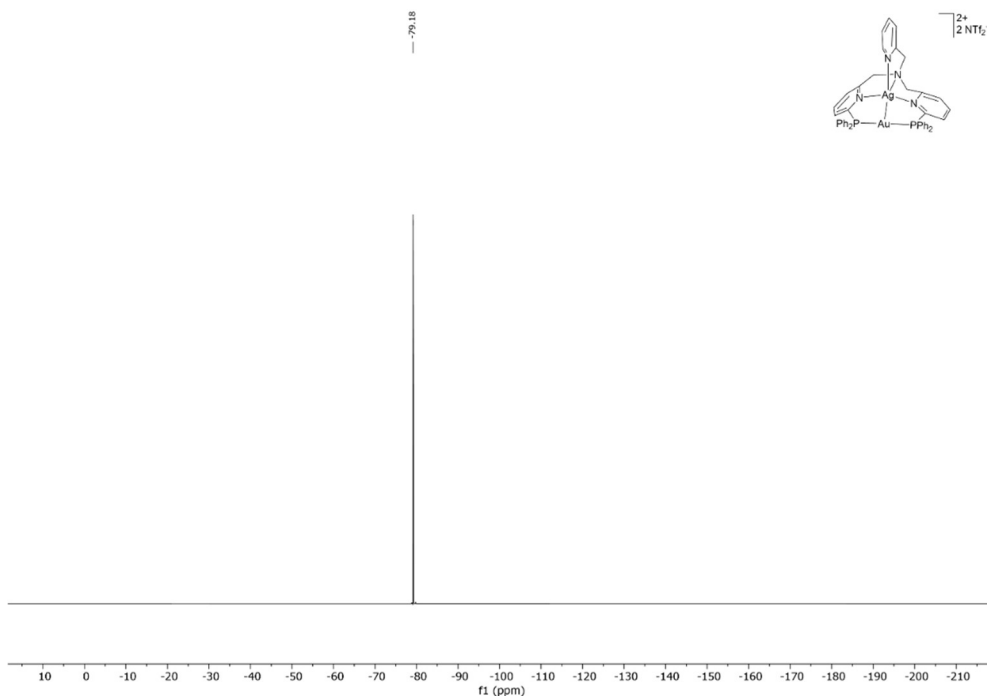


**Figure S32.** <sup>19</sup>F-NMR (THF-d<sub>8</sub>) of **12**.

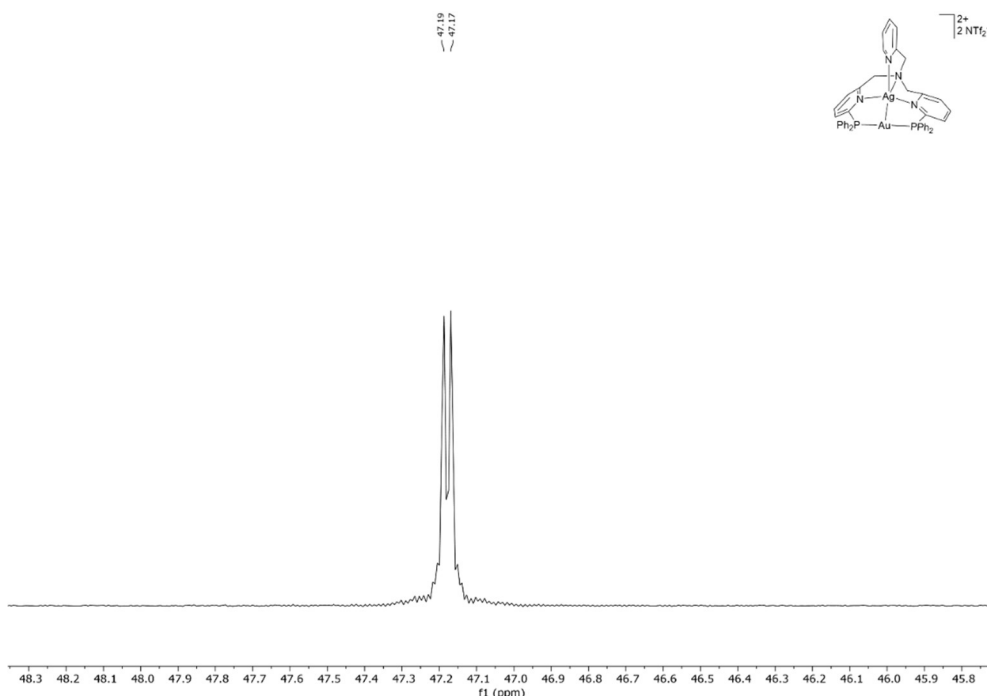


**Figure S33.** <sup>31</sup>P-NMR (THF-d<sub>8</sub>) of **12** at 225K.

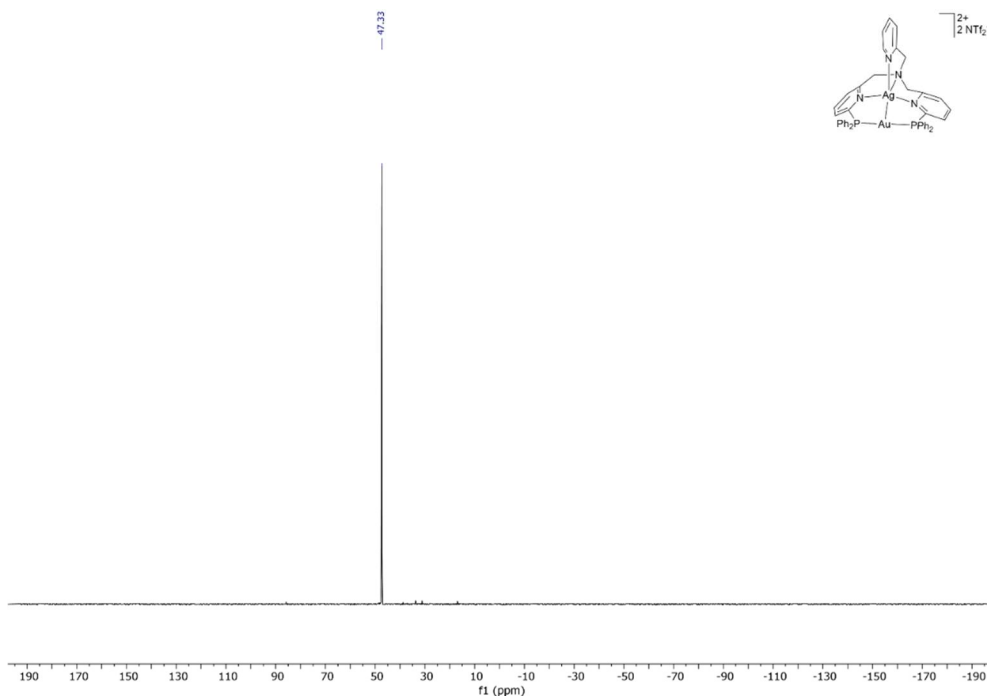


**Figure S34.** <sup>31</sup>P-NMR (THF-d<sub>8</sub>) of **12** at 300K.

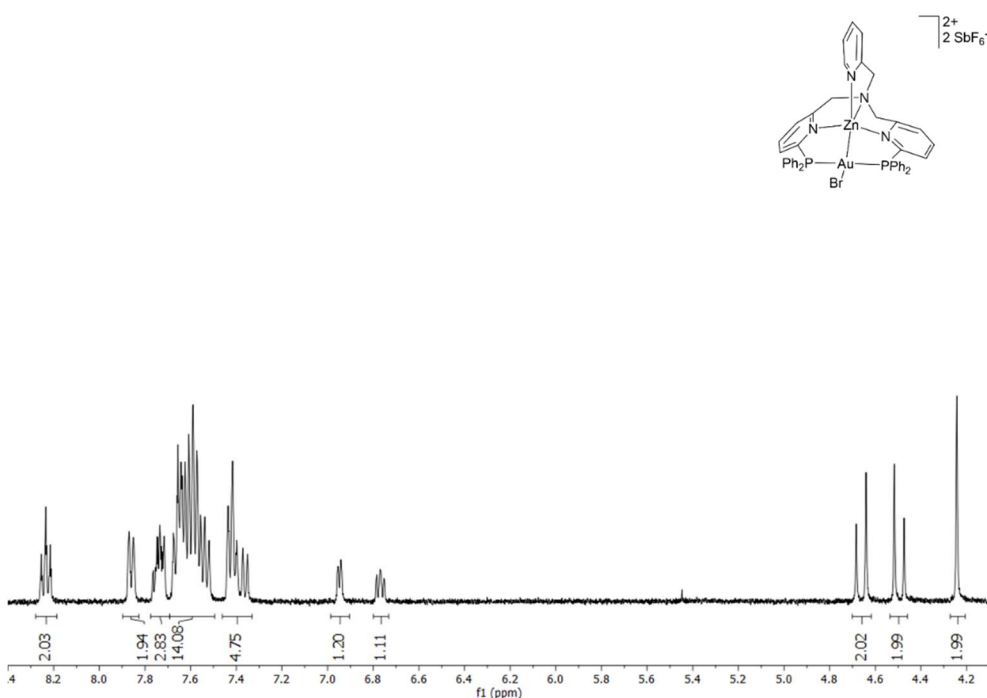


**Figure S35.** <sup>1</sup>H-NMR (MeCN-d<sub>3</sub>) of **17**.

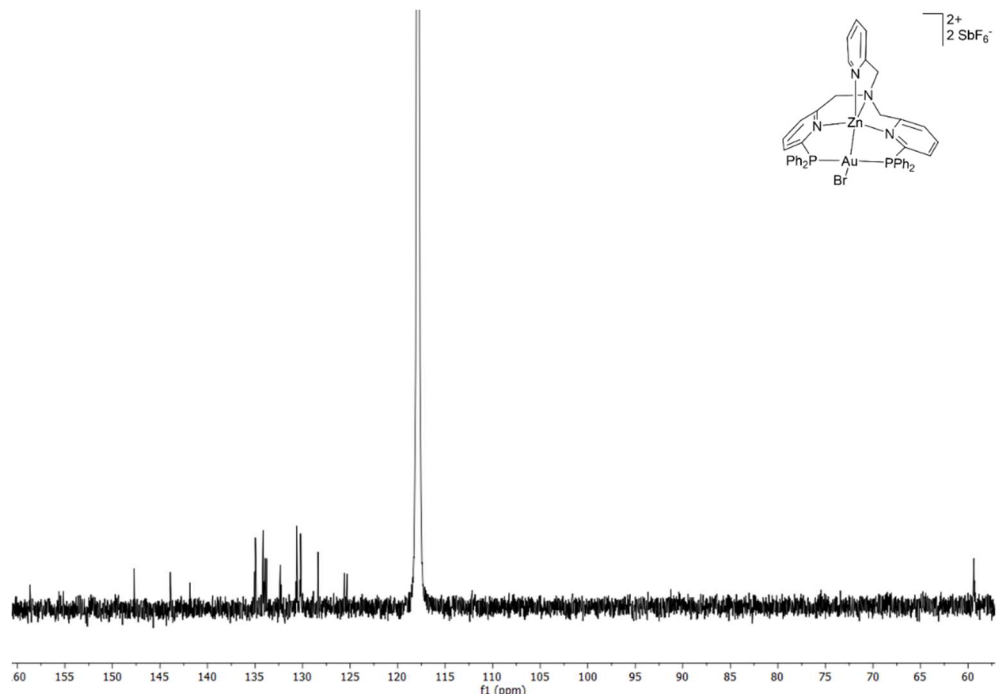


**Figure S36.**  $^{13}\text{C}$ -NMR (MeCN-d<sub>3</sub>) of 17.

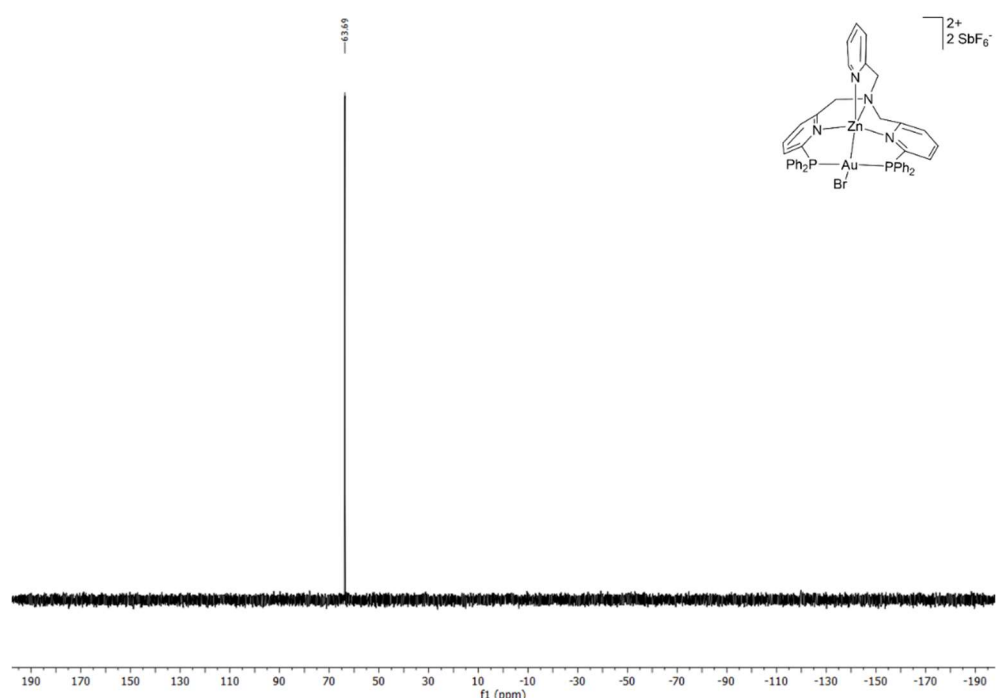


**Figure S37.**  $^{31}\text{P}$ -NMR (MeCN-d<sub>3</sub>) of 17.

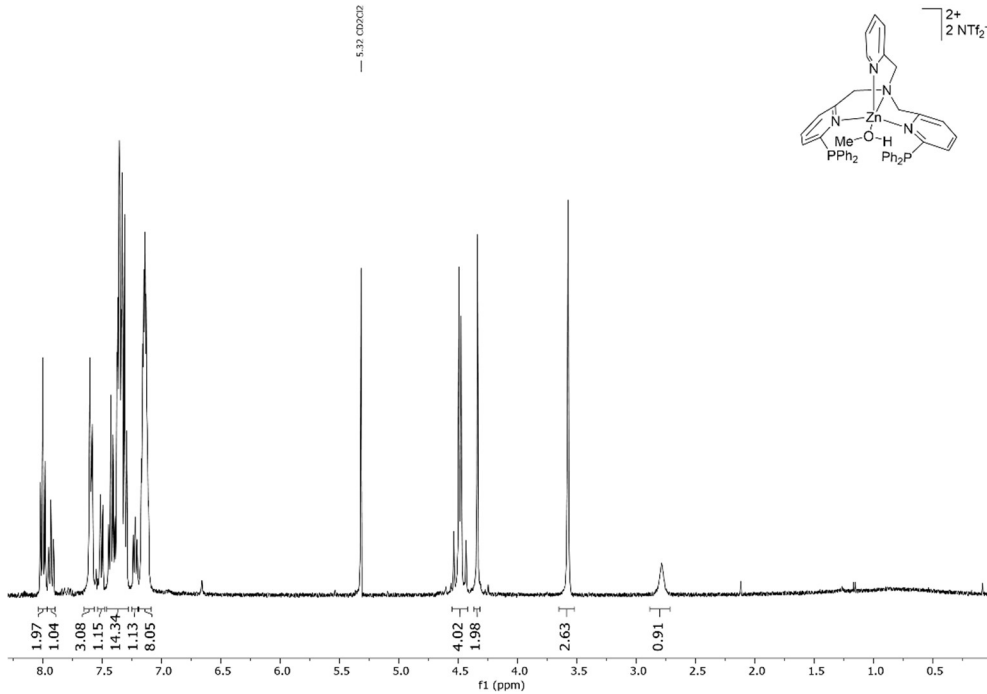


**Figure S38.**  $^1\text{H}$ -NMR (DCM- $\text{d}_2$ ) of **6**.

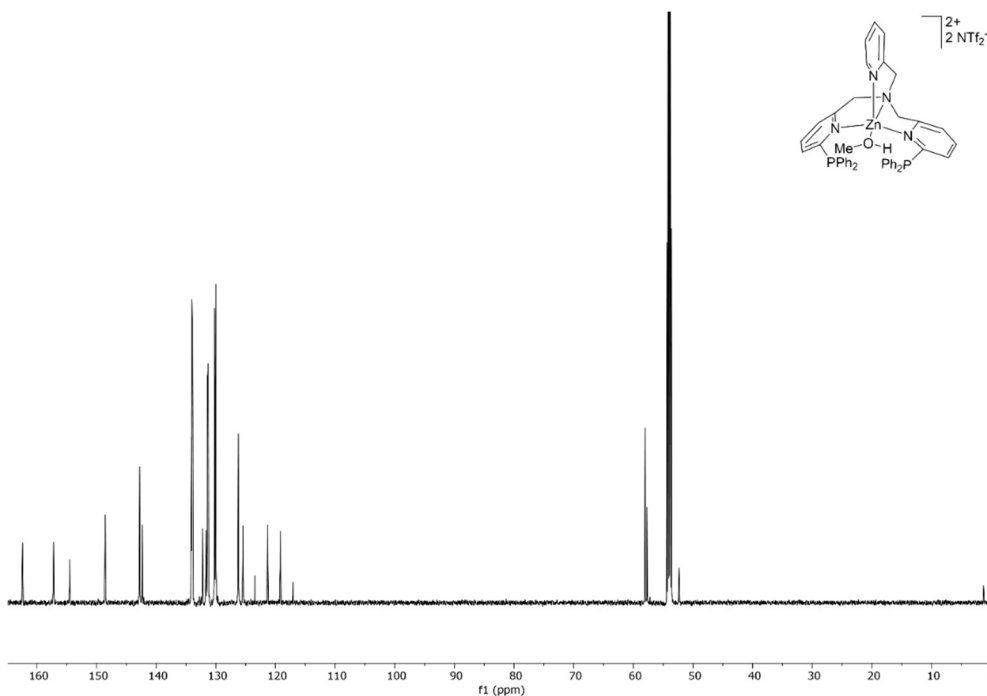


**Figure S39.**  $^{13}\text{C}$ -NMR (DCM-d<sub>2</sub>) of **6**.

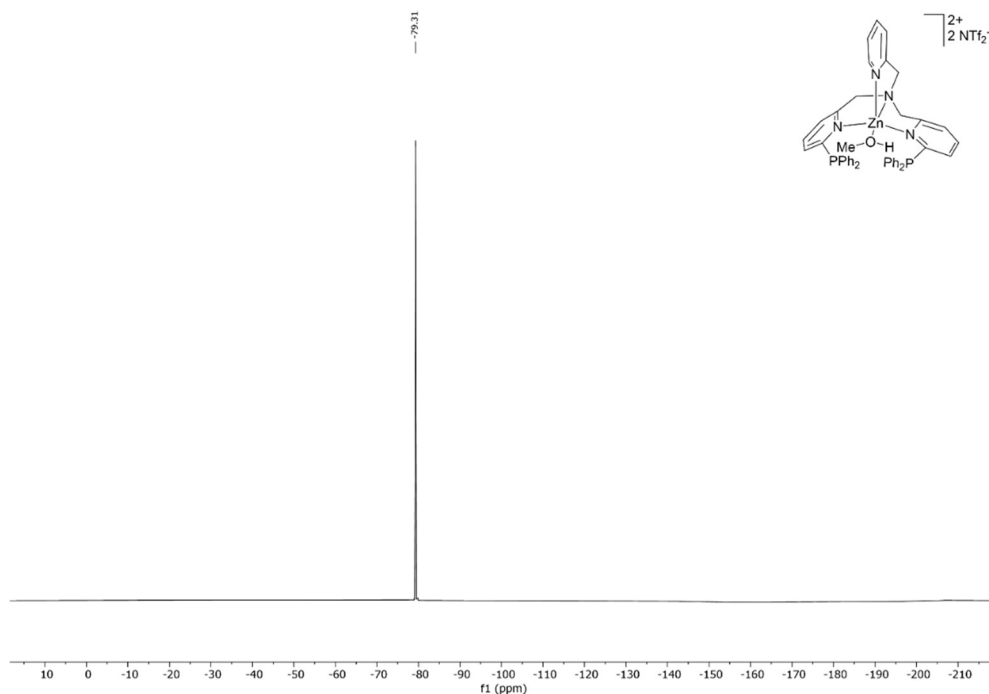


**Figure S40.**  ${}^{19}\text{F}$ -NMR (DCM-d<sub>2</sub>) of **6**.

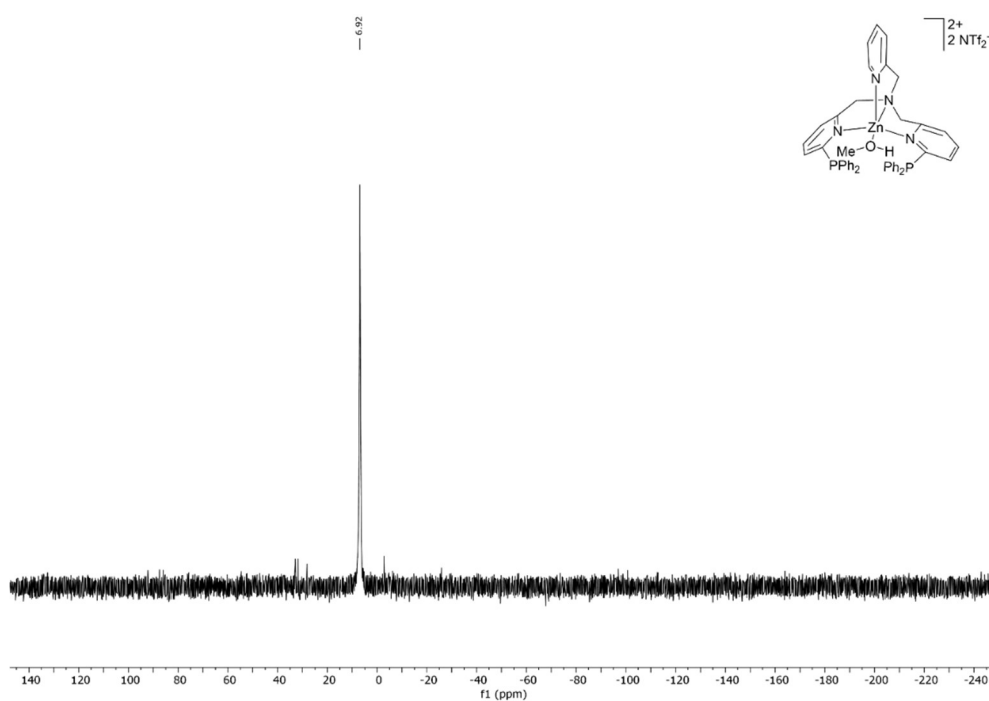


**Figure S41.**  ${}^{31}\text{P}$ -NMR (DCM-d<sub>2</sub>) of **6**.

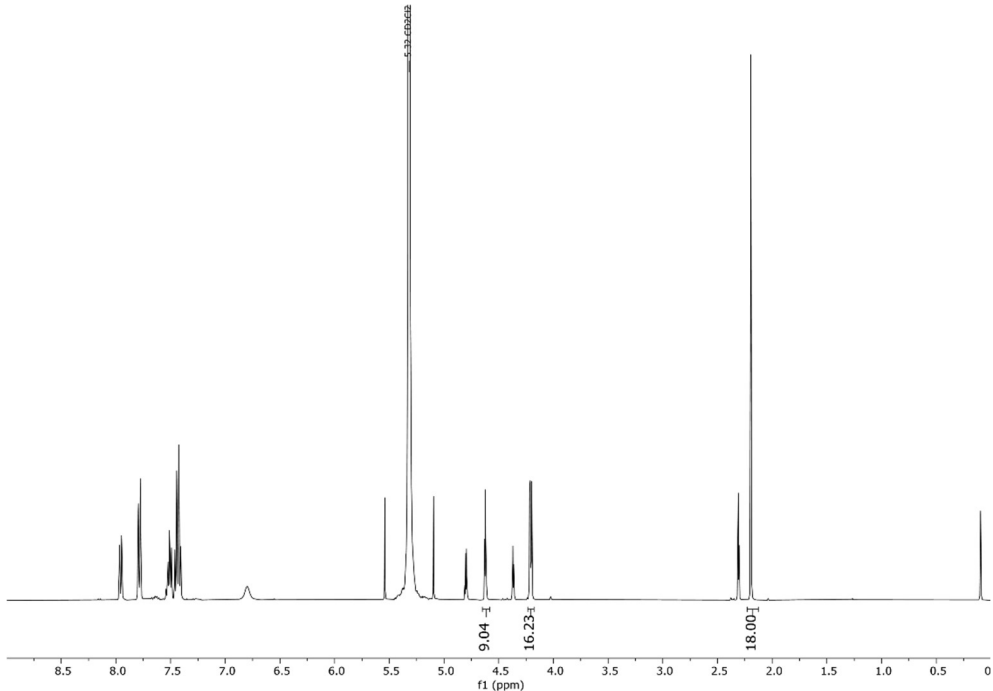


**Figure S42.**  $^1\text{H}$  NMR (DCM-d<sub>2</sub>) of reaction mixture from table 1 entry 1.

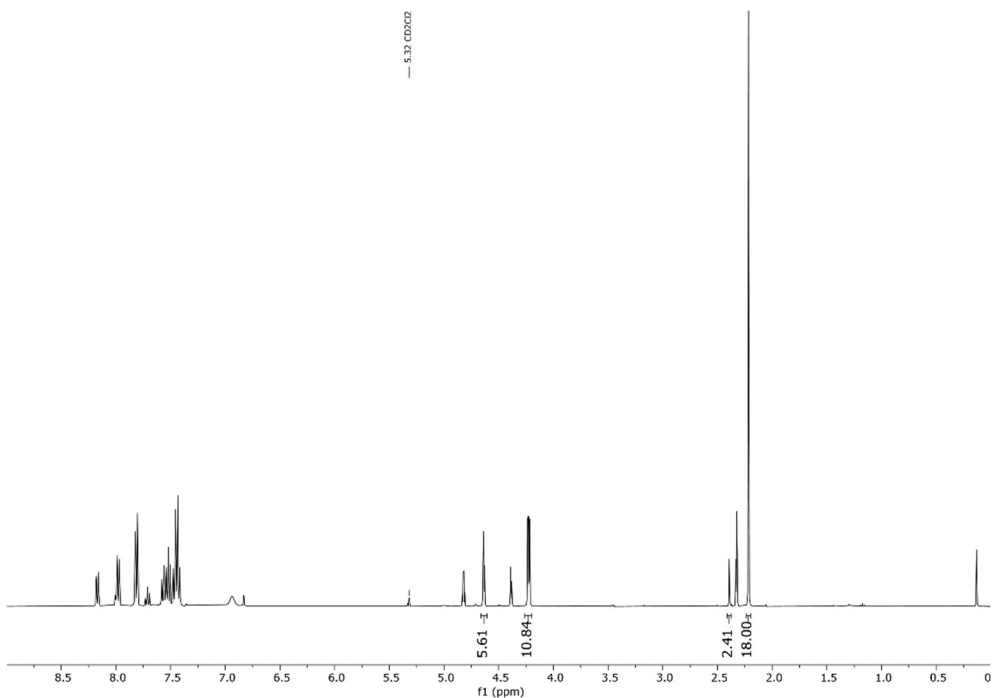


**Figure S43.**  $^1\text{H}$  NMR (DCM-d<sub>2</sub>) of reaction mixture from table 1 entry 2.

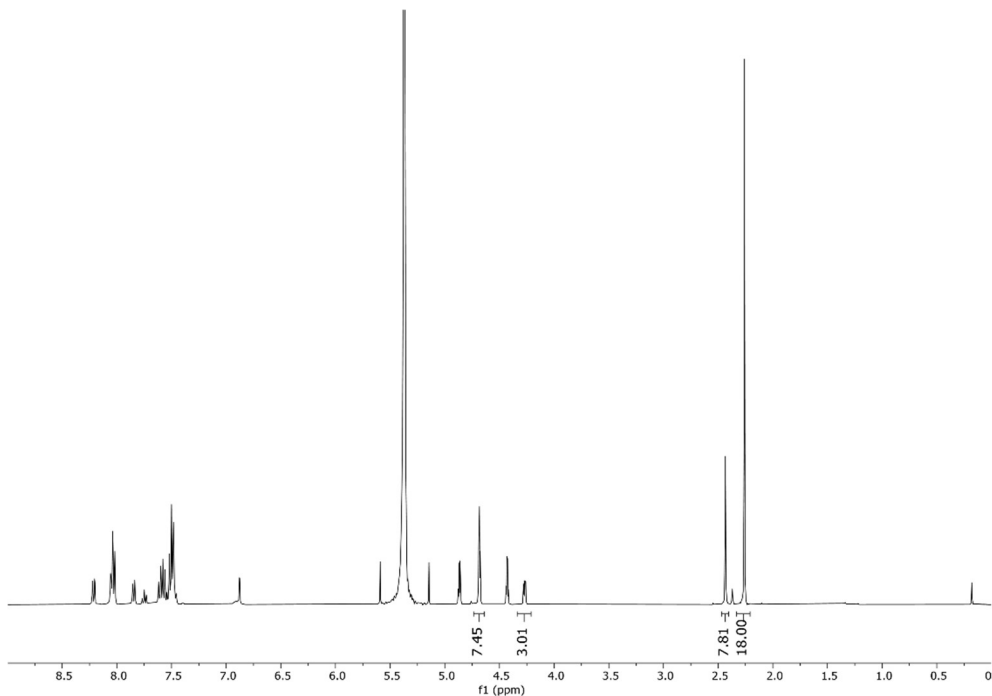


**Figure S44.** <sup>1</sup>H NMR (DCM-d<sub>2</sub>) of reaction mixture from table 1 entry 3.

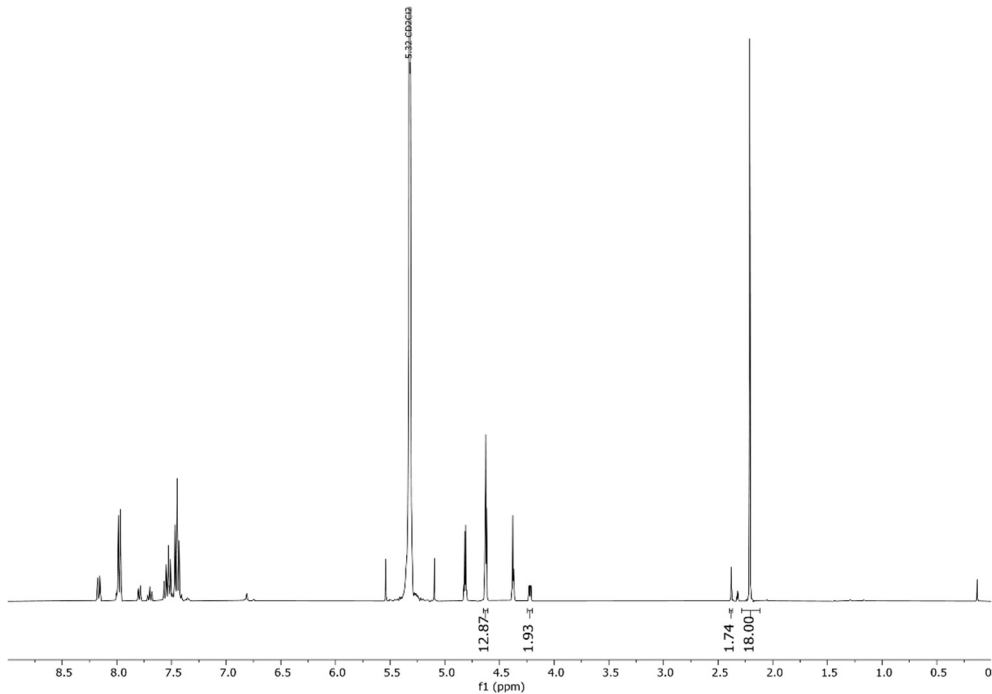


**Figure S45.** <sup>1</sup>H NMR (DCM-d<sub>2</sub>) of reaction mixture from table 1 entry 4.

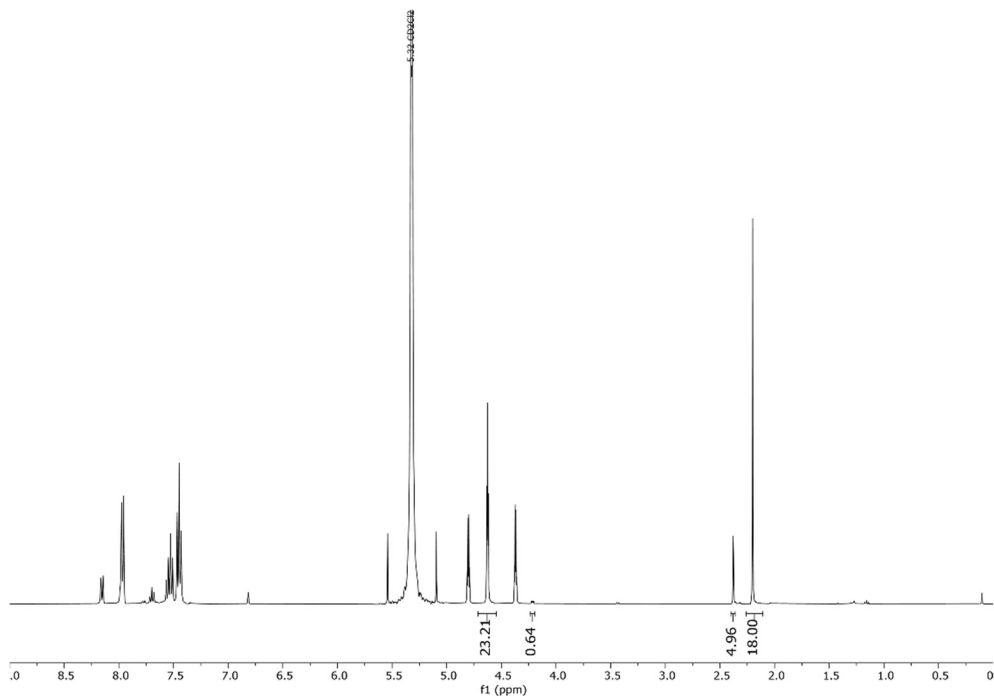


**Figure S46.** <sup>1</sup>H NMR (DCM-d<sub>2</sub>) of reaction mixture from table 1 entry 5.

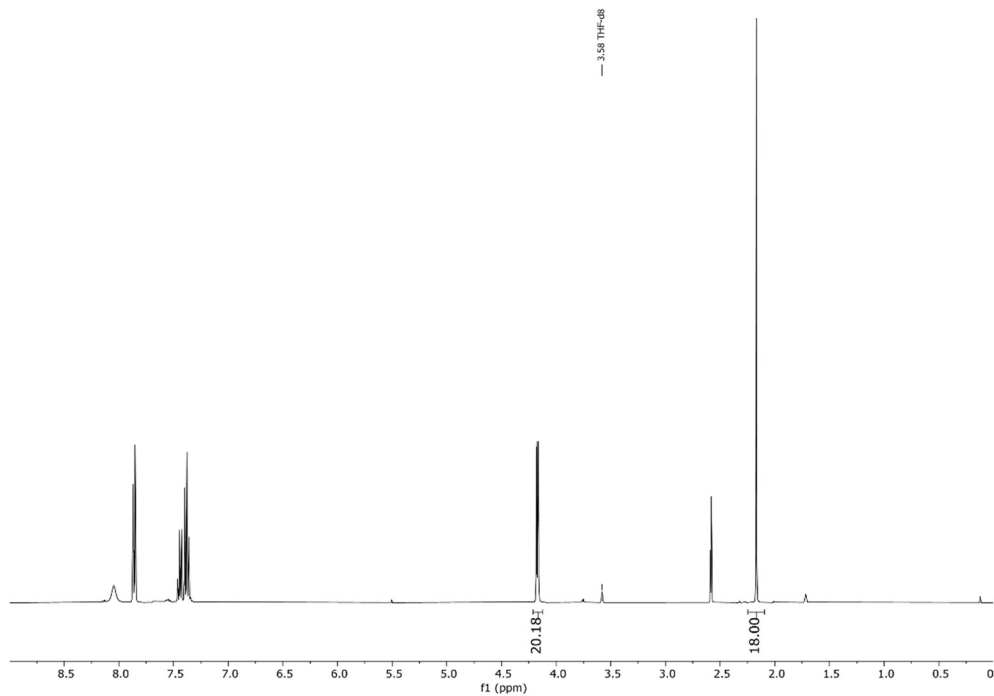


**Figure S47.** <sup>1</sup>H NMR (THF-d<sub>8</sub>) of reaction mixture from table 1 entry 6.

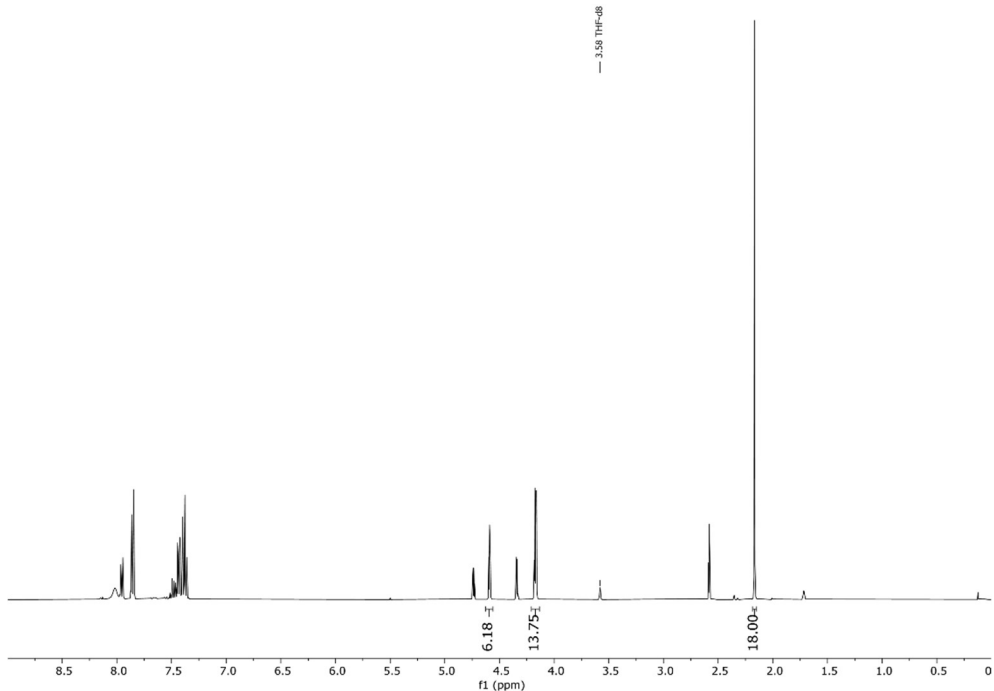


**Figure S48.** <sup>1</sup>H NMR (THF-d<sub>8</sub>) of reaction mixture from table 1 entry 7.

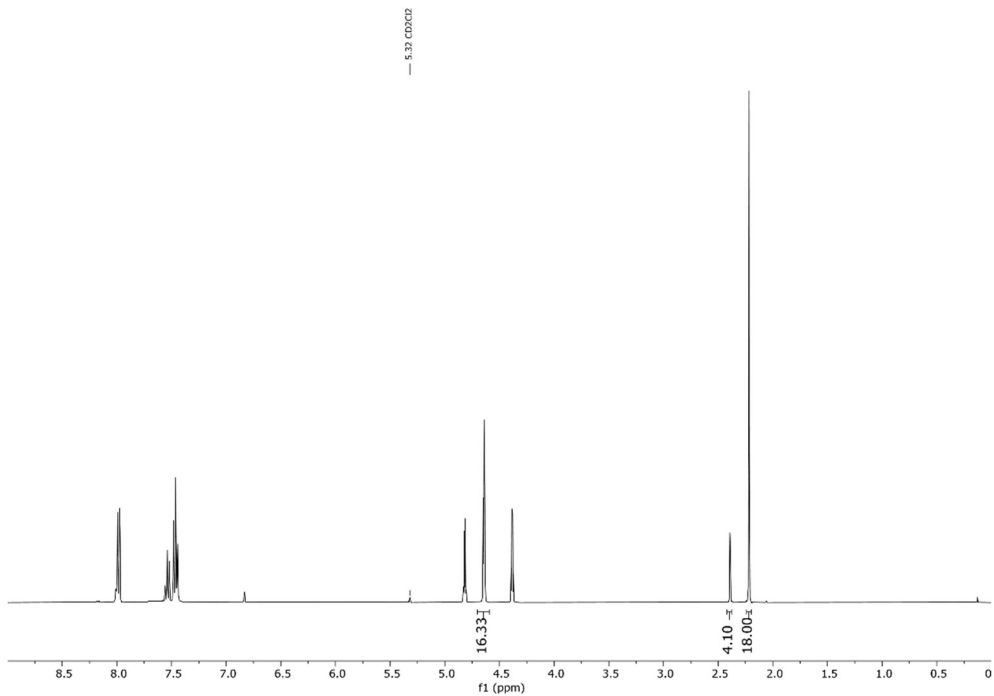


**Figure S49.** <sup>1</sup>H NMR (DCM-d<sub>2</sub>) of reaction mixture from table 1 entry 8.

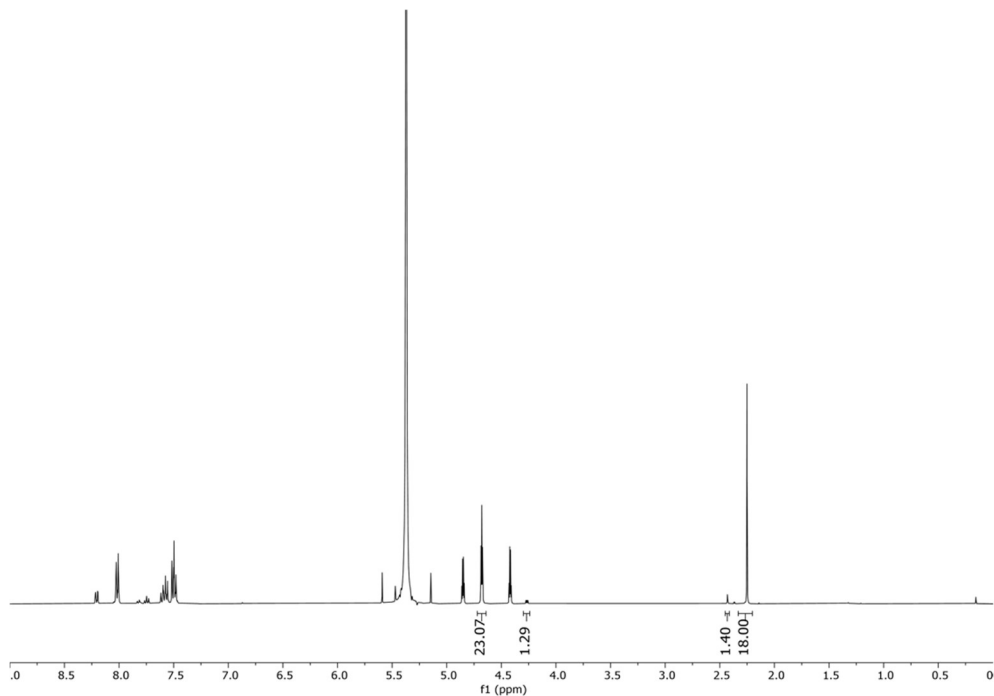


**Figure S50.** <sup>1</sup>H NMR (DCM-d<sub>2</sub>) of reaction mixture from table 1 entry 9.

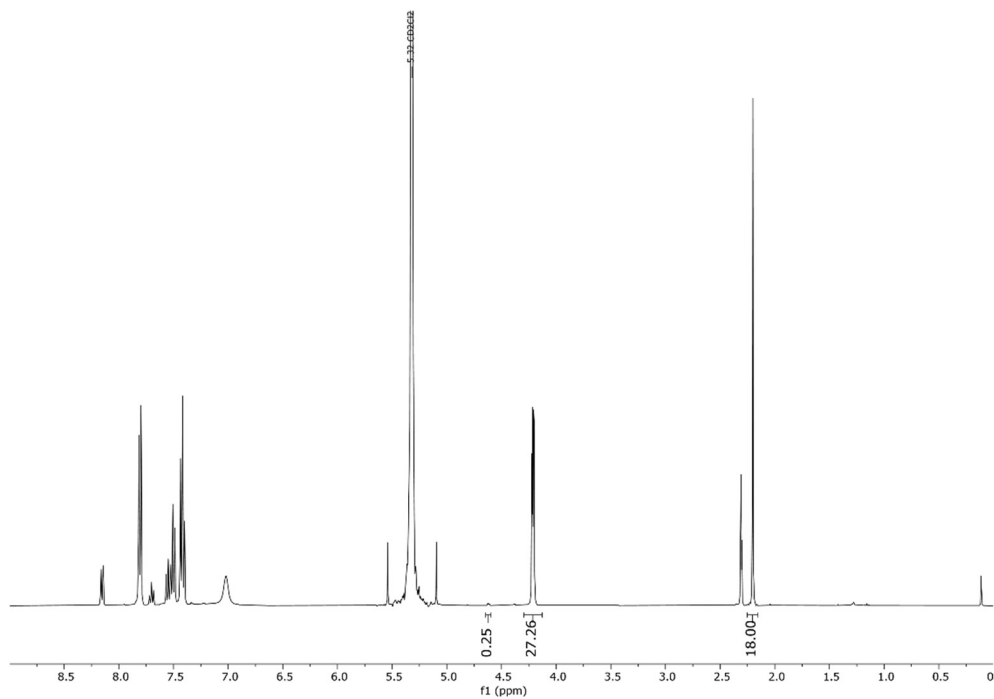


**Figure S51.** <sup>1</sup>H NMR (DCM-d<sub>2</sub>) of reaction mixture from table 1 entry 10.

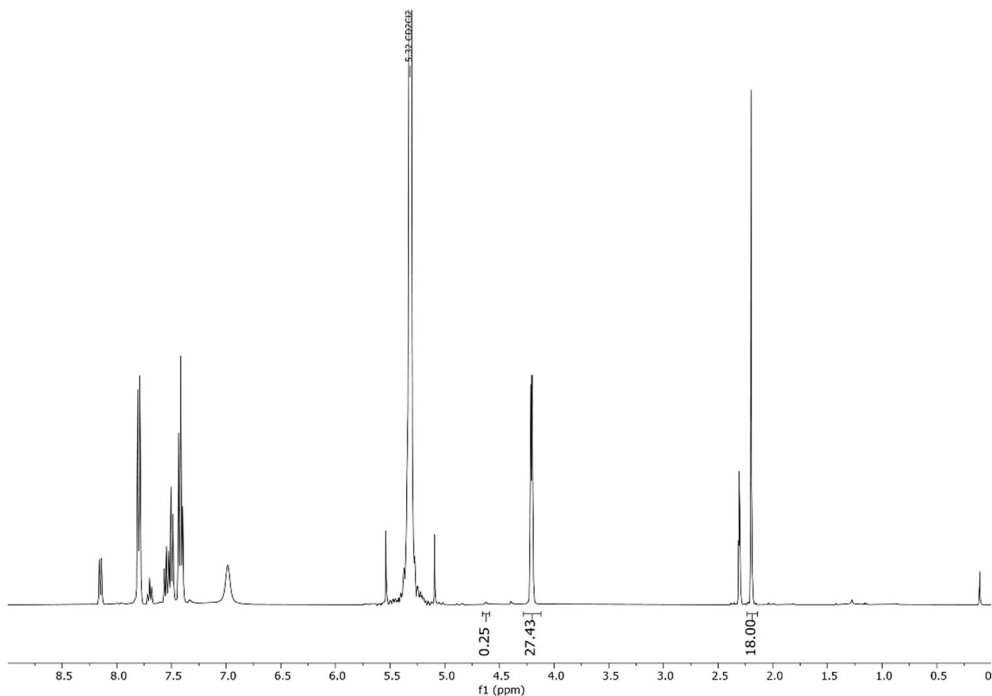


**Figure S52.** <sup>1</sup>H NMR (DCM-d<sub>2</sub>) of reaction mixture from table 1 entry 11.

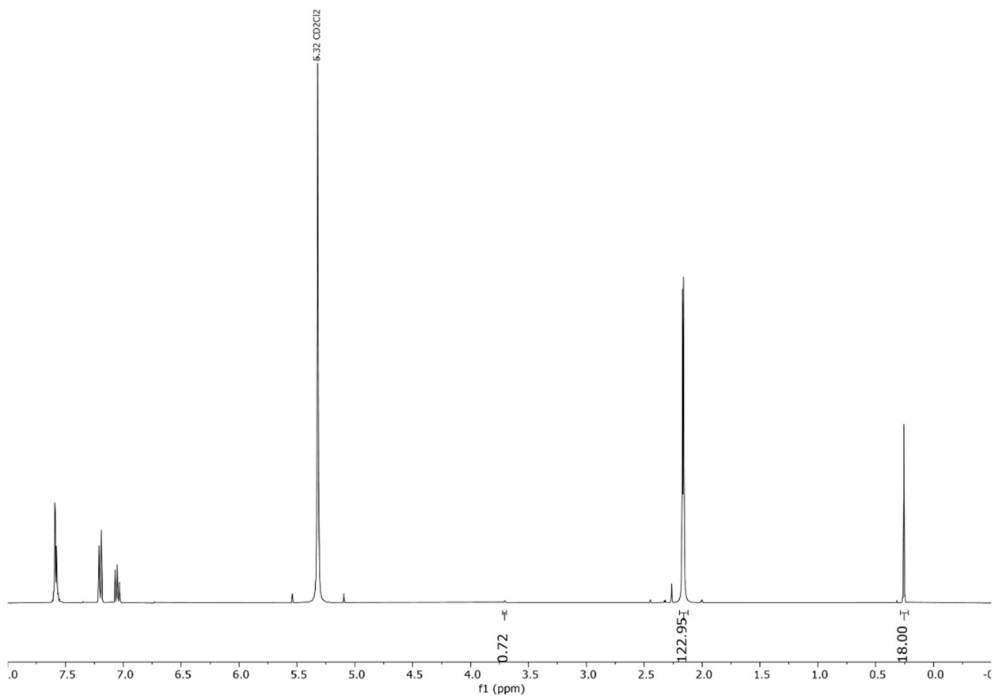


**Figure S53.** <sup>1</sup>H NMR (DCM-d<sub>2</sub>) of reaction mixture from table 2 entry 1.

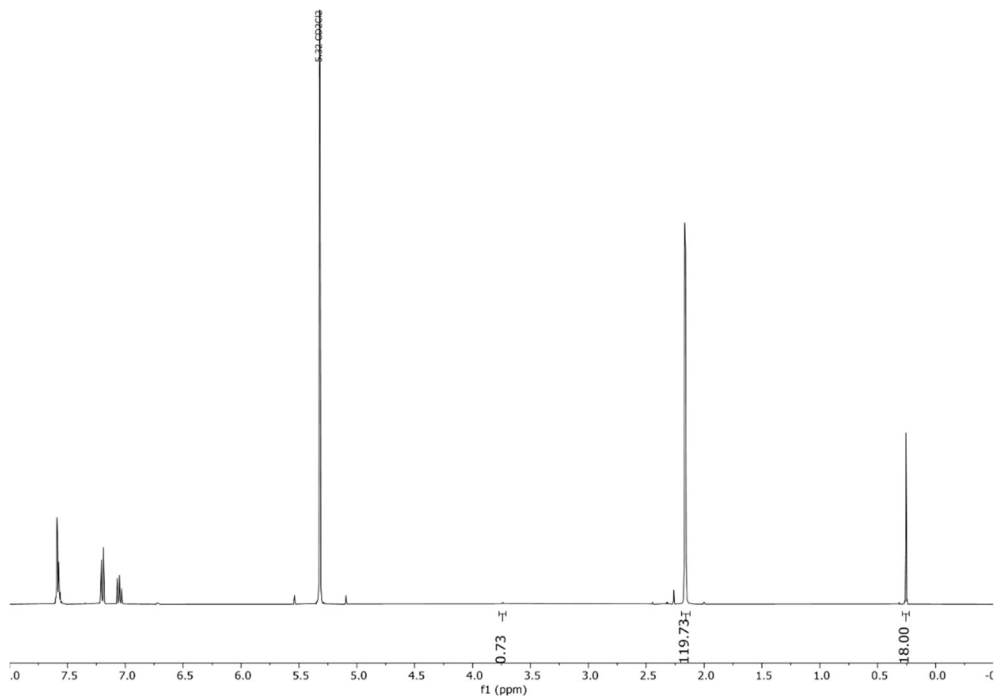


**Figure S54.** <sup>1</sup>H NMR (DCM-d<sub>2</sub>) of reaction mixture from table 2 entry 2.

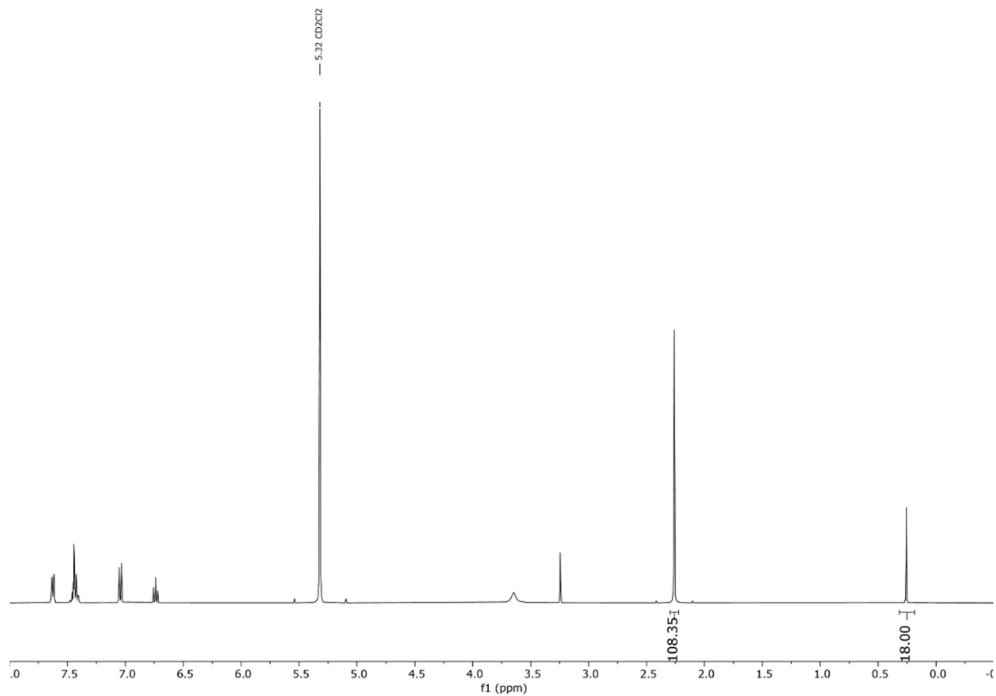


**Figure S55.** <sup>1</sup>H NMR (DCM-d<sub>2</sub>) of reaction mixture from table 2 entry 3.

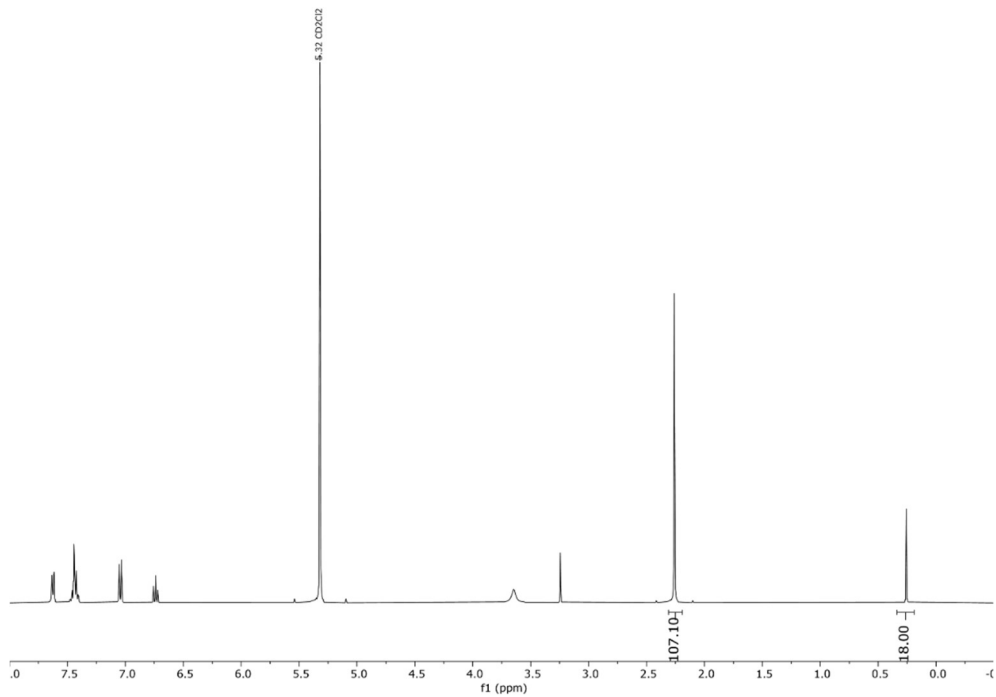


**Figure S56.** <sup>1</sup>H NMR (DCM-d<sub>2</sub>) of reaction mixture from table 2 entry 4.

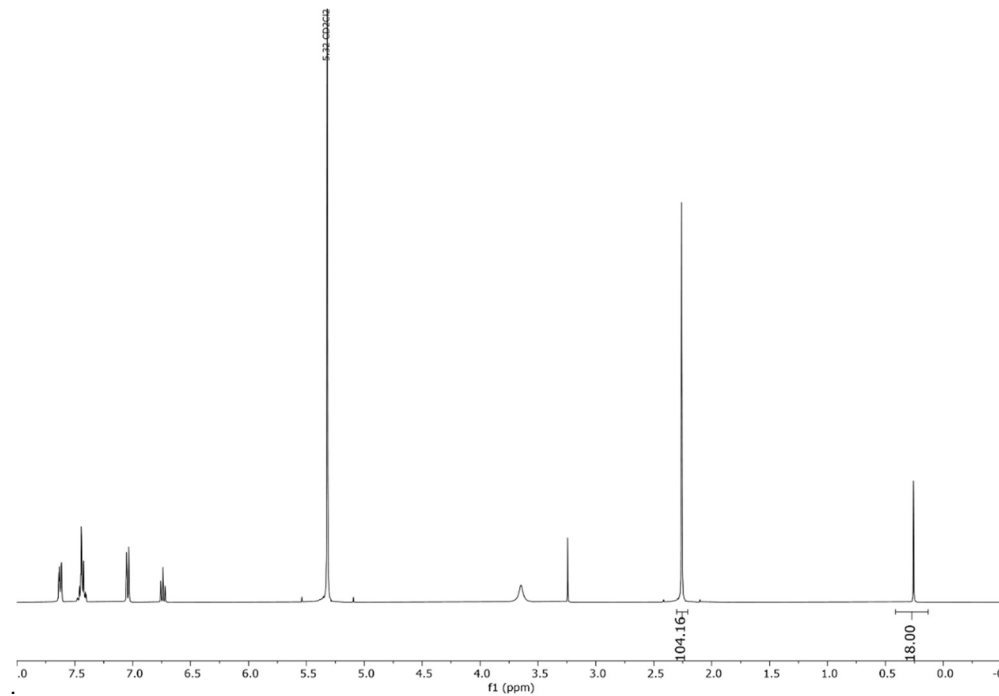


**Figure S57.** <sup>1</sup>H NMR (DCM-d<sub>2</sub>) of reaction mixture from table 2 entry 5.

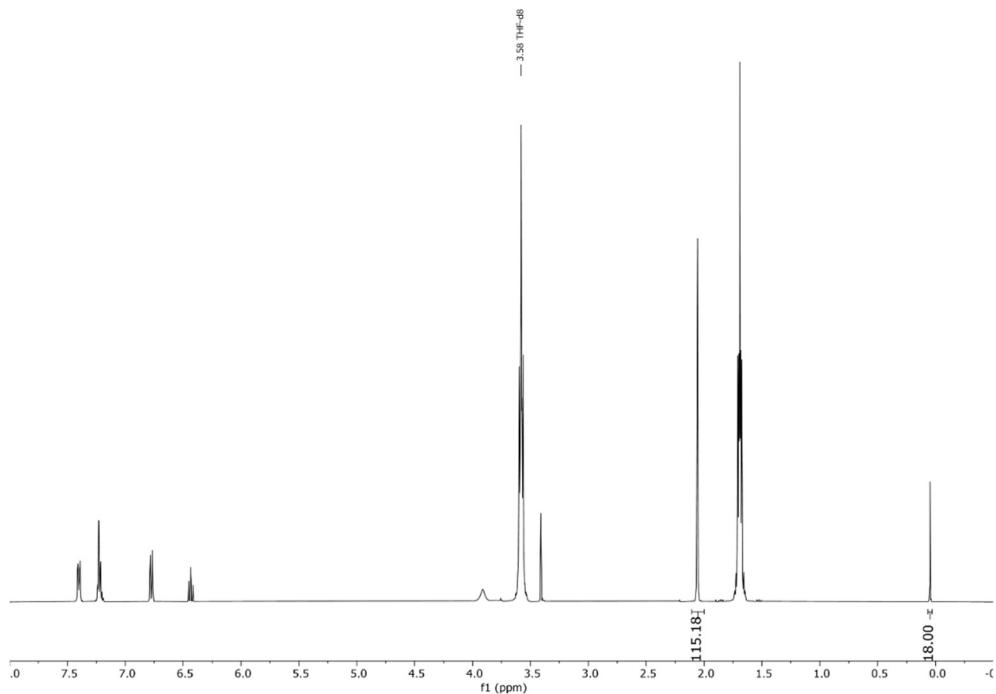


**Figure S58.** <sup>1</sup>H NMR (THF-d<sub>8</sub>) of reaction mixture from table 2 entry 6.

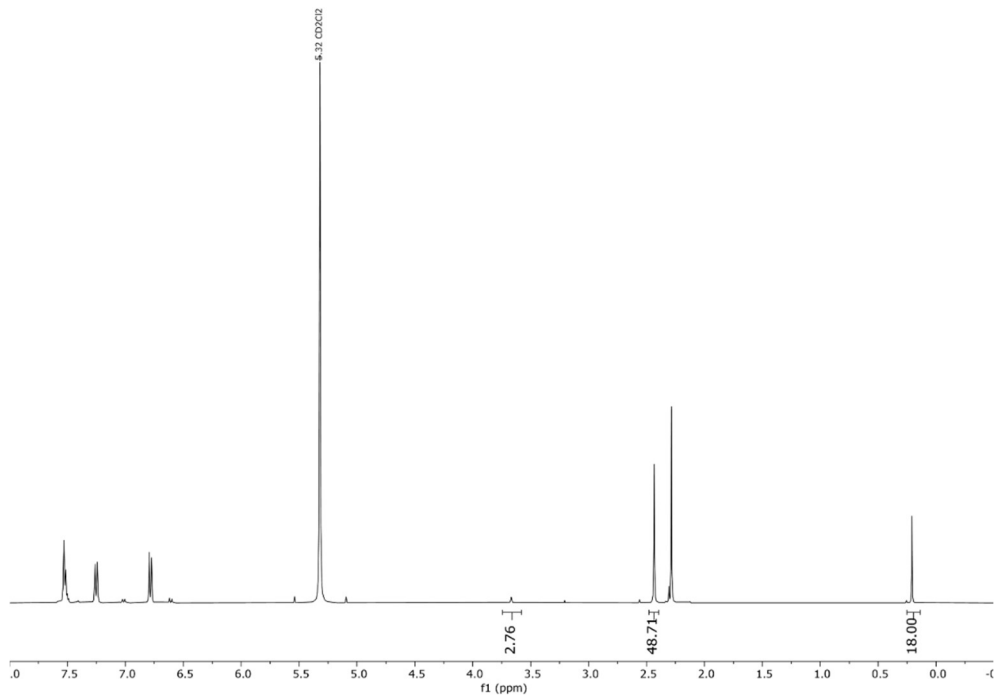


**Figure S59.** <sup>1</sup>H NMR (DCM-d<sub>2</sub>) of reaction mixture from table 2 entry 7.

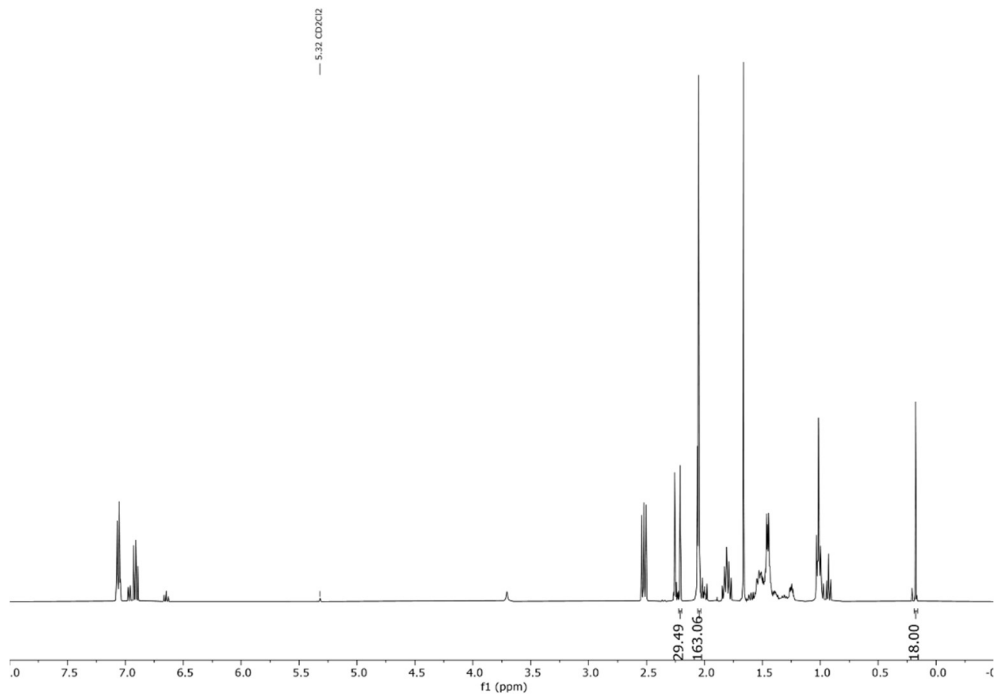


**Figure S60.**  $^1\text{H}$  NMR (DCM-d<sub>2</sub>) of reaction mixture from table 2 entry 8.

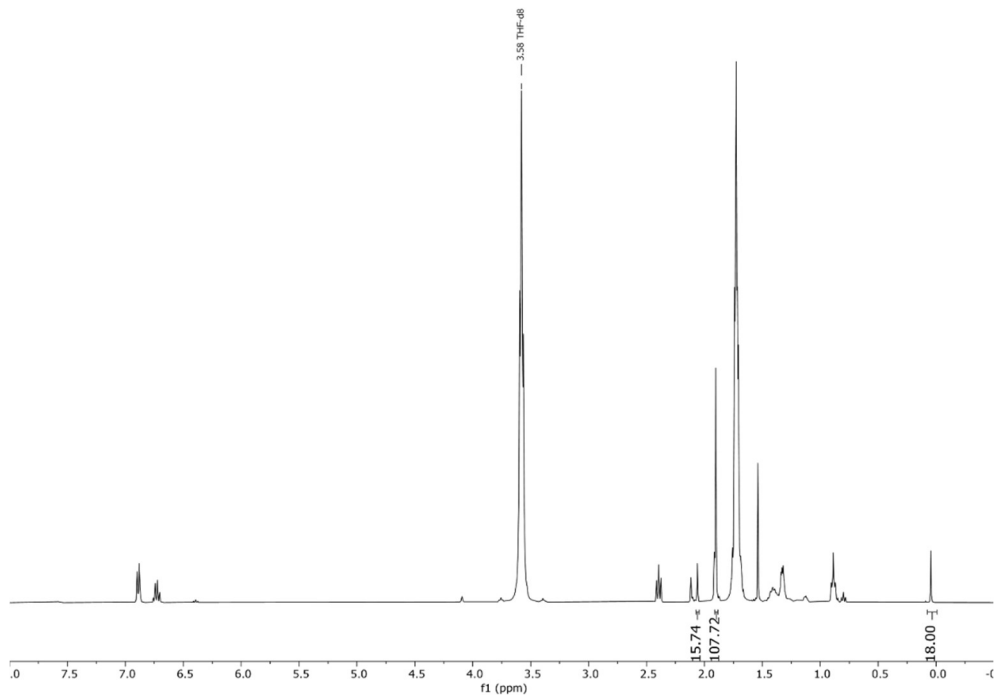


**Figure S61.**  $^1\text{H}$  NMR (THF-d<sub>8</sub>) of reaction mixture from table 2 entry 9.

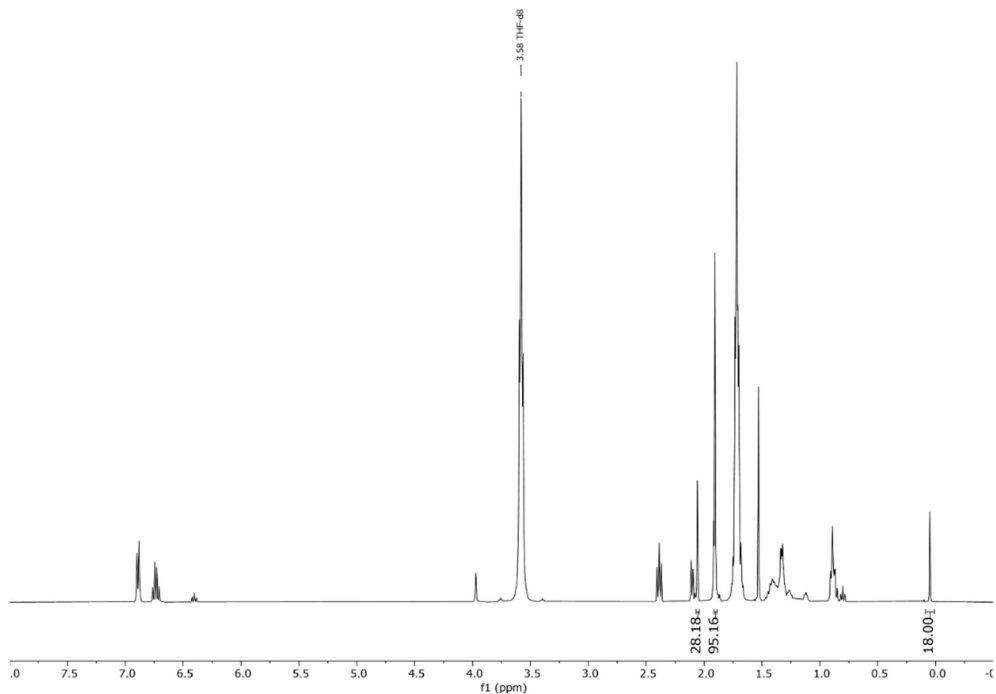


**Figure S62.** <sup>1</sup>H NMR (THF-d<sub>8</sub>) of reaction mixture from table 2 entry 10.

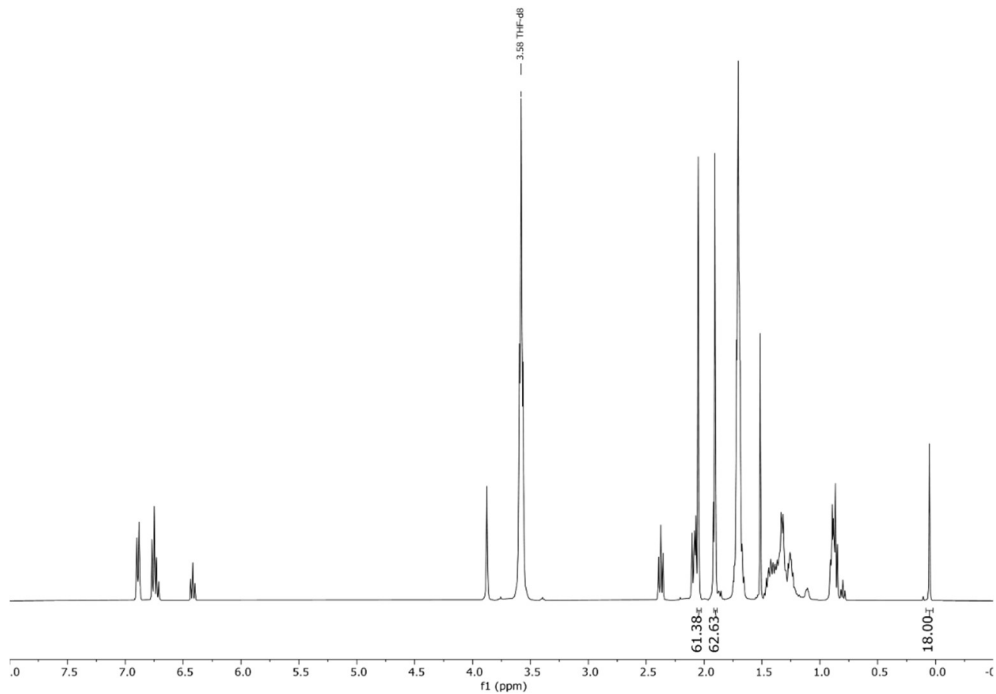


**Figure S63.** <sup>1</sup>H NMR (THF-d<sub>8</sub>) of reaction mixture from table 2 entry 11.

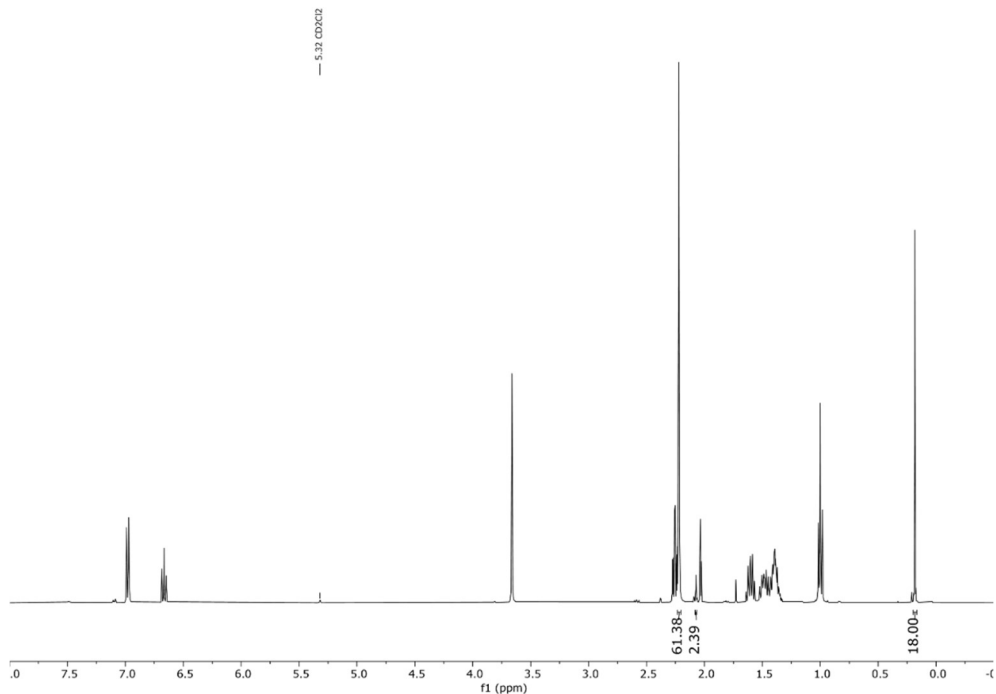


**Figure S64.** <sup>1</sup>H NMR (DCM-d<sub>2</sub>) of reaction mixture from table 2 entry 12.

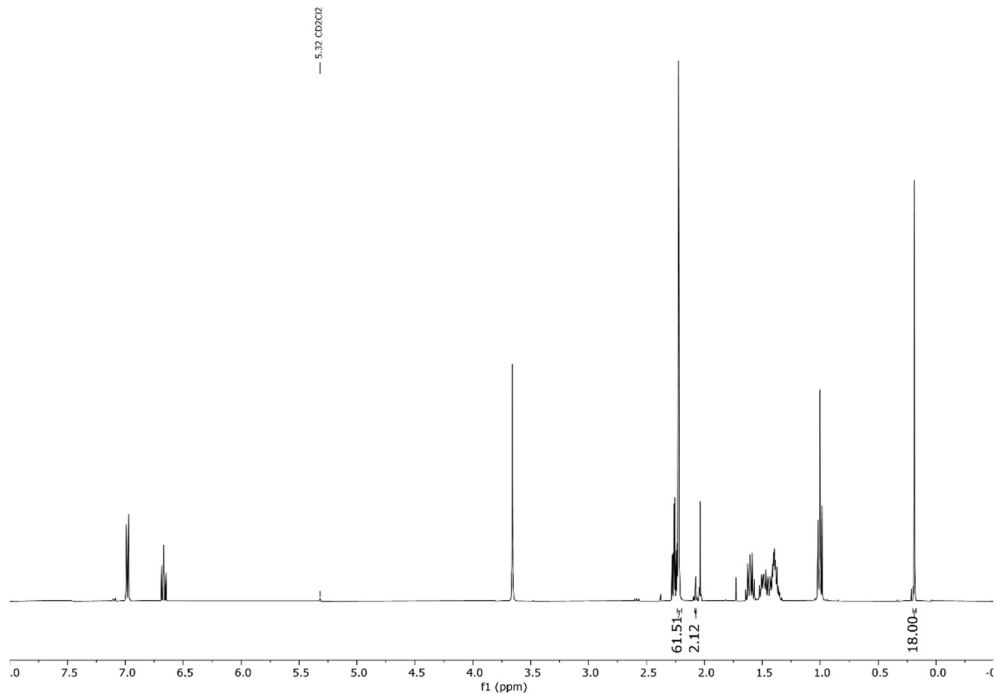


**Figure S65.** <sup>1</sup>H NMR (DCM-d<sub>2</sub>) of reaction mixture from table 2 entry 13.

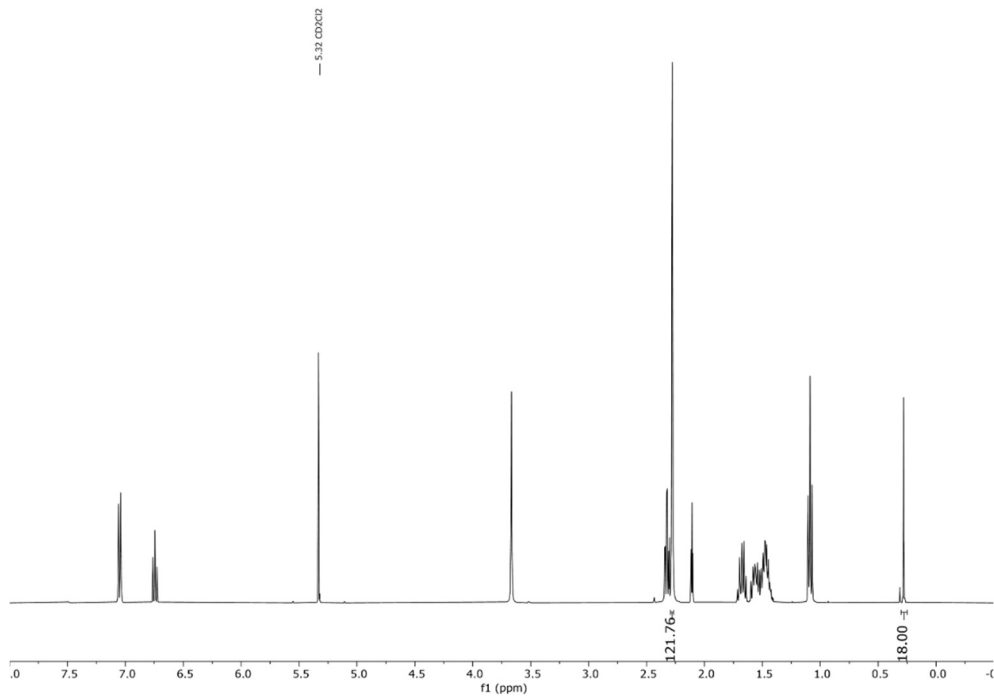


**Figure S66.** <sup>1</sup>H NMR (DCM-d<sub>2</sub>) of reaction mixture from table 2 entry 14.

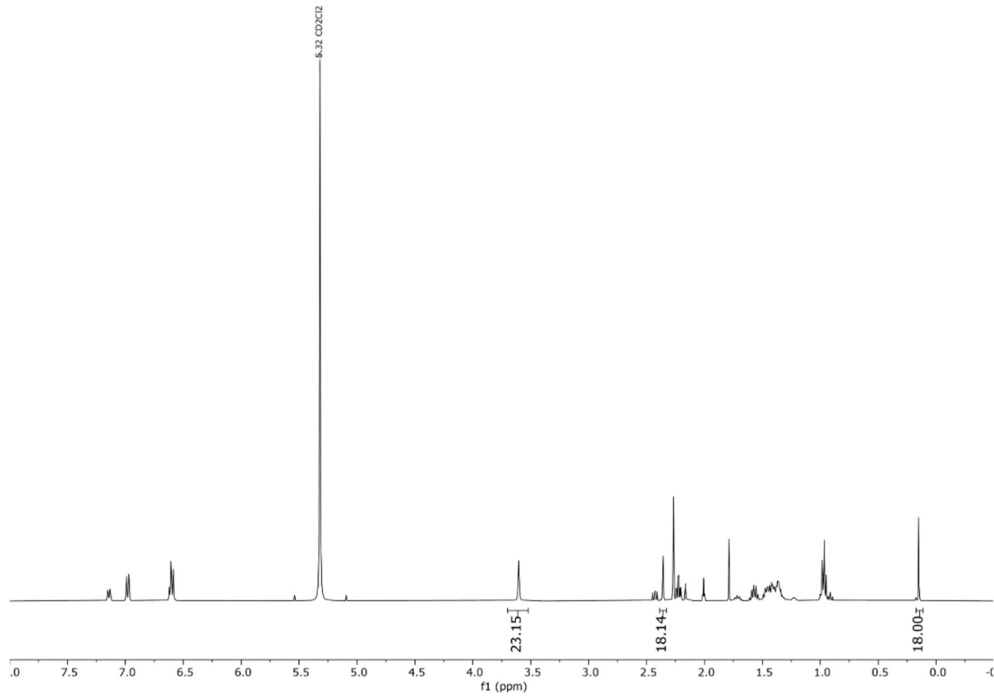


**Figure S67.** <sup>1</sup>H NMR (DCM-d<sub>2</sub>) of reaction mixture from table 2 entry 15.

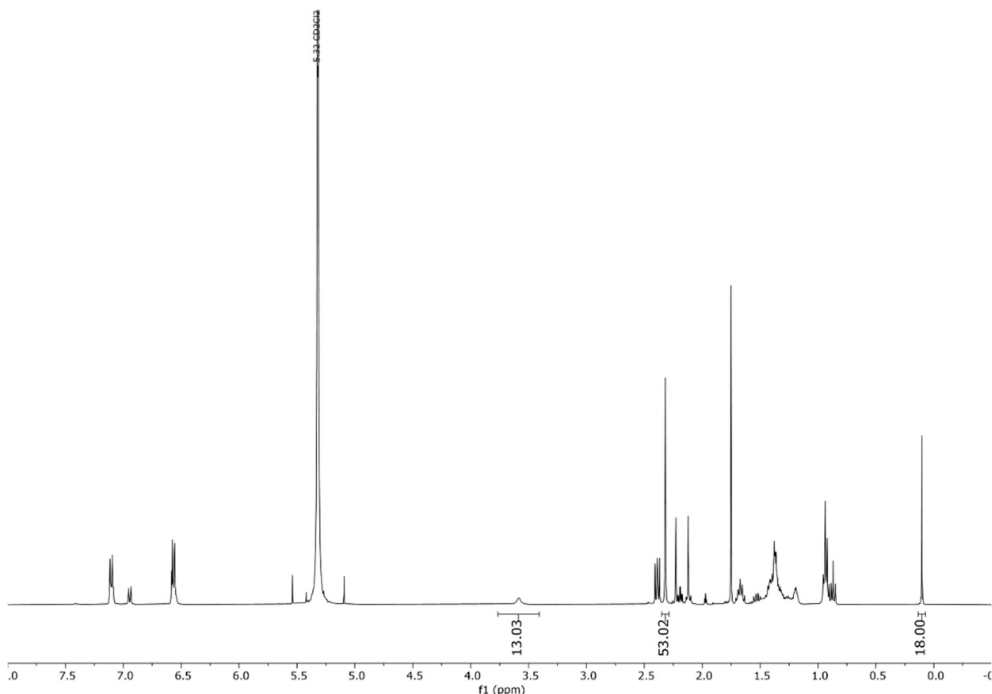


**Figure S68.**  $^1\text{H}$  NMR (DCM-d<sub>2</sub>) of reaction mixture from table 2 entry 16.

## 8 References

1. G. R. Fulmer, A. J. M. Miller, N. H. Sherden, H. E. Gottlieb, A. Nudelman, B. M. Stoltz, J. E. Bercaw and K. I. Goldberg, *Organometallics*, 2010, **29**, 2176-2179.
2. P. Steinhoff, R. Steinbock, A. Friedrich, B. G. Schieweck, C. Cremer, K. N. Truong and M. E. Tauchert, *Dalton T*, 2018, **47**, 10439-10442.
3. A. J. Martinez-Martinez and A. S. Weller, *Dalton Trans*, 2019, **48**, 3551-3554.
4. J. Schießl, J. Schulmeister, A. Doppiu, E. Wörner, M. Rudolph, R. Karch and A. S. K. Hashmi, *Adv. Synth. Catal.*, 2018, **360**, 2493-2502.
5. C. M. Conifer, D. J. Law, G. J. Sunley, A. J. P. White and G. J. P. Britovsek, *Organometallics*, 2011, **30**, 4060-4066.
6. M. Sircoglou, S. Bontemps, M. Mercy, N. Saffon, M. Takahashi, G. Bouhadir, L. Maron and D. Bourissou, *Angew. Chem. Int. Ed.*, 2007, **46**, 8583-8586.
7. R. Strothmann, S. van Terwingen, I. Kalf and U. Englert, *CrystEngComm*, 2021, **23**, 841-849.
8. Bruker, *SAINT+. Program for Reduction of Data Collected on Bruker CCD Area Detector Diffractometer*, 2012.
9. Bruker, *SADABS* 2008.
10. J. Kozíkova, F. Hahn, J. Richter and J. Kožíšek, *Acta Chim. Slovaca*, 2016, **9**, 136-140.
11. G. M. Sheldrick, *Acta Crystallogr. A Found. Adv.*, 2015, **71**, 3-8.
12. G. M. Sheldrick, *Acta Crystallogr. C Struct. Chem.*, 2015, **71**, 3-8.
13. C. F. Macrae, P. R. Edgington, P. McCabe, E. Pidcock, G. P. Shields, R. Taylor, M. Towler and J. van de Streek, *J. Appl. Cryst.*, 2006, **39**, 453-457.
14. A. Spek, *J. Appl. Cryst.*, 2003, **36**, 7-13.
15. A. Spek, *Acta Cryst. ,* 2009, **D65**, 148-155.
16. A. L. Spek, *Acta Crystallogr. D Biol. Crystallogr.*, 2009, **65**, 148-155.
17. C. R. Groom, I. J. Bruno, M. P. Lightfoot and S. C. Ward, *Acta Cryst. B*, 2016, **72**, 171-179.
18. M. E. Olmos, A. Schier and H. Schmidbaur, *Z. Naturforsch. B*, 1997, **52**, 203-208.
19. S. Nayeri, S. Jamali, A. Jamjah, J. R. Shakirova, S. P. Tunik, V. Gurzhiy, H. Samouei and H. R. Shahsavari, *Inorg. Chem.*, 2020, **59**, 5702-5712.
20. M. T. Dau, J. R. Shakirova, A. J. Karttunen, E. V. Grachova, S. P. Tunik, A. S. Melnikov, T. A. Pakkanen and I. O. Koshevoy, *Inorg. Chem.*, 2014, **53**, 4705-4715.
21. S. D. Adhikary, L. Jhulki, S. Seth, A. Kundu, V. Bertolasi, P. Mitra, A. Mahapatra and J. Dinda, *Inorg. Chim. Acta*, 2012, **384**, 239-246.
22. M. Dahlen, E. H. Hollesen, M. Kehry, M. T. Gamer, S. Lebedkin, D. Schooss, M. M. Kappes, W. Klopper and P. W. Roesky, *Angew. Chem. Int. Ed.*, 2021, **60**, 23365-23372.
23. L. Cao, S. Huang, W. Liu and X. Yan, *Organometallics*, 2018, **37**, 2010-2013.
24. K. Chen and V. J. Catalano, *Eur J Inorg Chem*, 2015, **2015**, 5254-5261.

25. I. O. Koshevoy, J. R. Shakirova, A. S. Melnikov, M. Haukka, S. P. Tunik and T. A. Pakkanen, *Dalton T*, 2011, **40**, 7927-7933.
26. R. Kobayashi, T. Yumura, H. Imoto and K. Naka, *Chem. Commun.*, 2021, **57**, 5382-5385.
27. C. E. Strasser and V. J. Catalano, *J. Am. Chem. Soc.*, 2010, **132**, 10009-10011.
28. V. J. Catalano, A. L. Moore, J. Shearer and J. Kim, *Inorg. Chem.*, 2009, **48**, 11362-11375.
29. H. Ito, T. Saito, T. Miyahara, C. M. Zhong and M. Sawamura, *Organometallics*, 2009, **28**, 4829-4840.
30. F. Meyer, E. Hupf, E. Lork, S. Grabowsky, S. Mebs and J. Beckmann, *Eur J Inorg Chem*, 2020, **2020**, 3829-3836.
31. C. Khin, A. S. K. Hashmi and F. Rominger, *Eur J Inorg Chem*, 2010, **2010**, 1063-1069.
32. C. Tschersich, C. Limberg, S. Roggan, C. Herwig, N. Ernsting, S. Kovalenko and S. Mebs, *Angew. Chem. Int. Ed.*, 2012, **51**, 4989-4992.
33. M. Viotte, B. Gautheron, M. M. Kubicki, Y. Mugnier and R. V. Parish, *Inorg. Chem.*, 2002, **34**, 3465-3473.
34. E. Hupf, E. Lork, S. Mebs and J. Beckmann, *Inorg. Chem.*, 2015, **54**, 1847-1859.
35. F. Kutter, A. Denhof, E. Lork, S. Mebs and J. Beckmann, *Z. Kristallogr. – Cryst. Mater.*, 2018, **233**, 627-639.
36. G. W. T. M. J. Frisch, H. B. Schlegel, G. E. Scuseria, M. A. Robb, J. R. Cheeseman, G. Scalmani, V. Barone, G. A. Petersson, H. Nakatsuji, X. Li, M. Caricato, A. V. Marenich, J. Bloino, B. G. Janesko, R. Gomperts, B. Mennucci, H. P. Hratchian, J. V. Ortiz, A. F. Izmaylov, J. L. Sonnenberg, D. Williams-Young, F. Ding, F. Lipparini, F. Egidi, J. Goings, B. Peng, A. Petrone, T. Henderson, D. Ranasinghe, V. G. Zakrzewski, J. Gao, N. Rega, G. Zheng, W. Liang, M. Hada, M. Ehara, K. Toyota, R. Fukuda, J. Hasegawa, M. Ishida, T. Nakajima, Y. Honda, O. Kitao, H. Nakai, T. Vreven, K. Throssell, J. A. Montgomery, Jr., J. E. Peralta, F. Ogliaro, M. J. Bearpark, J. J. Heyd, E. N. Brothers, K. N. Kudin, V. N. Staroverov, T. A. Keith, R. Kobayashi, J. Normand, K. Raghavachari, A. P. Rendell, J. C. Burant, S. S. Iyengar, J. Tomasi, M. Cossi, J. M. Millam, M. Klene, C. Adamo, R. Cammi, J. W. Ochterski, R. L. Martin, K. Morokuma, O. Farkas, J. B. Foresman, D. J. Fox, *Journal*, 2016.
37. F. Weigend and R. Ahlrichs, *Phys. Chem. Chem. Phys.*, 2005, **7**, 3297-3305.
38. J. P. Perdew, *Phys. Rev. B. Condens. Matter.*, 1986, **33**, 8822-8824.
39. K. Eichkorn, F. Weigend, O. Treutler and R. Ahlrichs, *Theor. Chem. Acc.*, 1997, **97**, 119-124.
40. K. Eichkorn, O. Treutler, H. Öhm, M. Häser and R. Ahlrichs, *Chem. Phys. Lett.*, 1995, **242**, 652-660.
41. D. Andrae, U. Huermann, M. Dolg, H. Stoll and H. Preu, *Theor. Chim. Acta*, 1990, **77**, 123-141.
42. M. Dolg, U. Wedig, H. Stoll and H. Preuss, *J. Chem. Phys.*, 1987, **86**, 866-872.
43. B. Metz, H. Stoll and M. Dolg, *J. Chem. Phys.*, 2000, **113**, 2563-2569.
44. C. Adamo and V. Barone, *J. Chem. Phys.*, 1999, **110**, 6158-6170.
45. M. Ernzerhof and G. E. Scuseria, *J. Chem. Phys.*, 1999, **110**, 5029-5036.
46. J. P. Perdew, K. Burke and M. Ernzerhof, *Phys. Rev. Lett.*, 1996, **77**, 3865-3868.
47. F. Weigend, *Phys. Chem. Chem. Phys.*, 2006, **8**, 1057-1065.
48. F. Weigend and R. Ahlrichs, *Phys. Chem. Chem. Phys.*, 2005, **7**, 3297-3305.
49. E. D. Glendening, J. K. Badenhoop, A. E. Reed, J. E. Carpenter, J. A. Bohmann, C. M. Morales, P. Karafiolou, C. R. Landis and F. Weinhold, *NBO 7.0*, 2018, Theoretical Chemistry Institute, University of Wisconsin.
50. U. D. S, F. Julia, A. Luridiana, J. J. Douglas and D. Leonori, *Nature*, 2020, **584**, 75-81.
51. N. Iranpoor and F. Panahi, *Adv. Synth. Catal.*, 2014, **356**, 3067-3073.
52. M. Virant, M. Mihelac, M. Gazvoda, A. E. Cotman, A. Frantar, B. Pinter and J. Kosmrlj, *Org Lett*, 2020, **22**, 2157-2161.
53. H. F. Yang and F. P. Gabbaï, *J. Am. Chem. Soc.*, 2015, **137**, 13425-13432.
54. M. L. Buil, M. A. Esteruelas, A. M. López and A. C. Mateo, *Organometallics*, 2006, **25**, 4079-4089.
55. C. G. Hartung, A. Tillack, H. Trauthwein and M. Beller, *J Org Chem*, 2001, **66**, 6339-6343.
56. S. Sen, I.-S. Ke and F. P. Gabbaï, *Organometallics*, 2017, **36**, 4224-4230.
57. S. Yazdani, G. P. Junor, J. L. Peltier, M. Gembicky, R. Jazzaar, D. B. Grotjahn and G. Bertrand, *Acs Catal*, 2020, **10**, 5190-5201.
58. T. Scherpf, C. Schwarz, L. T. Scharf, J. A. Zur, A. Helbig and V. H. Gessner, *Angew. Chem. Int. Ed.*, 2018, **57**, 12859-12864.
59. X. Hu, D. Martin and G. Bertrand, *New J. Chem.*, 2016, **40**, 5993-5996.
60. A. Ueno, K. Watanabe, C. G. Daniliuc, G. Kehr and G. Erker, *Chem. Commun.*, 2019, **55**, 4367-4370.
61. T. Witteler, H. Darmandeh, P. Mehlmann and F. Dielmann, *Organometallics*, 2018, **37**, 3064-3072.
62. J. E. Siewert, A. Schumann, M. Fischer, C. Schmidt, T. Taeufer and C. Hering-Junghans, *Dalton T*, 2020, **49**, 12354-12364.
63. E. Campos-Dominguez, J. Vasquez-Perez, S. Rojas-Lima, H. Lopez-Ruiz and D. Mendoza-Espinosa, *Appl. Organomet. Chem.*, 2020, **35**.
64. S. Ibáñez, M. Poyatos and E. Peris, *Organometallics*, 2017, **36**, 1447-1451.
65. E. Alvarado, A. C. Badaj, T. G. Larocque and G. G. Lavoie, *Chem-Eur J*, 2012, **18**, 12112-12121.
66. J. Li, X. Li, L. Sun, X. Wang, L. Yuan, L. Wu, X. Liu and Y. Wang, *Eur J Inorg Chem*, 2021, **2021**, 4230-4237.
67. S. Gonell, M. Poyatos and E. Peris, *Angew. Chem. Int. Ed.*, 2013, **52**, 7009-7013.
68. M. Flores-Jarillo, D. Mendoza-Espinosa, V. Salazar-Pereda and S. González-Montiel, *Organometallics*, 2017, **36**, 4305-4312.
69. C. Dash, M. M. Shaikh, R. J. Butcher and P. Ghosh, *Inorg Chem.*, 2010, **49**, 4972-4983.
70. S. A. Wolfarth, N. E. Miner, N. E. Wamser, R. K. Gwinn, B. C. Chan and C. Nataro, *J. Organomet. Chem.*, 2020, **906**.
71. A. Leyva and A. Corma, *Adv. Synth. Catal.*, 2009, **351**, 2876-2886.
72. J. P. Weyrauch, A. S. Hashmi, A. Schuster, T. Hengst, S. Schetter, A. Littmann, M. Rudolph, M. Hamzic, J. Visus, F. Rominger, W. Frey and J. W. Bats, *Chemistry*, 2010, **16**, 956-963.

73. M. Devillard, E. Nicolas, C. Appelt, J. Backs, S. Mallet-Ladeira, G. Bouhadir, J. C. Slootweg, W. Uhl and D. Bourissou, *Chem. Commun.*, 2014, **50**, 14805-14808.
74. S. Doherty, J. G. Knight, D. O. Perry, N. A. B. Ward, D. M. Bittner, W. McFarlane, C. Wills and M. R. Probert, *Organometallics*, 2016, **35**, 1265-1278.
75. S. Vanicek, M. Podewitz, J. Stubbe, D. Schulze, H. Kopacka, K. Wurst, T. Muller, P. Lippmann, S. Haslinger, H. Schottenberger, K. R. Liedl, I. Ott, B. Sarkar and B. Bildstein, *Chemistry*, 2018, **24**, 3742-3753.
76. O. Bárta, I. Císařová, J. Schulz and P. Štěpnička, *New J. Chem.*, 2019, **43**, 11258-11262.
77. M. Rigo, L. Hettmanczyk, F. J. Heutz, S. Hohloch, M. Lutz, B. Sarkar and C. Muller, *Dalton T*, 2016, **46**, 86-95.
78. M. Rigo, E. R. M. Habraken, K. Bhattacharyya, M. Weber, A. W. Ehlers, N. Mezailles, J. C. Slootweg and C. Muller, *Chem-Eur J*, 2019, **25**, 8769-8779.
79. P. Brüggemann, M. Wahl, S. Schwengers, H. Buhl and C. Ganter, *Organometallics*, 2018, **37**, 4276-4286.
80. A. S. K. Hashmi, Y. Yu and F. Rominger, *Organometallics*, 2012, **31**, 895-904.
81. M. M. Hansmann, F. Rominger, M. P. Boone, D. W. Stephan and A. S. K. Hashmi, *Organometallics*, 2014, **33**, 4461-4470.
82. A. Franchino, A. Marti, S. Nejrotti and A. M. Echavarren, *Chemistry*, 2021, **27**, 11989-11996.
83. D. Rendón-Nava, A. Álvarez-Hernández and D. Mendoza-Espinosa, *Eur J Inorg Chem*, 2021, **2021**, 840-847.
84. S. Sen and F. P. Gabbai, *Chem. Commun.*, 2017, **53**, 13356-13358.
85. S. Tšupova, M. Rudolph, F. Rominger and A. S. K. Hashmi, *Adv. Synth. Catal.*, 2016, **358**, 3999-4005.
86. A. Padunnappattu, C. Duhayon, V. César and Y. Canac, *Organometallics*, 2022, **41**, 2868-2878.
87. B. Wang, K. Koshino and R. Kinjo, *Chem. Commun.*, 2019, **55**, 13012-13014.